NASA CR-134837

NASA/Navy Lift/Cruise Fan Preliminary Design Report

by

GENERAL ELECTRIC COMPANY
EVENDALE, OHIO

PREPARED FOR

National Aeronautics and Space Administration

LEWIS RESEARCH CENTER

CLEVELAND, OHIO

NAS3-19411

1. Report No.	2. Government Accession No.	3. Recipient's Catalog No.
NASA CR-134837		

4. Title and Subtitle	5. Report Date
NASA/NAVY LIFT/CRUISE FAN PRELIMINARY DESIGN REPORT	JULY, 1975
	6. Performing Organization Code
7. Author(s)	8. Performing Organization Report No.
GENERAL ELECTRIC COMPANY	R75AEG414
	10. Work Unit No.
9. Performing Organization Name and Address	
GENERAL ELECTRIC COMPANY CINCINNATI, OHIO 45215	11. Contract or Grant No. NAS3-19411
	13. Type of Report and Period Covered PRELIMINARY DESIGN
12. Sponsoring Agency Name and Address	
NATIONAL AERONAUTICS AND SPACE ADMINISTRATION CLEVELAND, OHIO 44135	14. Sponsoring Agency Code

15. Supplementary Notes

16. Abstract

Preliminary design studies were performed to define a turbotip lift/cruise fan propulsion system for a Navy multimission aircraft. The fan is driven by the exhausts of the YJ97-GE-100 turbojet or a 20 percent Growth J97 configuration as defined during the studies. The LCF459 fan configuration defined has a tip diameter of 1.50 meters (59.0 inches) and develops a design point thrust of 75,130 N (16,890 lbs) at a fan pressure ratio of 1.319. The fan has an estimated weight of 386 kg (850 lbs). Trade studies performed to define the selected configuration are described.

17. Key Words (Suggested by Author(s))	18. Distribution Statement
TURBOTIP, FAN, MULTIMISSION, J97, V/STOL	UNCLASSIFIED - UNLIMITED

19. Security Classif. (of this report)	20. Security Classif. (of this page)	21. No. of Pages	22. Price*
UNCLASSIFIED	UNCLASSIFIED	180	

* For sale by the National Technical Information Service, Springfield, Virginia 22151

TABLE OF CONTENTS

TABLES

TABLES

FIGURES

FIGURES

FIGURES

FIGURES

SUMMARY

The LCF459 is an advanced remote turbo tip lift/cruise fan designed to meet the requirements of a Navy multimission aircraft. This report documents the trade studies which led to the definition of the LCF459, and describes the configuration established for the ensuing preliminary design studies.

The LCF459 is a 1.50 meter (59 inch) diameter lift/cruise fan with an aerodynamic design pressure ratio of 1.319 and a tip speed of 343 meters per second (1125 feet/sec). The fan is designed to operate with the J97 gas generator, either as a growth configuration or the existing YJ97-GE-100 turbojet engine. The LCF459 is capable of installation as a pod-mounted lift/cruise fan and as a horizontally installed lift only system. Estimated static vertical take-off lift on a 32°C (90°F) day for three fans operating with two growth engines is 144.7 kN (32,530 lbs). Comparable lift for three YJ97-GE-100 engines is 173.0 kN (38,894 lbs).

The fan cross section layout, as shown below, shows the features included in the fan design to provide a long-life, easily maintainable propulsion system.

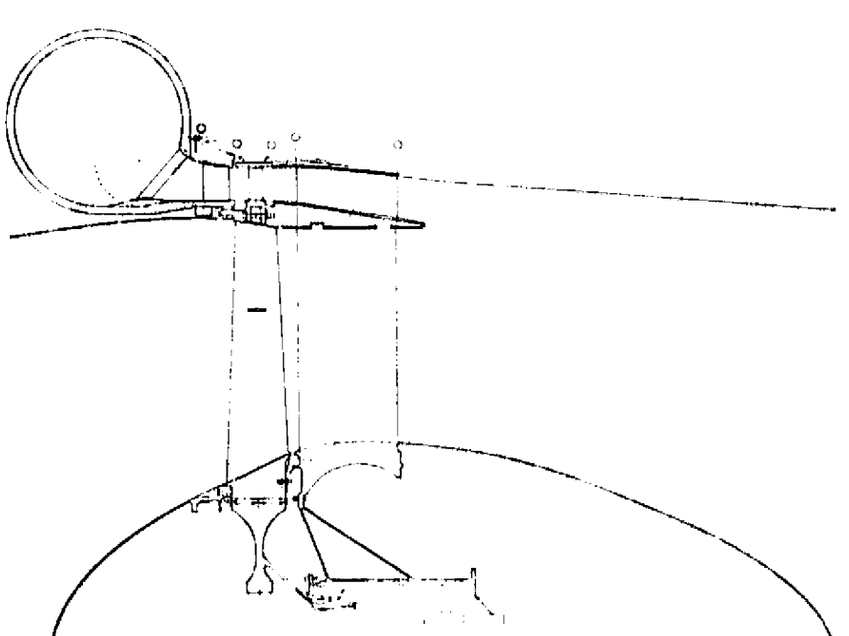

The fan is designed for a minimum life without repair of 3000 hours for hot components and 6000 hours for all other parts. Maintainability features are numerous and include the capability for single fan blade removal or complete rotor, disk and bearing removal without additional fan disassembly. The fan configuration employs a single structural rear frame which provides an unobstructed fan inlet consistent with the design approach used in current high bypass turbofan engines. Thus, fan anti-icing is not required.

Fan reliability and ruggedness are provided through consideration during the studies of bird ingestion requirements and fan reaction in the event of fan or turbine blade failures. Analytical studies show that the LCF459 is capable of sustained operation following ingestion of a 1 kg (2.2 lb) bird. Safe fan shutdown is also possible following loss of a complete fan blade/turbine carrier assembly.

Design features are also included in the fan to permit safe continuous operation following shutdown of gas generators. The fan system is capable of operating with only one gas generator by virtue of the multi-inlet scroll and interconnect ducting. Integral fan lubrication and cooling systems are provided to permit fan operation during these conditions without requiring the complexity of interconnected systems. Power take-off is also provided in the fan system for operating aircraft accessories. This feature provides the needed redundancy to cover aircraft systems operation during the single engine condition and still provides high levels of power extraction.

The scroll configuration of the fan can be configured to meet the particular aircraft installation requirements. Typical scroll cross-sectional shapes are the circular bubble, as shown in the fan cross-section, and a multilobe configuration selected to minimize fan frontal area at a small, about 10 kg (23 lb), increase in weight. The number and orientation of the scroll inlets is a design variable which is established by the relative location of the engines and fans in the aircraft, and the methods of interconnection used. This versatility of fan design permits a large degree of freedom for optimization of the aircraft configuration and selection of the propulsion component location for minimum interference effects and hot gas ingestion.

The weight of the referenced LCF459 fan with a circular scroll configuration is 386 kg (850 lbs). This weight yields a fan design point thrust-to-weight ratio of 19.9.

As part of these design studies, a growth configuration of the J97 engine was established. This engine represents a 20 percent power growth above the YJ97-GE-100 configuration. The selected growth was achieved through resizing the compressor for a 16 percent increase in airflow and a

20 percent increase in compressor pressure ratio. The estimated weight for the growth engine is 379 kg (835 lbs) as compared to the YJ97-GE-100 with a weight of 335 kg (735 lbs).

Ratings were defined for operation of both J97 engine systems. The definition of the ratings include the option of four percent pre-combustor water injection. The four rating points defined for sea level static operation of a 32°C (90°F) day are:

INTER - A 30 minute rating applicable to maximum performance during conventional flight operation.

VTO - A one minute rating applicable to the vertical take-off operation of the aircraft.

MAX - A short time, less than three second, rating available during application of maximum aircraft attitude control during powered lift operation.

EMERG - A one minute emergency rating to provide increased power during occurrences such as engine-out operation.

Fan performance during application of these short-time ratings was determined for three fans operating with either two growth or three YJ97-GE-100 engines. The VTO, 32°C (90°F) lift ratios relative to intermediate power, standard day, are as follows:

	VTO (No Water)	EMERG* (No Water)	VTO (4% Water)	EMERG* (4% Water)
2 Growth	0.951	0.603	1.047	0.642
3 YJ97-GE-100.	0.970	0.785	1.040	0.825

* One Engine Out

1.0 INTRODUCTION

The General Electric Company, in a joint effort with NASA, has been engaged in a continuing program to define advancements in component and system technology which will lead to advanced lift fan systems applicable to V/STOL aircraft. Specific objectives of these programs include improvements in areas of performance, weight, size, time response, and reliability and maintainability of the turbotip lift fan systems.

The turbotip lift fan concept of V/STOL propulsion was initially demonstrated as a viable propulsion system during flight tests of the XV-5A aircraft. This aircraft has been actively engaged in various flight test programs beginning with the first flight in 1964 and terminating with tests at NASA Ames Research Center in 1972. NASA-sponsored programs have included the LF336, the LF446, the LF460 and advanced commercial lift fan system design studies. The LF336 lift fan program, initiated in early 1967, included design and development of two turbotip lift fan test vehicles. The lift fan was designed to develop a fan pressure ratio of 1.30 with a fan tip diameter of 0.91 meters (36 inches). The LF336 fans were involved in numerous static and wind tunnel test programs. Later programs were initiated to modify the fan to include acoustic features such as rotor-stator spacing, variable stator vane numbers, stator lean and exhaust noise suppression. This acoustic technology demonstrator program continued through August of 1972. The fan configuration was then modified into a statorless, rotor only, configuration, with tests occurring in 1973 and 1974 for both serrated and unserrated leading edge rotor blading. It is presently engaged in testing of advanced deflecting exhaust nozzles for V/STOL aircraft.

The design studies of advanced fan concepts were initiated with studies of the LF446 fan system. This lift fan, a 1.35 pressure ratio, was designed for future application, with an advanced gas generator, in the XV-5 aircraft flight research program. In late 1969, the program was redirected by NASA toward a large research aircraft which would provide technology applicable to the design of future V/STOL commercial transports. With this redirection, the LF446, a 1.17 meter (46 inch) diameter fan was increased in size to 1.52 meter (60 inch) diameter. The configuration was identified as the LF460 turbotip lift fan system and was driven by the exhaust gases of the YJ97 engine. Preliminary and detail design studies of the LF460 lift fan were completed in May, 1971, and are reported in Reference 1.

In mid-1973, NASA initiated study programs for the evaluation of lift fan powered V/STOL aircraft systems applicable to a proposed carrier on-board delivery (COD) mission. Aircraft and propulsion studies were initiated through the joint efforts of the NASA Ames and Lewis Research

Centers. The aircraft studies were later expanded to include numerous other Navy missions such as Antisubmarine Warfare (ASW), Surveillance (SURV), Surface Attack (SA) and Combat (Strike) Search and Rescue (CSAR). These aircraft studies identified the need for a rugged, reliable, long-life lift/cruise fan to power this new family of multimission aircraft. The fans for this aircraft would be used for both V/STOL lift and conventional cruise power. These new requirements compelled revision of several of the design features used in fans employed for lift operation only. Typical changes are; oil lubricated versus grease-packed bearings, fewer number of blades for improved FOD resistance, no front frame because of anti-icing requirements and minimum frontal area for ease of installation in cruise nacelles. In addition, improvements for long life without repair are needed to reduce life cycle costs.

This study is a preliminary design of a lift/cruise fan which meets the requirements of the multimission Navy aircraft. The propulsion system reflects the requirements as established during concurrent aircraft studies performed by the McDonnell Aircraft Company and Rockwell International, Los Angeles Aircraft Division. The gas generator selected for driving the fan system was the J97 turbojet engine. The J97 engine has been developed through preliminary flight rating. This engine is a lightweight, high-energy gas generator which is the most optimum to meet the requirements of temperature, flow and pressure for the single stage turbotip fan. Low risk growth of the engine is considered for advanced applications, but the YJ97-GE-100 engine is ideally suited for the technology research aircraft due to its availability and size.

This report documents the results of trade studies performed during selection of the design features of the lift/cruise fan. These design features are incorporated into a preliminary design configuration which was used to establish weight, performance and installation features. This design study provides a solid base for the detail design, fabrication and test of a lift/cruise fan for the technology aircraft.

An economic analysis was also performed, and is presented in a separate report. This analysis includes program plans and schedules, risk assessments and estimated costs.

2.0 DESIGN CRITERIA

The lift/cruise fan propulsion shall be designed to meet the requirements of a Navy multimission type of aircraft. Tentative design requirements have been defined based on applicable engine design specifications, General Electric lift fan experience and the results of concurrent aircraft studies conducted by McDonnell Douglas and Rockwell International, LAAD.

2.1 Fan Design Point

2.1.1 Gas Generators

The lift/cruise fan will operate with the exhaust gas provided by a J97 engine operating as the gas generator. Two J97 engines were considered:

J97-GE-100: an existing engine system which has completed a 60 hour PFRT program in 1969, after 1300 hours of accumulated development testing.

Growth J97: a derivative of the J97-GE-100 engine designed to produce 20 percent more exhaust gas power than the existing engine.

The aircraft study programs have identified two particular combinations of engine/fans which were the most promising arrangements; three fans with two Growth J97 gas generators and two fans with two J97-GE-100 gas generators. The three fans on two gas generator configuration is shown schematically in Figure 2.1. This arrangement employs two fans and two gas generators during cruise. A third fan is utilized during V/STOL operation, with the gas flow from the two engines divided equally among the three fans. The condition for maximum power to the fans is during cruise operation and, thus establishes the design operating point for the system.

The two-on-two configuration is shown in Figure 2.2. Two gas generators are interconnected to supply gas power to the two lift fans during both cruise and V/STOL operation. For this arrangement, the maximum power to a fan occurs during the flow transfer case in V/STOL operation. The maximum power transfer operating point, as defined in Section 3.0, establishes the gas conditions for the fan design point.

The gas conditions for these two operating modes are given in Table 2.1 for uninstalled engine systems. The flow for the two-on-two arrangement includes the flow transfer between pairs of engines and the fan scroll inlet pressure includes an estimated three percent pressure loss of the interconnect

ducting. Comparing the total available gas power for the two conditions, the difference in power is 5.8 percent, which is equal to the change of density between the standard and hot day conditions as required for equal fan speed operation, hot and standard day. With the exception of minor changes in turbine design, the fan designed for either configuration would be identical. The difference in turbine designs occurs primarily in the fan turbine throat area. The two-on-two configuration using the -100 engine requires a turbine area 18 percent smaller than the growth system. The growth configuration design is the more difficult task, because it contains a larger turbine annulus and thus represents a larger tip load on the rotor in addition to having larger diameter frames. Conversion of the fan designed for growth could be accomplished through simple blank-off of part of the turbine arc or reorientation of the turbine nozzles to provide the required area. In either case, it is simpler to decrease than to increase the area. For this reason, the three-on-two growth system was selected for the design configuration for this study.

At the initiation of the fan design point studies, the Growth J97 engine cycle had not been firmly defined. Tentative gas conditions to the fan scroll were selected to initiate the design studies. These gas conditions are listed in Table 2.2 and agree with the selected growth cycle power within two percent. The fan design point selected for the mechanical design studies was based on these initial gas conditions. For continuity of design activities, the fan was not redefined to match the new gas conditions. However, the performance and cycle data does reflect the increased power capability.

2.1.2 Fan Design Point

The fan design point was selected by a process of optimization of fan thrust for a range of design variables including fan diameter, inlet specific flow, fan and turbine exit Mach numbers and fan tip speed. For each set of design assumptions, a particular combination of fan and turbine exit pressure ratio was determined to produce maximum fan system thrust.

A base point fan design was selected having 1.50 meter (59.0 inch) tip diameter and the design parameters as given in Table 2.3. Figure 2.3 shows the effects of fan pressure on design thrust for these assumptions, and indicates a maximum thrust level at a fan pressure ratio of 1.31. The significant design variables for this configuration are given in Table 2.4.

The second step in the design process was to systematically change each of the remaining design variables to establish changes in fan thrust performance. The results of these studies are summarized in Table 2.5 and show that fan tip speed, specific flow and fan diameter are the most significant design parameters. For the final selected design, the fan inlet

specific flow was increased from 195 to 203 kg/sec-meter^2 (40 to 41.5 lb/sec-ft^2) as a reasonable technology level for a fan with a relatively long cruise type of inlet geometry. The aircraft studies had identified a fan diameter of 1.50 to 1.52 meters (59 to 60 inches) as being the optimum size. The selected base point fan diameter of 1.50 meters (59 inches) was retained. The design parameters for this selected design are given in Table 2.6 and indicate a design point thrust of 74.46 kN (16,740 lbs) at a fan pressure ratio of 1.319. These fan design parameters are based on the original estimated Growth J97 cycle. As discussed previously, the final cycle yielded about a two percent higher gas power. This increased power was used for performance calculations by adjustment to the turbine area at the fan/turbine mixing location with a slight increase in design point thrust.

2.2 Mechanical Design Criteria

The Mechanical Design Criteria established for the lift/cruise fan propulsion system were derived based on:

MIL-E-5007D, Engine Design Specification, Reference 2

FAR 33-1B, FAA Ingestion Requirements, Reference 3

General Electric Experience in Military and Commercial Applications

The significant design criteria included in these references which have a direct influence on the fan design are described in the following paragraphs.

2.2.1 Maneuver Loading

The maneuver loading criteria was based on MIL-E-5007D, with revisions to reflect deletion of catapult take-off and arrested landing requirement. The revised loading criteria are given in Figure 2.4. The criteria were further revised by limiting the maximum gyroscopic moment to 2.0 radians per second to reflect the maneuver capability of a typical V/STOL aircraft system.

2.2.2 Foreign Object Ingestion

The lift/cruise fan will contain no provisions for anti-icing because of the absence of a front frame and inlet guide vanes. The fan will be capable of ingesting ice formations which may develop on the rotating fan bulletnose.

The bird ingestion objectives were established as follows:

Safe shutdown after ingestion of a 1 kg (2.2 lb) bird

Less than 25 percent loss in power after ingestion of 16 50-to-100 gram (2 to 4 ounce) birds

2.2.3 Containment

Containment in the lift/cruise fan configuration is limited to a turbine blade failure. Containment of a complete fan rotor blade would require substantial structure with increased weight. Local protective shielding should be considered at critical areas of the aircraft.

2.2.4 Blade-Out

The fan assembly will be capable of a safe shutdown following failure of a fan blade. The fan frames and bearings shall be designed to accept the forces due to rotor unbalance following the failure for 30 seconds of operation. Frame deformations and minor failures are acceptable providing the rotating components are constrained until shutdown.

2.2.5 Design Life

The design life criteria for the lift/cruise fan is given in Table 2.7 for the typical Antisubmarine Warfare Mission (ASW) as defined in Section 2.3. During the V/STOL take-off and landing portions of the mission, the fan system was designed to the control duty cycle as shown in Figure 2.5. The frequency for the control applications was assumed to be at a rate of 0.5 to 1.0 cycles per second. The design levels of control power were based on the maximum short-time control power setting, as defined later, or 25 percent of the operating fan thrust, whichever is limiting.

2.2.6 Flight Envelope

The operating envelope for the lift/cruise fan is shown in Figure 2.6. Operation at high speed-low altitude required for Combat (Strike) Search and Rescue (CSAR) mission was considered in the studies, but at reduced fan life.

2.2.7 Maintainability

The lift/cruise fan system was designed to include numerous low cost maintenance features. The significant design criteria used in this area are as follows:

On-wing removal of fan blades and turbine carrier assemblies

Removal of disk, bearing and sump as a complete sub-assembly with the fan installed in the aircraft

Easily-separable fan sub-assemblies such as scroll, frame, rotor and sump

Field balance capability without major fan rotor disassembly

Conventional materials

2.2.8 Installation

The lift/cruise fan is capable of installation as either a cruise fan or a lift fan without significant configuration changes. The mounting system employs a three-point determinant arrangement.

The fan lubrication and cooling systems are designed to be self-sufficient without relying on the gas generator systems. This feature is highly desirable for engine-out operation when two or more fans are operating with a single gas generator. Lack of this feature would require interconnect of the engine lubrication and cooling systems.

The fan systems also include the option for mounting aircraft accessories, hydraulic pumps and generators, in the fan exhaust tailcone. A direct drive is provided on the fan shaft for supplying up to 111.8 kw (150 hp) to the accessory package. Figure 2.7 shows a typical accessory package considered in the design studies.

2.3 Missions

The applicable aircraft studies were required to consider five representative missions as listed below:

Anti-Submarine Warfare (ASW)

Surveillance (SURV)

Surface Attack (SA)

Combat (Strike), Search and Rescue (CSAR)

Vertical On-Board Delivery (VOD)

The missions as defined for the aircraft studies are presented in Figure 2.8. The ASW mission was selected as the design mission to

establish the duty cycle for life analysis of the lift/cruise fan. Two of the missions, SURV and VOD, are less severe with regard to propulsion life while the SA and CSAR missions are more severe. The life of the lift/cruise fan must be adjusted to reflect the severity of the SA and CSAR missions. A considerably shorter fan life will exist for repeated CSAR missions because of the high power settings required for the mid-mission low altitude dash and hover segments.

The mission flight conditions and power requirements were established during the related aircraft studies and are summarized in Table 2.8 for a typical ASW mission. This mission provides the basis for fan life analysis not established by low cycle fatigue.

3.0 ENGINE STUDIES

The gas generator for driving a turbotip fan is required to provide sufficient power for a level of VTO lift in excess of the aircraft gross weight, to exhibit low specific fuel consumption and to meet the requirements and limits of the fan turbine system. Studies of multimission aircraft have identified a gross weight requirement of between 12,500 and 14,500 kg (28,000 and 32,000 pounds). Figure 3.1 compares aircraft gross weight with the gas generator power requirements for a two, three or four engine aircraft. For the range of aircraft weights of interest, the gas generator size is about 8,202 kw (11,000 hp) to 13,049 kw (17,500 hp) respectively, for a three or two engine system. Considering maintenance and engine costs, the four engine system would be prohibitive for the relatively small aircraft size. For this study, the engine size for a two gas generator system was selected with a gas power output of about 12,304 kw (16,500 hp). For a three gas generator system, the existing YJ97-GE-100 engine provides adequate gas power.

For reasonable turbine efficiency with the lightest weight in the single stage tip turbine, the turbine pressure ratio should not exceed about 4.0. At sea level static operation, this establishes an engine discharge pressure limit of about 400 kN/m^2 (58 psia). Engine discharge pressures in excess of this level would exhibit poorer turbine efficiency for the turbine tangential speeds as established by the fan system. Also, in the interest of light weight and low cost, the scroll (engine discharge) temperature should not exceed a maximum steady state engine discharge temperature of 1030 to 1060°K (1850 to 1900°R).

In addition to the above requirements, the gas generator should employ high pressure ratio compressors and high turbine inlet temperature for minimum specific fuel consumption. For simplicity and low weight, a single spool axial flow compressor is also desirable. Based on available and projected compressor aerodynamic technology, this establishes a maximum compressor pressure ratio of about 18.

3.1 J97 Engine

The previous discussion has established the following desirable features of a gas generator for the turbotip fan system in the multimission aircraft:

Gas power of 12,304 kw (16,500 hp)

Maximum discharge pressure of 400 kN/m^2 (58 psia)

Maximum discharge temperature of 1030 to 1060°K (1850 to 1900°R)

Maximum single spool compressor pressure ratio of about 18

Maximum turbine inlet temperature in consonance with the above engine exit conditions

Figure 3.2 presents engine parametric data, discharge pressure and specific gas power, as a function of design values of turbine inlet temperature and compressor pressure ratio. At a discharge temperature of 1020°K (1836°R), the optimum gas generator would have a compressor pressure ratio of between 17 and 20 with a moderate technology level of turbine inlet temperature of 1390 to 1420°K (2500 to 2550°R). For this gas generator, the discharge specific power is about 335 kW-sec/kg (200 hp-sec/lb). Engine airflow required would then be about 38.5 kg/sec (85 lb/sec).

A survey was made to determine what General Electric engines, or derivatives thereof, would meet the requirements for the turbotip fan system. The J97 with a 20 percent gas horsepower increase met the size requirements. A study to define the changes required for this growth was performed and is discussed in the following section. One interesting feature of the existing J97-GE-100 engine is that for a three engine aircraft, the match is quite good, with a small amount of excess power. For the technology aircraft being considered, a three engine system is almost mandatory because of the engine-out requirements.

The J97-GE-100 is an existing engine which is defined in Reference 4 and was developed through PFRT. The -100 configuration was never placed in production, but a derivative YJ97-GE-3 engine was placed in limited production with about 30 engines built. Most of these engines are still in existence with relatively low operating times.

The availability of these engines, in adequate numbers, is beneficial to a low cost technology aircraft program. The changes required for conversion from the -3 to the -100 configuration are as follows:

Increase main fuel pump capacity to a higher flow rate

Removal of the engine exhaust gas temperature cutback control system

Change of seal pressurization from the 14th stage in the compressor for the -3 configuration to the 8th stage for the -100 configuration

Modification of the No. 1 bearing carbon seal to increase clearance around the oil jets

Replacement of the No. 2 bearing with a modified bearing

The first three items can be accomplished through external modifications of the engine. The last two items require an engine teardown, but are not essential for engines used exclusively for ground testing. Thus, a minimum effort would involve only external modifications for ground test engines with both internal and external conversion of those engines required for flight tests.

3.2 Growth Studies

The approximate power required for a multimission aircraft is 12,304 kw (16,500 hp). A study was performed to define the cycle and configuration changes required to provide this level of growth for a derivative of the YJ97-GE-100 engine. The growth can be accomplished using combinations of increased airflow, rotational speed and turbine inlet temperature.

Figure 3.3 gives the variation of engine ideal power with combinations of increased airflow and turbine inlet temperature. The required engine rotational speed change is also presented. The least risk growth condition was selected at a flow increase of 16 percent and a turbine inlet temperature of 1358°K (2445°R). A small increase of compressor speed is associated with this selection. Other selected growth conditions include no change of turbine blade cooling and no change of turbine efficiency. Table 3.1 compares the cycle parameters of this growth configuration with the original YJ97-GE-100 design point. A comparison of the ideal gas power shows a 22 percent growth over the original cycle. The design point power for the selected growth J97 engine is 11,707 kw (15,700 hp) as compared to an aircraft requirement of 12,304 kw (16,500 hp). Use of short-time VTO engine ratings are more than adequate to increase the gas power to the required levels.

The engine changes required to achieve this level of growth include:

Design airflow increase of 16 percent

Turbine inlet temperature increase of 40°K (70°R)

Compressor speed increase of four percent

3.2.1 Compressor

With the growth configuration established, studies were performed to evaluate the effects of these changes on engine configuration and life. A

study was performed to define the compressor flowpath and blading changes required to produce the 16 percent increased airflow. The revised compressor flowpath is shown in Figure 3.4 and identifies an increase of 5.1 cm (2.0 inches) in length and 3.8 cm (1.5 inches) in rotor inlet diameter. All blading and flowpath changes occur forward of the Stage 5 rotor inlet. Blade chords have been lengthened and the flowpath expanded primarily at the rotor tip.

The aerodynamic performance of the revised compressor was estimated as follows for design, 100 percent, speed operation.

Overall pressure ratio, 16.7

Inlet airflow, 36.30 kg/sec (80.03 lb/sec)

Rotational speed, 14,231 rpm

Efficiency, 83.6 percent

Stall Margin, 22.15 percent

The mechanical changes anticipated in the growth compressor include a new compressor case for the increased length and diameter, and new blading for the first four stages. The air design retains the blade geometry through the remainder of the compressor. All stator vanes will be changed from titanium to nickle base alloy, Inco 718. Some of the rear stage rotor blades may require a material change.

3.2.2 Turbine

The two stage turbine of the growth engine will retain essentially the same aerodynamic design as that of the base engine. Some minor restaggering of blades and stators will be made to match the new cycle flow function and to yield low levels of turbine exit swirl. Turbine cooling will remain unchanged. Nozzle film cooling and first stage convection cooling schemes will be retained. The second stage blades will remain uncooled. The major change in the turbine blades will be material substitution of René 125 in place of the Rene 100 used in the YJ97-GE-100 and -3 engines.

Life analysis of the turbine blades is summarized in Figure 3.5. The analysis was performed at an engine speed of 103 percent, which is the one minute take-off rating. This and other ratings will be described in the engine performance section. The turbine inlet temperature at this operating point is 1467°K (2640°R). At this condition, limiting life of the Stage 1 blades is 125 hours. Based on the reference ASW mission cycle given in

Table 2.8, the fraction of the mission at power settings above 95 percent is about 9.1 percent of the total mission time. Assuming all high power settings are equivalent in terms of material damage, the total service life of the Stage 1 blades is 1370 hours. This design life is comparable with the criteria established for the turbotip fan system. Some minor changes of blade design and cooling could be used to increase the life to approximately 3000 hours.

An analysis of temperature-speed limits during the maximum control excursions and engine emergency operation was performed. Figure 3.6 gives the maximum turbine inlet temperature limits for engine speeds in the range of interest. These limits will be compared with the short-time ratings during the discussion of engine performance.

Other design changes anticipated in the turbine include changes of the stator from brazed-fabricated to cast construction. The disk systems would also be redesigned to reflect the change of blade stagger and the increased centrifugal load associated with the redefined design speed.

3.2.3 Weights

The growth engine would involve redesign from the current engine and would represent an improvement over the current engine. Table 3.2 gives the estimated weights of the growth engine, with the comparable J97-GE-100 weight. The growth engine system yields a 20 percent increase in power for about a 13 percent increase in weight. On a thrust-to-weight basis, this is about a one-for-one trade.

3.3 Water Injection

Water injection in turbojet engines is a well-known method of increasing thrust during the short period of aircraft take-off. In V/STOL operation, increases in thrust associated with short-time take-off ratings and water injection yield a significant improvement in the payload or fuel-carrying capability of the aircraft. A study was performed to define a water injection system for the J97 engine and to determine the thrust gains associated with the use of water injection.

There are presently two locations considered for water injection, compressor inlet and combustor inlet. Compressor inlet water injection is the most effective method because the work of compression is reduced during vaporization of the water. Performance improvements associated with this method are unpredictable and must usually be determined during actual engine testing. Compressor inlet water injection also has the additional problem of changing compressor clearances due to the quenching action of the water.

Combustor water injection is the easier method to develop and predict. This method was selected for the engine studies to determine the advantages of such a system. A water flow rate of four percent compressor flow was established for the performance studies based on a reasonable compromise between improved performance and reduced compressor stall margin.

3.3.1 System Description

The system selected for the J97 engine consists of the components identified in Figure 3.7. Components installed on the engine include:

12 spraybars

Water manifold

Mounting pads on compressor rear frame

Pressurization valves

Components remote from the engine are:

Water storage tank

Feed pump

Water cooler

Electrically-actuated control valve

Connecting plumbing

The spraybars are similar in design to the spraybars used to deliver fuel to afterburners. Each spraybar spans the compressor discharge flowpath and contains a pressurization valve which prohibits external flow leakage from the compressor or water leakage into the engine except when the water pressure exceeds a predetermined pressure level of about 440 kN/m^2 (140 lb/in^2). During the operating conditions when water injection is intended to be used or anticipated as an emergency measure, the feed pump will be operating continuously. The bypass control valve is open and the bypass flow prevents build-up of manifold pressure. A small amount of water flow passes through the manifold for cooling and priming. A cooler is inserted in the cooling flow return to remove the heat gain which occurred due to the hot compressor discharge environment. The pressurization valve does not permit water to flow into the engine.

When water injection is commanded, the bypass valve is closed and the manifold pressure increases almost instantaneously producing water injection into the combustor. Water flow continues until the supply is consumed or the bypass valve is again activated. This system provides a nearly constant flow rate, independent of the engine power setting. Feed pump pressure and spraybar orifice size are the prime factors which establish the flow quantity.

3.3.2 Weights

The weights of the engine-mounted components of the water injection system were estimated to represent an added weight of 9.5 kg (21 lbs) per engine.

3.4 Performance

The following discussion covers the performance of the basic J97 gas generator, particularly the definition of engine short-time ratings and effects of water injection. System performance, fan and engine, will be discussed in Section 5.4.

The use of engine short-time ratings is an effective way to increase V/STOL payload, range and time-on-station at small increases of weight or slight reductions of life of the propulsion components. Three rating conditions have been defined:

VTO - A vertical take-off power rating which has been assumed to occur not longer than one minute per aircraft mission

MAX - A maximum demand type control power setting which is required for not longer than three seconds per application

EMERG - An emergency power setting which is established to provide increased power during occurrences such as engine-out operation. Following usage of this power setting, not to exceed one minute, the engine must be inspected or removed for evaluation of hot parts

The MAX and VTO power settings both occur at the same engine speed. At VTO, the engine operation is established by the nominal trimmed fan turbine area. To achieve the MAX power setting, flow transfer between pairs of engines is required to raise the engine operating line to the limiting level. This concept of flow transfer between pairs of interconnected engines is a concept commonly referred to as ETAC. In defining the engine operation at the MAX rating point, it was assumed that the flow transfer was through a

no loss duct. This assumption has only small effects on performance because of the small levels of flow transfer, about seven percent. Short-time rating limits for the two J97 engine cycles are given in Table 3.3.

Performance of the Growth and YJ97-GE-100 engines was determined at the three rating conditions, both with and without combustor water injection. The engine discharge gas conditions at these rating points is given in Tables 3.5 and 3.6. Similar performance data, using an assumed set of installation assumptions, given in Table 3.4, is also given in Tables 3.7 and 3.8. Additional engine performance data will be included with the system performance presented in Section 5.4 of this report and in Reference 5.

4.0 FAN DESIGN STUDIES

As a prelude to the selection of a lift/cruise fan preliminary design configuration, numerous studies were performed to determine the most suitable features which would meet the design criteria, yield best performance at the lightest weight and produce a low cost configuration attractive to the aircraft installations. At the onset of the study, certain desirable design features were initially established. These include:

Structural Rear Frame - for application as a cruise fan, a front frame fan configuration would require strut anti-icing to meet the design criteria. Previous lift fans employed front frame configurations for minimum installation thickness and support of the shallow inlet bellmouth. These are not requirements for a lift/cruise fan system and are consistent with current large turbofan technology. Other design studies, Reference 6, had shown that a structural rear frame fan is the lightest configuration. A structural rear frame was successfully demonstrated during tests of the 2.03 meter (80 inch) LCF380 lift/cruise fan.

Conventional Cruise Inlet - the airframe studies use the fans installed as either a lift/cruise fan or pure lift fan in the nose of the aircraft. Both installations employ deep straight inlets.

Lubricated Bearings - conventional lubricated bearings are required to meet the life requirements. Grease packed bearings used in lift only fans are the lightest system but were not intended for continuous cruise duty cycles. The fan lubrication systems must be self-contained for each fan to eliminate the requirement of interconnect for an engine driven lube system.

Confluent Flow Exhaust - due to the thrust vectoring requirements of the lift/cruise fan, all fan and turbine exhaust thrust must be deflected downward during V/STOL operation. Thrust vectoring can be accomplished more efficiently when the two flows are mixed prior to entering the thrust deflector.

The design features which were considered during the studies were:

Aerodynamics
- Fan Stall Margin
- Shrouded or Unshrouded Turbine

Scroll
- Flowpath Cross-Section Shape

Mounting
Fan Inlet Sealing Methods

Rotor
Number of Fan and Turbine Blades
Midspan Shroud Requirements
Conventional or Twin Web Disk
Blade to Turbine Carrier Attachment
Shrouded or Unshrouded Turbine Blades

Vane/Frame
Number of Stator Vanes, Structural and Non-Structural
Vane Lean
Structural Cooling Methods

4.1 Aerodynamics

The aerodynamic design parameters for the LCF459 fan were established during the initial fan design selection studies. Design point airflow and pressure ratio were established to yield maximum static thrust for a fan tip diameter of 1.50 meters (59 inches). The initial design selection studies used one dimensional analysis to determine the flow properties and performance of the fan and turbine. The next step of the design process is to establish the aerodynamic design parameters using two dimensional axisymmetric analytical procedures. Normal fan performance indicators such as blade loading and fan stall margin were determined and compared with existing design criteria and previous General Electric experience of similar turbomachinery systems. The procedures involve iterations between the mechanical and aerodynamic designs to produce a viable fan configuration.

Similar design iterations were performed for the turbine considering items such as number of blades, levels of turbine reaction and the requirements for a tip shrouded turbine. The following discussion presents some of the highlights of these studies.

4.1.1 Fan Stall Margin

Estimates of the stall margin potential of the initial fan aerodynamic design were on the order of 12 to 13 percent at design point. This design featured a discharge Mach number of 0.5, 56 rotor blades, 30 stator vanes and a cylindrical tip flowpath contour. This level of stall margin is probably inadequate to sustain the operating environment which would include exit static pressure distortion due to the exhaust deflector, conventional levels of inlet distortion and hot gas reingestion. The largest levels of these distortions will most likely occur during V/STOL operation. A design study was undertaken to determine the most desirable means of increasing the stall margin potential using a procedure based on a correlation of the known static

pressure rise capability of tested turbomachinery. Consideration was given in the studies to determine the effects of blade and vane aspect ratios, blade and vane numbers, flowpath contour and exit Mach number.

Reductions in blade number, vane number and aspect ratios increased the estimated stall margin, but the increases of rotor moment of inertia and fan weight limited the benefit available. The resulting fan design was selected to have 52 rotor blades and 27 stator vanes, based on the mechanical design limitations. Altering the fan flowpath to a rotor tip slope of 10 degrees was also used to increase the estimated stall margin in the selected design. The largest improvement in stall margin was obtained through increases of the fan discharge Mach number. A change in Mach number from 0.50 to 0.55 produced a 3.4 percent improvement in stall margin potential. Incorporating these features, 10 degrees tip slope and an exit Mach number of 0.55, yields a fan with a predicted stall margin of 18 percent at the design point. In the V/STOL operating mode the fan nominal speed is about 8 to 10 percent below design speed. At this condition, an increase in fan exit area will be used to produce increases in both fan thrust and stall margin. Figure 4.1 shows the stall margin for maximum sea level static net thrust. A stall margin of 25 percent was selected to define the fan operating characteristics during V/STOL operation.

4.1.2 Shrouded/Unshrouded Turbine

Early in the design, it was recognized that for turbines, with high radius ratios and large tip diameters, tip clearance could have a very important effect on performance. The question also arose as to whether or not tip shrouds should be used on the turbine buckets. A design study was therefore made to determine the sensitivity of turbine performance to tip clearance both with and without bucket tip shrouds.

Figure 4.2 is a correlation of turbine efficiency and tip clearance based on a number of unshrouded test turbines. The data is plotted against the bucket tip value of "$\sin\beta_1/\sin\beta_2$" which is an indication of tip reaction. All important operating points for the LCF459 turbine lie within a range of 0.95 to 1.05. Using this correlation, Figure 4.3 was obtained showing the design point efficiency decrement with tip clearance changes for the LCF459 turbine both with and without tip shrouds. The efficiency loss for a shrouded turbine is simply calculated based on the leakage over the shroud tip seal tooth, assuming a 1/8 inch open honeycomb tip seal. This comparison shows that the desirability of a tip shroud increases rapidly, from the performance point of view, as tip clearances become larger. At very small tip clearances an unshrouded turbine may be preferred. Thus, the desirability of a tip shroud depends strongly upon the clearances to be expected. Curves similar to Figure 4.3 can also be constructed for other

turbine operating points and will vary somewhat due to level of turbine tip reaction. Table 4.1 shows the tip clearances expected at several important operating points with the corresponding differences in turbine efficiency, and indicates that the loiter point is the most critical and the governing factor in the selection of a tip shrouded turbine for this design. A discussion of the analysis performed to determine these turbine operating clearances is presented in Section 5.2.

4.1.3 Fan Aero Design

The significant design parameters which describe the fan aero design are presented in Table 4.2. Selection of the fan airflow and pressure ratio was dictated basically by the installation thrust requirements and the available gas generator power. A maximum design tip speed of 343 m/sec (1125 ft/sec) and a minimum hub radius ratio of about 0.40 were selected primarily on the basis of rotor mechanical design considerations. A specific airflow of 199.2 Kg/s-m^2 (40.8 lb/sec-ft^2) was selected to insure good cruise efficiency with a minimum fan frontal area. The numbers of blades and vanes were selected based on the mechanical design requirements of the rotor and vane/frame, consistent with maximum stall margin. Other design parameters presented in Table 4.2 result from the selection of the above parameters.

The fan rotor is tip shrouded and incorporates a part-span shroud at 65 percent of the blade span. The leading edge of the tip shroud also serves as a single tooth seal restricting the flow of turbine cooling airflow into the fan tip region. The fan stator vanes are leaned 25 degrees at the hub as shown in Figure 4.4 for aerodynamic as well as mechanical reasons, to be discussed later. The aerodynamic purpose of the stator vane lean is to help turn the flow radially inward and thus relieve the low static pressure which occurs at the fan hub and the tendency of separation along the aft centerbody.

The fan stator vanes are of non-uniform thickness; every third vane being a thicker structural vane. These structural vanes have a maximum thickness-to-chord ratio of eight percent, while the intermediate, non-structural vanes are four percent thick. The fan exit total pressure profile is skewed as shown in Figure 4.5 to reduce fan hub loading.

Figures 4.6 through 4.15 present a number of fan aerodynamic design details. The calculation of the vector diagrams and fluid properties upon which these details are based was accomplished with the aid of the General Electric NEWCAFD computer program. This program numerically solves the axisymmetric differential equations of fluid flow along desired calculation lines within arbitrary axisymmetric boundaries. The analysis

considers flow with or without blade rows, non-uniform total pressure and temperature profiles and leaned or swept blade rows.

Figure 4.6 shows the fan flowpath and the calculated axisymmetric streamlines. Figures 4.7 and 4.8 show, respectively, contours of equal meridional Mach numbers and static pressures. For purposes of this analysis, the turbine exhaust flow streamline was assumed as the boundary for the fan flow in the exhaust duct. Figures 4.9 through 4.15 show radial distributions of a number of parameters of common interest. The abscissas on these plots are fan stream function which is the ratio of flow to total fan flow. Figure 4.16 relates the stream function to the blade edge radial stations.

Only one area of minor concern is evident on examining these results. Figure 4.12 shows the stator hub D factor to be high locally due to a low static pressure at the stator hub leading edge. This produces a predicted high stator hub loss coefficient as shown in Figure 4.11. Minor reshaping of the hub flowpath in a detail design will alleviate this problem.

Radial distributions of loss coefficient were estimated for the rotor and stator as a function of the local D factor, solidity, inlet relative Mach number, and exit air angle. Adders representative of end losses were applied at the inner and outer blade regions. The average fan adiabatic efficiency calculated using these loss coefficients was 0.882. Additional efficiency decrements were estimated for the part-span shroud and forward seal leakage as -0.014 and -0.018, respectively, with a resulting net fan efficiency of 0.850.

4.1.4 Turbine Aero Design

Table 4.3 presents a number of the basic turbine design point parameters. The inlet gas conditions, total pressure ratio and energy extraction are determined by the gas generator discharge gas conditions and the fan power requirements. The turbine exit Mach number is set at a relatively high value of 0.55 for minimum bucket length and to reduce the static pressure differences between the turbine and fan streams. The exhaust flow is diffused to a Mach number of about 0.45 before mixing with the fan discharge flow.

At design point, the turbine was selected to have a small amount of reaction, 10 percent at the hub and 20 percent at the tip. With this amount of reaction, the exit swirl angle is about 8.5 degrees and turbine outlet guide vanes are not needed to straighten the exhaust flow. At the cruise operating point, exit swirl angles and reaction levels are similar to the design point. At reduced power settings and full admission arc, such as the loiter operating

point, the reaction tends to decrease toward the impulse condition. Thus, incorporating some reaction at the turbine design point helps to prevent part speed turbine efficiency from dropping as rapidly as it would with an impulse design. Turbine reaction also tends to decrease with partial arc operation. At the nominal VTOL operating point with 240 degrees admission arc, the turbine hub reaction will operate near impulse. For positive reaction, bucket aerodynamic loading parameters (i.e. Zweiffel numbers) decrease, and thus lower bucket solidities are permitted, compared to impulse turbine. Lower bucket solidities represent lower rotor weights and inertias.

An accurate evaluation of turbine efficiency changes with reaction is difficult to obtain short of conduct of actual test programs. Based on previous test experience, an estimated two percent improvement of turbine efficiency may be attributed to the levels of reaction included in the selected design. The improvements are achieved primarily through reductions of turbine nozzle exit and bucket inlet Mach numbers. Similar or larger improvements in turbine efficiency can be expected during off-design operation of the turbine.

Aerodynamic loading of the turbine is modest with a pitch line stage work coefficient ($gJ\Delta H/2u_p^2$) of 0.83 and a pitch line stage velocity ratio (u_p/V_o) of 0.475. The turbine wheel speed was established by the fan rather than by turbine aerodynamic loading criteria.

Figure 4.17 shows the turbine hub and tip vector diagrams and Table 4.4 presents aerodynamic parameters at hub, pitch and tip locations. The calculations were made assuming free vortex simple radial equilibrium at each station.

A turbine base design point efficiency was estimated to be 0.88, not including tip leakage and partial admission losses which are accounted for separately. At the design point with a tip shroud and with 1.4 mm (0.055 in) clearance, Figure 4.3 shows an expected tip leakage loss of 2.0 percent in efficiency. At the design point, without partial admission losses, the efficiency is therefore 0.86. For full arc operation at other than design speed, performance was determined using an estimated turbine performance map, described in Section 5.5.

During partial arc operation, additional losses will occur because of the inactive bucket windage loss and the losses which occur at each end of the admission arc.

Dimensional analyses substantiated by test data, Reference 7, have shown that the power consumed by windage or pumping in the inactive buckets of a partial admission turbine can be represented by an equation of the form

$$P_{WL} = K_F \rho A (u_p/100)^3$$

where

P_{WL} = windage loss, kW

ρ = fluid density in inactive arc, kg/m^3

A = annulus area of inactive arc, m^2

u_p = mean peripheral bucket velocity, m/sec

K_F = a constant depending on the geometry of the bucket and its surrounding structure.

For performance estimates for the LCF459 turbine, a value of 34.0 was used for K_F based on the test results given in the reference. This value was increased slightly to allow for the extra windage of the tip shroud and bucket carrier. Using this value for K_F and the design values for A and u_p, we can write the following equation for windage loss for the LCF459 turbine:

$$P_{WL} = 479.5 \rho_{54} (1-F) (\%N/100)^3$$

where

ρ_{54} = turbine exit air density, kg/m^3

F = fraction of admission arc

%N = percent of design physical speed

Further partial admission losses occur at each end of the active admission arc due to inefficiencies and flow losses. These losses may be represented by an equation of the form

$$P_{EL} = K_E \rho A_B (\Delta H) W$$

where

P_{EL} = end loss, kW

A_B = projected bucket area (length x projected chord), m^2

ΔH = turbine energy extraction, J/g

W = turbine gas flow, kg/sec

This form of the equation is equivalent to saying that the end loss power is proportionate to the energy available in the flow which is swept into the inactive arc by the moving buckets. Although good test data on end losses in turbines are scarce, past tip turbine performance estimates have assumed a loss equal to 1.5 times the energy contained in the theoretical flow swept into the inactive arc and have shown good correlation with measured tip turbine performance.

Using the LCF459 design values, the end losses become:

$$P_{EL} = 0.6868\ \rho(\Delta H)\ (\%\ N/100)$$

Performance of the LCF459 during partial arc operation includes corrections of turbine performance using the mathematical representation for both the end and partial admission losses. Table 4.5 gives a listing of these estimated losses at selected fan operating conditions.

4.2 Scroll

4.2.1 Design Considerations

The primary function of the scroll is to efficiently distribute the engine discharge gas to the tip turbine. This requires a flow passage with approximately a constant velocity and a minimum of internal flow obstruction or blockages which would result in high pressure losses. A second design consideration is the alignment of the nozzle discharge with the tip turbine during operating conditions. The large diameter scroll undergoes significant radial thermal expansion compared to the short tip turbine annulus.

The forward fan seal is supported by the scroll structure and controls the leakage of turbine gas into the fan flowpath. The seal must be dimensionally stable and not influenced by the large relative radial thermal growth of the scroll compared to the fan. Excessive leakage will adversely effect the fan performance.

In some aircraft installations, an increase in the aircraft payload will occur for a low profile scroll design due to the decrease in nacelle weight and the reduction of the frontal area. The magnitude of the increased payload as a function of scroll height is dependent on the aircraft installation and the mission. A low scroll profile is a desirable design objective if it is provided without excessive increases of pressure losses, weight or cost.

4.2.2 Shape Studies

The design studies of the scroll considered two different scroll flowpath shapes. The most simple, lightweight scroll configuration uses circular cross-sections to form the full or 360 degree flowpath. For the design trade studies, it was assumed that the scroll was supplied through two inlets, one feeding 240 degrees of arc and the other feeding the remaining 120 degree arc. This inlet arrangement represents only one possible configuration of many which are strongly aircraft installation dependent. Alternate scroll inlet configurations were considered in the studies and are described in Section 5.4.

A second scroll configuration was established to provide a minimum fan system frontal area. This scroll incorporates three circular cross-sections blended together to form a multilobe flowpath. Reduction of frontal area using the multilobe scroll can be obtained at increases in cost, weight and pressure losses of the scroll. The following discussion presents a comparison of these two scroll shapes. Selection of a scroll shape for the final configuration was not required since its effects on the other fan components is very minor. The scroll configuration selection can be withheld until initiation of the detail design of the LCF459 fan.

The circular scroll configuration is shown schematically in Figure 4.18. The scroll is held in position by 36 pins welded into the scroll mounting flange as shown in Figure 4.19. The pins slide in radial slots in the forward fan casing flange. This allows the scroll to expand and contract radially during high temperature cyclic operations. The pins are also used to react the 42.25 kN (9500 lb) tangential thrust load on the scroll. The axial thrust load, 21.17 kN (4760 lb), on the scroll is resisted by a 360 degree retainer plate bolted to the forward fan casing flange. The retainer also provides a positive air seal against leakage into the surrounding aircraft cavity.

The forward fan seal is supported from the fan casing by 18 equally-spaced struts which pass through hollow turbine nozzle vanes and are bolted to the fan seal support ring. This allows the forward fan seal to ramain stationary and concentric as the scroll expands and contracts radially during operation. Cooling air is ducted from the fan exhaust into a plenum chamber surrounding the outer surface of the nozzle ring. The fan air flows through all of the 160 hollow nozzles into the inner plenum as shown schematically in Figure 4.19. The fan air then passes through the perforated outer seal into the cavity between the two seals and discharges into the fan inlet. The method of supplying this seal buffer air will be described in detail in Section 4.6. The forward seal support ring will operate at a fan discharge air temperature, except for the small amount of heat addition as the flow passes through the hollow nozzle passages.

The internal flow area of the circular scroll is designed for an inlet Mach number of 0.25. The flow area is linearly decreased to a minimum 15.3 cm (6 in) diameter section. This minimum cross-section is required to maintain a rigid structure throughout the remaining scroll circumference.

In the nozzle transition section, 80 hollow struts as shown in Figure 4.18 are brazed into the face sheets to carry the pressure hoop loads around the shell. The struts are oriented to minimize local bending so that the strut is essentially a tensile load-carrying member. The struts also include camber to aid in turning the flow into the fan turbine nozzles and thus yield a reduction of the overall pressure losses.

The multilobe scroll shown in Figure 4.20 is similar in construction to the circular scroll except for the geometry of the shell. The forward air seal, scroll mounting and turbine nozzle systems are identical. The primary advantage of the multilobe scroll is the reduced section height and projected frontal area. The multilobe scroll design employs tie rods at the junction of the intersecting cylinders to transfer the pressure hoop loads between opposite sides of the pressure vessel. The aerodynamically shaped tie rods are spaced on 2.5 cm (1.0 inch) centers at the two locations of intersecting scroll lobes. Each tie rod has a cross-sectional area of 0.078 sq cm (0.012 sq in) with a resulting maximum tensile stress of 172,000 kN/m^2 (25.0 ksi). This low stress level is established to provide for tie rod failures without sequential failures of the adjacent rods.

The results of the trade-off study between the circular and multilobe scroll are summarized in Table 4.6. The circular scroll showed significant improvements in all categories except in the projected fan frontal area. The 0.56 square meter (882 square inch) reduction in the projected frontal area of the multilobe scroll may prove significant in increasing the aircraft payload. However, the improvement in the aircraft payload was not evaluated since it is dependent on the aircraft configuration and its application and is beyond the scope of the current design study. Although the multilobe scroll has a better installed performance due to its smaller projected area, the circular scroll internal performance is higher due to the absence of tie rods. A tabulation of the estimated pressure losses of the two scroll configurations is given in Table 4.7.

Manufacturing costs of the circular scroll will be less than the multilobe scroll even though the same number of die-formed pieces are required since the circular scroll dies are less complicated and require less welding in joining the segments into a finished unit. The addition of tie rods would also increase the machining and joining costs for the multilobe scroll. The 5.9 kg (23 lb) weight disadvantage of the multilobe scroll is due to the added tie rods and local shell reinforcements at the junction of the intersecting cylinders.

4.2.3 Stress/Life Analysis

René 41 was selected as the scroll material since it is considered the most versatile high temperature alloy available. It is highly oxidation resistant to temperatures of 816°C (1500°F). René 41 can be inert-gas welded with or without filler material using arc or electron beam welding. The material properties can also be controlled through variations of heat treatment temperatures to provide the best balance between rupture and tensile properties. The 0.02 percent yield and rupture strength for the selected René 41 material are shown in Figure 4.21. These material properties were used in the scroll life analysis as described in the following paragraph.

The scroll life analysis was based on a 3000 hour life for the representative ASW mission. The scroll temperature, pressure, number of cycles per mission and stress are shown in Table 4.8. Approximately 98 percent of the scroll life is used up in the take-off and landing portions of the mission. Only 22.5 percent of the stress rupture life of the scroll is used during the 3000 hour life.

4.2.4 Defect Analysis

A scroll defect analysis was performed to establish the sensitivity of the scroll to manufacturing defects and survivability to foreign object damage or small arms fire. The results of this study are shown in Table 4.9 and show that the scroll could survive a 2.0 cm (0.8 inch) defect sustained during flight and still complete the mission. Similarly, if the defect occurred during the take-off maneuver, the maximum size limit is 1.5 cm (0.58 inch) to still enable the aircraft to complete the mission.

A life analysis of the scroll, with typical weld defects, was performed to determine the capability of meeting the 3000 mission cycle criteria. For a typical maximum allowable defect of 2.0 cm (0.8 inches), the scroll will be capable of sustaining 50,000 start-stop cycles which greatly exceeds the design criteria.

4.3 Rotor

4.3.1 Design Considerations

The rotor system was designed to meet the LCF459 requirements which include 6000 hours minimum life and 6000 mission cycles. The critical design objectives which have a direct influence on the rotor design are:

Bird strike capability

Time response (minimum inertia)

Blade-disk system stability margin

Torsional flutter stability

Design studies initiated early in the program showed that the combined bird strike criteria and response requirements established a rotor system containing between 52 and 56 titanium blades. A single mid-span shroud would also likely be required in addition to a tip shroud lock-up. This configuration was used as the starting point for the trade studies.

Other significant design criteria used in the studies were:

15 percent margin of blade-disk frequency over the 2/rev at 100 percent speed

Stresses less than 0.2 percent minimum yield strength

Stresses less than 10^7 cycles in stress range diagram

15 percent margin on blade natural frequencies over anticipated excitation sources

Burst speed greater than 122 percent design speed

Disk dovetail capable of restraining adjacent blades with one blade out

Single blade removal on-wing

Blade flutter shall not occur prior to fan stall

4.3.2 Blade Midspan Shrouds

Figure 4.22 shows the initial fan airfoil geometry generated for a 52 bladed rotor. Based on this geometry, an investigation was initiated to establish the number and location of fan blade midspan shrouds. Figure 4.23 relates the torsional reduced velocity, the blade airfoil stage weight and the number of rotor blades for a non-midspan shrouded rotor and a rotor with midspan shrouds. A low torsional reduced velocity parameter is required to insure a stable, flutter-free blade configuration. The trends indicate that for a given reduced velocity parameter a midspan shrouded stage represents a significant weight savings over the non-shrouded stage. Effects of the spanwise location of the midspan are also shown. A midspan shrouded blade provides comparatively better bird strike resistance and a higher blade-disk system frequency. The lighter weight of the midspan shrouded rotor stage will also exhibit lower rotor inertia as required for low thrust time constants.

From a mechanical design objective standpoint, the midspan shrouded blade design is thus superior to a non-shrouded design. Figure 4.24 shows a midspan shroud sized for the 65 percent span height location on a 52 bladed fan rotor.

Based on the conclusions derived from this analysis, the blade configuration for the remainder of the studies will include a single midspan shroud, an integral tip shroud and a single hook dovetail for blade attachment. The tip shroud defines the fan outer flowpath while providing a seal against the hot gas leakage into the fan stream. The inner flowpath is formed by integral platforms on the blade. The use of two forward buffer seals and cooling air in the blade-turbine attachment region restricts the heat flow and reduces the blade shroud temperature to permit the use of titanium rather than steel fan blades. The material selected for the blade was titanium (Ti 17) which offers the best strength margins at elevated temperatures of any of the titanium alloys. Figure 4.25 compares the strengths of several titanium alloys, and shows that the Ti 17 material is superior at temperatures above 260°C (500°F).

4.3.3 Disk

A comparative study of the two disk configurations shown in Figure 4.26 was made to determine their compatability with a 52 or 56 bladed fan. The limiting design consideration for comparison of the two designs was the first two diameter coupled blade-disk frequency margin over the 2/rev excitation line. Results of the study are shown in Figures 4.27 through 4.31 and are summarized in Table 4.10. The conventional disk can provide the same frequency margin as the twin-web (hollow) disk but with a lighter weight design. It can also be manufactured at a lower cost with fewer processes and represents a lower risk to the program.

Figure 4.27 illustrates comparative disk effective stresses for designs which are equal weight. This data shows that the conventional disk design has lower local stresses than the twin-web configuration and consequently could produce a lighter weight design from an equivalent stress and life design standpoint. Weight reduction efforts in the rotor area resulted in a final configuration as shown in Figure 4.28. The disk and bearing shaft are Ti 6-4 material inertia welded to provide the lightest weight assembly.

This disk meanline stress distribution is shown in Figure 4.29. The disk dovetail fatigue diagram is shown in Figure 4.30. A comparison with the blade dovetail fatigue diagram reveals that the disk dovetail has more stress margin than the blade dovetail and therefore satisfies the criteria that the disk dovetail be stronger than the blade dovetail which should be stronger than the airfoil.

The blade-disk system frequency curves presented in Figure 4.31 were generated based on a rotor configuration utilizing a structural spinner and a blade midspan location of 65 percent span height. The concept of a structural spinner was initially demonstrated on the CF6-50 engine. The concept employs a rotating fan inlet spinner which is bolted directly to the outer rim of the fan stage disk. The combination of disk and spinner provides a unified structure which exhibits a significant stiffness increase above the disk alone stiffness. Increases in blade root retention stiffness produce increases of the blade-disk vibratory mode frequency and thus increased margin over the potential two-per-revolution excitation. With an initial objective for the first two diameter blade-disk frequency margin of 15 percent at 100 percent speed rpm, and a minimum allowable of 10 percent, some improvement was required for the initial 52 bladed rotor configuration with a conventional disk. A study was made to determine the effect of the midspan shroud location on the margin of the first flex frequency over 2/rev. Figure 4.32 illustrates that the blade first flex rigid rim (no disk effect) margin must be 30 percent for a 15 percent margin with a conventional disk. The data also show the general improvement of the first flex margin as the midspan height is lowered. This method of margin increase can be achieved without any weight penalty, but is limited to a height band since an effective midspan design becomes pitch limited due to interlock crushing stress as the midspan location is lowered.

The requirement of the blade design for this lift/cruise fan to satisfy frequency and weight criteria while meeting bird strike requirements is best accomplished with a blade-disk system utilizing a conventional disk design.

4.3.4 Blade Thickness Distribution

The limiting criteria for theLCF459 fan blade design was the coupled blade-disk first two wave frequency margin over the 2/rev excitation at 100 percent speed. A study of a blade geometry change to improve the first two wave blade-disk frequency margin over 2/rev was conducted with the results shown in Figure 4.33. The study showed that a change in the blade thickness distribution from the original or base configuration effectively increases the percent margin over 2/rev by approximately five percent without any weight penalty. The revised thickness distribution uses a distribution established by configuration 4 from root to pitch and configuration 1′ from pitch to tip. This revised blade geometry was used for stress and frequency analysis.

4.3.5 Bird Strike

The bird strike capability of the LCF459 fan blade design was

evaluated using an analytical procedure which employs a semi-empirical method based on an energy balance theory. The method has consistently been able to predict with good correlation the bird impact results for new fans. Empirical data from whirligig tests and actual bird impact incidents on previous fans in conjunction with analytical simulation of the incidents were used to determine a damage boundary. The capability of the LCF459 fan blade design was measured against this boundary.

The study included analysis of effects of blade number containing either single or double midspans. Midspan location was also treated as a variable in the analysis. The study yielded the following results:

A single midspan configuration was more favorable from a stress standpoint than the double midspan configuration.

For the comparative case with a single midspan at 65 percent height and 70 percent height, the deformation characteristics were about the same while the 65 percent height midspan location produced lower stress buildup at the shroud for various strike locations.

The greater the maximum thickness the better the bird strike capability.

The study also included variations of bird weights, bird axial speed relative to the inlet and strike locations to determine the critical strike location for each blade configuration. The critical strike location of a blade configuration is the location on the blade which, when struck, incurs the greatest normal displacement. Figure 4.34 summarizes the results of the bird strike capability for a configuration employing a single midspan at 65 percent span.

The results show that for the LCF459 configuration with 52 Ti 17 blades a 1.0 kg (2.2 lb) bird strike could result in torn or missing pieces of the blade, while the 0.45 kg (1.0 lb) bird strike is marginal and the 113 gm (0.25 lb) bird strike should not tear the blade. These results are based on the predicted improvement with the high strength Ti 17 relative to the semi-empirical damage boundary based on Ti 6-4 and Ti 8-1-1 fan blade material. The improvement in bird strike capability is also identified for reduced numbers of blades.

Adjustments in the blade geometry during detail design phase will improve the bird strike capability of the blade by using the following techniques:

Generous blends to hard point locations, tip and midspan shrouds, to reduce stress concentrations.

Local thickness distribution changes to improve susceptible areas

of the blade.

Chordwise location of the shroud away from the leading edge so that chordwise plastic deformation can absorb some of the energy.

4.3.6 Turbine Blades

The initial concept for the turbine incorporated a non-shrouded blade with hollow turbine buckets integrally cast to the turbine carrier. The non-shrouded turbine rotor is desirable from a design standpoint in that it requires less cost to manufacture and provides a lighter weight configuration in an area where weight greatly affects the rotor inertia. Figure 4.35 shows the proposed bucket cross-section which would be integrally cast to the turbine carrier with the inside cavities and stiffeners formed by Electro-Chemical Machining (ECM). The integral casting process would eliminate any brazing operations. The turbine bucket and carrier material would be cast René 80. The tabulation also identifies the weight and rotor inertia changes for various combinations of rotor blades and number of turbine buckets per blade. With a turbine bucket aspect ratio limit of approximately 3.0 based on aerodynamic considerations, the maximum number of buckets allowed is seven per blade or 364 total for a 52 bladed rotor. Figure 4.36 shows the turbine stage weight savings as the number of buckets per blade is increased. Wall thickness for the buckets is 0.0635 - 0.0762 cm (0.025 - 0.030 inch) which is applicable to thin wall castings and will provide the required strength and a high level of FOD resistance.

Figure 4.37 shows the unshrouded bucket stress range and frequency-speed diagram. The material properties are for cast René 80 at 1033°K (1400°F) which corresponds to design point operating conditions. The turbine frequency-speed diagram shows no critical excitation in the 70 to 100 percent speed operating range.

Aero-mechanical studies performed to identify the effects of tip clearance on turbine performance showed appreciable performance improvements for a shrouded compared to an unshrouded turbine. As described above, the turbine contribution to the total rotor weight decreased as the number of turbine buckets was increased. Large numbers of turbine buckets also have the additional benefit that addition of turbine shrouds produce only small increases in rotor weight. The turbine configuration with seven turbine buckets per fan blade was modified to include a tip shroud. The shroud could either be cast integral with the turbine buckets or brazed on as a separate part.

Figure 4.38 shows the stress range diagram and frequency-speed curve for a shrouded turbine bucket design. The addition of the turbine rotor tip shroud will add approximately 1.36 kg (3.0 lbs) to the rotor weight

and 0.097 kg-m-sec^2 (0.7 lb-ft-sec^2) to the rotor inertia.

4.3.7 Tang Attachment

The initial concept for the turbine carrier attachment was the use of a dovetail arrangement with the male member similar to the fan blade root dovetail machined on the top of the blade tip shroud and the female member, or slot, broached through the turbine carrier. The intent was to position the dovetail form on the tip shroud along the blade outline to effectively transfer the centrifugal and torque load of the turbine to the fan blade without transition problems and resulting high local stress buildup. However, with the dovetail skewed at a steep angle relative to the axial direction, the blade tip dovetail and turbine carrier disk post develop higher corner stresses than would occur with an axially-oriented dovetail. The skewed dovetail also added difficulty in removal of single fan blades without complete fan disassembly. As the number of turbine blades per fan blade is increased, the problems associated with the skewed dovetail became more difficult as the space between turbine blades becomes smaller. An axial turbine dovetail slot was therefore considered as an alternate to ease the problem. Figure 4.39 illustrates this configuration.

A dovetail form on the tip shroud similar to the fan blade root form could satisfactorily meet the design requirements since both the centrifugal load and length at the tip dovetail are approximately 1/3 of that at the blade root dovetail. The turbine drive loads would be taken out across the dovetail contact surface with minimal wear problems. The key to the dovetail arrangement is support of the disk post sections at the sides of the broached slot to keep the slot from spreading open and inducing high bending stresses in the post sections. The figure shows channels running axially through the carrier at the base which would fit against support ribs on the blade tip shroud to react against the post bending. The posts are also supported at the forward and aft ends of the carrier by the faces of the carrier box and at the center by a stiffener web as illustrated. The dovetail arrangement would require an axial retention system for the carrier as well as sufficient axial clearances for sliding disengagement to allow on-wing turbine sector removal.

Changing of the carrier dovetail from a skewed to an axial configuration decreased the advantages of this type of design. For a skewed dovetail, the transition region between the dovetail and fan blade airfoil section could be accomplished easily because the dovetail and blade are approximately aligned. For the axial dovetail configuration, a transition region is required to distribute the loads efficiently into the fan blade tip. This configuration would not be too much different than that required for the bolted tang system used in most of the previous turbotip fan systems.

The bolted carrier-to-blade attachment was evaluated for the LCF459 fan for comparison with the dovetail arrangement. The studies showed no real advantage of the dovetail over the bolted arrangement, where considerable successful operating experience has been obtained. The selected axially-bolted attachment is shown in Figure 4.40.

The tip tang would be integrally machined as part of the fan blade tip shroud. The design would use a 0.9524 cm (0.375 inch) diameter high strength bolt with the carrier bosses and blade tip tang sized as shown for adequate safety margins on bearing stress and shear tearout. A bushing would minimize any wear problems in the titanium blade tip tang, and provide a means for correcting for any assembly mismatch. Tip turbine drive loads and carrier rotation on the bolts are counteracted by supports on the fan blade tip shroud. The bolted tang assembly is an axial retention system for the turbine carrier and disengages radially for ease of on-wing fan blade or turbine sector removal.

4.3.8 Stress and Stability Margins

The selected rotor configuration includes 52 titanium fan blades, 364 shrouded turbine blades and a single web disk. This configuration was selected to determine the blade stress distribution and blade frequency/stability margins.

The steady state spanwise stress distribution for the airfoil is shown in Figure 4.41. Estimated end effects for the blade root showed the peak airfoil stress of 510,000 kN^2/m^2 (74 ksi) will occur at the root on the convex side near the trailing edge. Figure 4.42 compares the blade dovetail peak stresses to the blade material capability. The dovetail vibratory stress was determined for the condition where the maximum blade vibratory stress is at its endurance limit. The comparison shows the dovetail to have stress margin above the failure of the airfoil in fatigue. Figure 4.43 shows peak stresses on the fan blade relative to Ti 17 material properties versus temperature.

The frequency-speed diagrams for the blade are shown in Figure 4.44. The lower fundamental modes have no excitation from the stators (27 per rev) within the fan operating range. Figure 4.45 shows the coupled blade-disk two wave frequency margin at 14 percent over the two per rev excitation line at 100 percent speed. Although this is slightly below the design objective of 15 percent, present turbofans operate successfully with margins as low as seven percent. The three wave mode crosses the three per rev line at the low end of the operating range around 73 percent speed.

An investigation of the blade design relative to a torsion instability

parameter was conducted. Torsional stall instability is characterized by large oscillatory vibrations at the blades' torsional frequency. Common design utilizes a non-dimensional "reduced velocity parameter" to predict the susceptibility of blading design to instability.

Reduced velocity parameter = $V/b\omega$

Relative air velocity = V (m/sec, ft/sec)

Blade chord = b (m, ft)

Blade natural frequency = ω (rad/sec) in torsional mode

A reduced velocity parameter value above some critical value normally indicates the possibility of blade instability depending upon the blade incidence angle. Figure 4.46 shows the design instability boundary used for investigation of the LCF459 blade design. The curve illustrates that an instability free design should result with a reduced velocity parameter of 1.2 or below.

The calculated reduced velocity parameters at design point for the blade panels for the 52 bladed rotor with midspan at 65 percent span height are shown and indicate that the blade design should be free from torsional instability for design and off-design incidence angles.

4.4 Lube System, Bearings and Seals

4.4.1 Lube System

The lubrication system of the lift/cruise fan is self-contained and composed of the following subsystems:

Oil supply subsystem

Oil scavenge subsystem

Seal pressurization air subsystem

Vent subsystem

A dry sump is used as in other General Electric gas turbine engines. Oil is pressure-fed to both engine bearings and the carbon oil seal, and is removed from the sump area by drainage. The bulk of the oil is thereby retained in the oil tank. The lubrication system schematic diagram is shown in Figure 4.47.

The oil supply subsystem consists of the oil tank, which serves as the main reservoir of oil in the system, the oil supply pump, oil supply filter,

oil cooler and oil supply nozzles. Oil is supplied to the inlet of the supply pump from the oil tank. Oil under pressure is then routed through supply filter and oil cooler and distributed to the engine by the oil supply nozzles. The oil supply pump is protected from contamination by an inlet screen.

The oil scavenge subsystem consists of the oil drain passages and the scavenge oil deaerator. The scavenge oil gravity drains back to the oil tank which is located in the bottom of the sump. A gravity deaerator is located in the upper part of the oil tank.

Main shaft oil seals require pressurization air in order to cause air to flow across the seals into the sumps at all operating conditions. If air is allowed to flow out of the sump through an air seal, some oil is carried with it. This oil leakage must be eliminated in order to prevent excess oil consumption and seal coking. Fan discharge pressurization air is supplied to the oil seal using the air system which provides seal buffer and impingement cooling air. This air system is described in Section 4.6.

The sump must be vented to remove pressurization air which enters through the oil seals. This also allows the sump internal pressure to remain low enough to prevent reverse airflow out through the oil seals during a rapid power reduction. The sump is center-vented through the accessory drive shaft. Air is vented overboard and oil is returned to the oil tank.

The oil tank is located in a bulge on the side of the sump at the bottom. The scavenge air/oil mixture drains by gravity back to the tank. Air removal will be accomplished by a static deaerator. The oil tank shape is such that the oil will gravity-drain back to the tank when the fan is mounted either vertical or horizontal.

The oil supply pump is located in the bottom of the sump and is driven by the fan accessory shaft. The pump is a positive displacement element which is protected by a non-bypassing debris screen.

The oil supply filter serves to protect the lube supply nozzles from contamination as well as remove contamination such that system cleanliness is maintained at an acceptable level. The filter will be a non-bypassing type with a filtration level of 46 microns nominal.

The oil cooler will be capable of transferring the engine lube system heat rejection to the fan discharge air. The cooler will be located on the inner flowpath.

4.4.2 Bearings and Seals

The main shaft bearings include one thrust bearing and one roller

bearing. The thrust bearing will be a CF6 No. 4B bearing. The roller bearing is an 1800 series bearing. Figure 4.48 shows a cross-section of the sump and bearings, and lubrication pump. Bearing design loads and life are also given on the figure.

The carbon seal is similar to the F101 No. 5 oil seal. The sealing portion of the seal will be identical to the F101 but a different design is required for the seal mounting flange.

4.5 Vane Frame

A lift/cruise fan incorporating a structural rear frame was a logical choice based on the design requirements. The vane frame or rear frame, being the main structural component of the fan, must perform the following functions:

Support the rotor and bearings

Provide fan mounting points

Incorporate the fan exit stator cascade

Support the scroll

Provide fan and turbine discharge flowpaths

4.5.1 Design Considerations

The frame was designed to meet the life and mission cycle criteria established for the fan system. The most critical design criteria for the frame are:

Maneuver loading, particularly the two radian per second angular precession requirement

Thermal loading due to the hot outer structure and cold vanes and centerbody

Restraint of the forces as established by the blade-out criteria

The frame must exhibit adequate stability to provide good seal clearance control and minimize relative deflections of the fan components, such as rotor-to-stator or scroll deflections during angular precession. Adequate frequency margins are also required to insure resonant free operation.

4.5.2 Vane Number and Lean

The vane frame established at the initiation of the design studies

contained 30 structural stator vanes spanning the fan flowpath between the hub and turbine splitter or mid-box. Ten struts tied the structural mid-box and outer case together. The assembly employed cast and welded structures to form the hub, stator vanes and outer rings. Film cooling was employed on the outer casing and mid-box to yield acceptable thermal stresses. This configuration was abandoned when initial weight estimates indicated that the frame design would not produce an efficient lightweight structure.

The studies were then directed towards an evaluation of frame configurations which incorporates intermixed structural and non-structural vanes. These configurations employed small numbers of structural vanes which span the hot and cold flowpaths with the other stator vanes, as required by aerodynamic considerations, acting as turning vanes only.

A two-dimensional computer model comprised of beam members, as shown in Figure 4.49, was used to calculate thermal and load stresses in the fan frames. A future detailed analysis would use three-dimensional models incorporating beams and plates. The predominant stresses considered in the frame analysis are produced by the two radians per second gyroscopic precession, the blade-out forces and the thermal growth. The blade-out analysis should be performed using a dynamic analysis where the frame spring coefficients are used to determine the forces reaching the fan frame. In view of the complexity of this analysis, it was decided to make an initial static estimate limiting the dynamic analysis to the final selected configuration. Stresses resulting from rotor thrust, stator vane gas loading and remaining maneuver loading were also initially calculated to ascertain order of magnitude and later recalculated for the final selected configuration.

The thermal stress analysis was used to establish the stator lean to be incorporated in the frame struts and the required metal temperatures for the mid-box and outer case structures. Relative stiffnesses of struts and structural rings and the number of structural struts are additional factors which influence thermal stress levels.

Vane lean is advantageous from both an aerodynamic and structural viewpoint. Aerodynamically, it imposes radially inward force on the flowfield. Mechanically, it promotes bending of the frame struts and rotation of the frame hub assembly relative to the outer structure to accommodate the thermal growth difference between cold vane struts and hot outer structure. The rotational action relieves the tendency to build up large stresses in the outer structural rings. Non-radial or leaned struts have been used in the hot sections of numerous General Electric engines for relief of thermal stresses due to temperature mismatch between the hub and casings. This proven concept is equally beneficial in this application. Table 4.11 indicates the favorable stress reduction with increasing vane lean. A practical limit

exists for the degree of lean, because the transition between strut and ring becomes difficult at high lean angles. The limit established for these studies was 25 degrees.

Frame stresses under thermal and gyroscopic precession conditions were determined for the all-structural and partially-structural vane configurations. For this analysis, the frame contained 20 degrees of lean, had a total of 30 vanes and used the structural temperatures as given in Table 4.12. The stresses, as listed for the two configurations, approach the capabilities of the properties of Inco 718 material. Even though both frame configurations exhibited acceptable stress levels, the frame weights were still excessive for an acceptable configuration.

The frame studies were next directed towards weight reductions through the elimination of redundant members. The major change in this area was use of flowpath fairings for the fan/turbine mid-box in place of the original structural configuration. In addition, the number of structural vanes was reduced to nine to provide a symmetrical arrangement of structural struts relative to the three mount locations spaced at 120 degree intervals. Vane and strut chord were increased from 15.24 cm (6.0 in) to 16.93 cm (6.67 in) to maintain constant solidity in the exit stator row.

4.5.3 Frame Analysis

The initial trade studies produced a frame with the following design features:

27 stator vanes with a chord of 16.93 cm (6.67 inches), leaned 25 degrees at the hub.

Nine of the stator vanes are hollow and fabricated using cast Inco 718 material. They span the complete flowpath from the fan hub to the outer case.

18 non-structural stator vanes of 7075 aluminum.

Non-structural flowpath fairings at the turbine/fan mid-box. The fairings are Hastelloy X and provide support for the tips of the aluminum vanes.

An outer case with forged rings of Inco 718. Temperature control is obtained by impingement cooling. Flowpath liners and insulation are used to minimize cooling requirements.

The fan hub section, for supporting the rotor and bearings, is a cast fabricated structure using Inco 718 material.

This configuration was employed for stress analysis including the effects of aerodynamic loading, maneuvers, gyroscopic precession and blade-out. The results of this stress analysis, exclusive of the blade-out analysis, is given in Table 4.13. A comparison of the calculated stresses with the material yield strength and low cycle fatigue stress limits shows that the frame design does meet the design life/cyclic requirements. The cast structures of the frame will be subjected to Hot Isostatic Pressing (HIP) to improve weldability and low cycle fatigue strength. The improvement in low cycle fatigue strength can be observed in Table 4.13 by comparison of 36,000 cycle strength limit of the densified and undensified material. The stresses of the aluminum turning vanes were obtained for the steady state aerodynamic loading and are compared with the material capabilities in Figure 4.50. The selected material exhibits a more than adequate vibratory stress margin.

The vibratory characteristics of both the structural and non-structural vanes were determined for comparison with possible sources of excitation, particularly the rotor blade passing frequency. This comparison is shown in Figures 4.51 and 4.52 and indicates that the frame should be free of objectionable resonances in the operating range between 60 and 100 percent speed.

The blade-out capability of the frame was determined using a dynamic model of the frame, bearing support and rotor shaft system.

The analytical model as shown in Figure 4.53 replaces the frame structure with spring elements distributed around the outer periphery of the bearing housing. The remaining structure including the bearing support cone, shaft, disk and spinner are modeled in the analysis. The radial stiffness of the bearings was replaced by the spring constants as shown in the figure. The mathematical analysis of the model determines both resonant frequencies of the spring-mass system and forces due to rotor unbalance which are transmitted to the fan frame. The resonant frequency or critical speed analysis showed that the lowest critical speed would be 7855 revolutions per minute, compared to a design speed of 4370 revolutions per minute. This yields an 80 percent margin below resonant operation and possible high vibration due to small rotor unbalances.

For the rotor operating at design speed, well below resonance, the forces on the frame were determined for a rotor unbalance equivalent to one blade missing. The forces as determined from the dynamic analysis were then applied to the static two-dimensional model of the frame. The blade-out stresses are compared to the material properties' low cycle fatigue limits in Figure 4.54 and indicate a minimum endurance of 2000 cycles, which is equivalent to 30 second operation at design speed following the blade failure.

This simplified analysis shows that the selected frame design has

the capability of sustained operation for a reasonable period of time following failure of a complete blade and turbine carrier assembly. During a detail design study, a more complete dynamic analysis would be conducted using inelastic structures. This type of analysis normally shows an improved capability to withstand large unbalance forces.

4.6 Structural Cooling

The capability to maintain acceptable thermal stresses as well as optimum seal clearances requires cooling of the outer casing structure. Thermal stresses result from the thermal gradients between the outer casing, heated by the turbine discharge, and the struts and inner hub kept near ambient by the fan discharge flow. If the hot casing were allowed to grow thermally without cooling the turbine tip clearances would be excessive because the rotor growth (thermal plus centrifugal) is not as great as the unrestrained hot casing. Additionally, the air seal at the forward fan blade tip would have increased clearances allowing turbine gas to leak into the fan stream causing a large efficiency loss. To eliminate the need for cooling system interconnection in the event a gas generator became inoperative, it was determined that the cooling system be designed using only fan air.

During initial design study phases a cooling system evolved using fan air, bled through struts, to film cool the outer rings and the mid-box structure and provide buffer air to the forward air seal. However, aerodynamic changes in turbine blade reaction and fan stream exit Mach number decreased the available pressure head, thereby creating a marginal source of cooling flow. It was thought that if the case cooling could discharge to atmospheric pressure the use of fan discharge flow could be utilized. Impingement cooling fits this requirement in addition to being able to place the cooling flow in the precise place it is required.

Impingement cooling of high temperature engine casings was first successfully used on the USAF TF39 Low Pressure Turbine Casing (Figure 4.55). As seen from the figure, the impingement cooling tubes are placed over the specific areas to be cooled; in this case, the stator vane support rings. The versatility of impingement cooling to vary temperature of an engine structure is demonstrated by Figure 4.56 where the temperature of the casing was changed significantly by simply opening a valve and increasing the flow. This cannot be achieved by any other type of cooling system without extensive modifications. An additional feature of impingement cooling is that the "fountains" of air created by the jets of air reduce not only the basic structure temperature but the localized thermal gradients as evidenced by Figure 4.57.

Extensive back-to-back testing of the TF39 engine with and without

impingement cooling on the LP turbine casing produced a net SFC improvement of 0.38 percent with only 0.18 kg/sec (0.4 lb/sec) cooling flow. This can only be attributed to improved turbine tip clearances due to the casing being "shrunk" tighter on the rotor. This impingement cooling proved so successful on the TF39 that similar systems are used on the CF6-6, CF6-50 and F103 High Bypass Turbofan engines. To date, impingement case cooling has proven it durable by operating for more than 3×10^6 flight hours without problems. Thus, impingement cooling was chosen as the best system for the lift/cruise fan because of 1) effectiveness, 2) versatility to allow cooling flow redistribution without extensive hardware changes, and 3) proven durability.

Impingement cooling flows were sized to maintain ring temperatures at 288°C (550°F) with allowance for some increased temperature in the intermediate shells. Proper utilization of the impingement cooling technique required the introduction of casing liners in order to shield structural components from high convective heat transfer and resulting large thermal gradients. It should be noted that at this point in the design, cooling of the mid-box was still accomplished by film cooling and the forward rotor seal pressurization design had not changed. Figure 4.58 shows the design at this point in its development. Advantages of the redesigned system include: 1) reduced cooling flow requirements due to the introduction of impingement cooling, 2) a larger positive pressure head resulting from exhausting to ambient rather than turbine stream pressures, and 3) a system more capable of facilitating design modifications without major, expensive structural hardware changes.

The final change in cooling flow requirements evolved from the elimination of the mid-box structure at the turbine stator/fan stator interface of the frame assembly. The absence of continuous rings and shells eliminates the need for film cooling at the inner turbine flowpath. The turbine flowpath fairings and aft rotor seal were changed to a construction similar to the outer casing liners. The use of individual liner sectors permit freedom of thermal growth thereby eliminating temperature induced stresses. Proper positioning is accomplished by the structural frame struts. Figure 4.59 depicts the final cooling configuration.

The source of cooling airflow must be of sufficient pressure to provide adequate margin to prevent backflow of turbine gas out of the forward air seal. Extensive studies indicated that the use of strut bleed ports would not provide sufficient margin because of the lack of total pressure recovery. The configuration utilizes four scoop type inlets manifolded together to supply not only the 0.7 kg/sec (1.5 lb/sec) impingement case cooling flow but the 0.7 kg/sec (1.5 lb/sec) forward seal buffer air. The proposed design of the scoop type inlets are shown on Figure 4.60.

Four inlet scoops are located in the exhaust flow of the fan. These scoops are designed to efficiently recover the fan total pressure, diffuse, turn and duct the flow to the outer fan case. The cooling flow is then distributed to three locations:

Seal buffer air, 0.68 kg/sec (1.5 lb/sec)

Impingement cooling air, 0.68 kg/sec (1.5 lb/sec)

Carbon seal pressurization air, 0.05 kg/sec (0.1 lb/sec)

5.0 SELECTED DESIGN

A lift/cruise fan was defined based on the results of the design trade studies. This fan, the LCF459, incorporates those features which exhibited the highest potential for meeting the design objectives and requirements for the Navy multimission aircraft. The LCF459 is a 1.5 meter (59.0 inch) diameter turbotip fan designed for operation with a Growth J97 engine. The fan design, with only minor modifications of the turbine, is also capable of operating with the YJ97-GE-100 engine.

Preliminary mechanical and aerodynamic design studies were completed for this configuration, which provide a sound base for initiation of the next step of the design process, the detail design of a turbotip lift/cruise fan. Performance, weight and installation data have been provided for the selected configuration for evaluation by the aircraft companies and the anticipated using agencies. This section of the report describes the design features of the selected configuration, defines installation requirements and presents extracts of significant performance.

5.1 Fan Design Features

The fan cross-section, as established by the design studies and shown in Figure 5.1, includes the following salient features in each major component:

5.1.1 Rotor

The rotor contains 52 fan blades incorporating a single mid-span and integral tip shrouds. A drawing of the rotor showing the design features is shown in Figure 5.2. The rotor blades include integral platforms to form the hub flowpath. A single web conventional disk retains the blades using single-hook dovetails. Drop down slots, with spacers for blade retention, are provided to permit single blade removal. An aluminum structural spinner is attached to the disk to provide added structural stability for increased blade disk mode frequency margin. The spinner includes features for installation of radial balance weights. This permits on-wing field balance without any rotor disassembly. The rotor stub shaft is integrally fabricated with the disk to produce a lightweight structure. A flanged joint could be provided for separation of the disk and shaft for ease of maintenance but at some increase in weight.

The turbine rotor system contains 52 carrier assemblies, each attached to a single fan rotor blade. Retention of the carrier to the blade is accomplished using bolted attachments as used in previous lift fan designs

which used separable carrier-blade designs. Each turbine carrier contains seven turbine blades, giving a total of 364 blades for the turbine rotor. The turbine carrier, including blades and seal runners, is an integral cast structure. Tip shrouds are included on the turbine. These shrouds may either be directly cast with the carrier assembly or fabricated, as a separate subassembly and then brazed to the turbine. A summary of the materials used in the major rotor components is given in Table 5.1.

5.1.2 Scroll

The scroll geometry is strongly dependent on the particular aircraft installation. For purposes of this study, two configurations were considered, a single bubble scroll and a multilobe scroll. The single bubble configuration, Figure 5.3, is the lighter weight and simpler mechanical configuration. The multilobe, Figure 5.4, incorporates increased complexity to yield a reduction in fan projected frontal area. The major portion of both scrolls is the same, only the pressure vessel is of different cross-sectional shape.

The scroll pressure vessels are designed to restrain the pressure loading in hoop tension using circular sections. Struts are provided for continuation of the loadpath across the gap formed by the flowpath to the nozzles. For the multilobe scroll, additional ties are required at the junctures of the circular cross-sections. Both the struts and tie rods are designed to permit failure of one member without self-propagation of the failure to the adjacent struts or ties.

The turbine stator row is formed by 160 hollow nozzle partitions. The leading edges of these nozzles are formed to match the incidence of the incoming flow. Different geometries are required in the opposite legs of the scroll. A series of five different types or families of nozzles will be required.

Scroll mounting to the fan structure is located near the outer diameter of the turbine stator structure. A machined flange with 36 pins is an integral part of the scroll. These pins mate with a fan case flange which has slots aligned with the pins. This combination resists all motion of the scroll, except in the radial direction which is the result of thermal growth. The fan outer case also provides methods for retention of the segmented fan turbine honeycomb tip seal. Seal radial position is thus determined by the fan case alone. Impingement cooling air, with internal insulation, is provided for control of the casing temperature and turbine tip seal clearance.

The stationary part of the fan inlet seal is also supported from the fan case. Eighteen struts are attached to the cool case, pass through the hollow nozzles and support the honeycomb seal box structure. This structure of seal box, fan case and 18 struts forms an integrated stable structure

capable of rigid support of the seal. As defined earlier, seal buffer air passes through the nozzles, cools the mid-box and enters the fan stream as seal leakage. This cooling air minimizes thermal growth in this area.

Both scroll configurations contain two circular inlets. Blocker plates are inserted in flanged sections between the scroll inlets and in the opposite side of the scroll to separate the two flowpaths. The location of the blocker plates may be changed to produce other scroll arc ratios in place of the 240/120 degree split used for the design studies. These features will be described later for several specific lift/cruise fan installations.

A listing of the material used in the various parts of the scroll-seal-casing structure is given in Table 5.2.

5.1.3 Vane Frame

The preliminary configuration of the LCF459 includes the selected fan frame configuration. The construction of the vane frame is shown in Figure 5.5. The main structural portion of the frame is a welded fabrication of the inner hub, the outer case and nine leaned structural struts. The hub structure is a one piece casting, while the outer case is a fabricated structure of castings, rings and sheet metal. Each structural strut is a welded assembly of two hollow cast structures, the inner airfoil shaped strut and the outer strut including the transition in the mid-box region. All castings will be subjected to the Hot Isostatic Pressing process (HIP) to improve welding and chemical milling characteristics coupled with improved low cycle fatigue characteristics.

Three mounting points are incorporated on the frame structure. These mounts are spaced at 120 degree angular locations. Each mount distributes the reactions to three of the structural members.

The outer casing structure is shielded from the high convective heat transfer of the turbine flow by nine sections of casing liner. The brazed honeycomb liner panels are keyed to the structural struts for free differential growth. Insulation is installed between the fairings and outer structure to reduce the effective heat transfer. The inner turbine flowpath fairings include the stationary component of the labyrinth seal assembly located immediately aft of the rotor and are similar in design to the outer casing liners. Eighteen liner segments comprise the outer flowpath of the fan stream. Each liner segment is bolted to a structural strut and provides support for one of the non-structural stator vanes. Thermal growth flexibility is achieved by the slip fit between adjacent liner segments.

The non-structural struts or stator vanes are forged, solid aluminum airfoils. The vanes are bolted to the frame hub and torsionally restrained by

pins at the outer liner segments. Molded nylon inserts are used to provide a smooth hub flowpath between vanes.

The materials used in fabrication of the frame are given in Table 5.3. Geometric data for the struts and vanes are summarized in Table 5.4.

5.2 Clearances

Most of the previous fan designs were required to operate as lift only devices during the take-off and landing mode and therefore only minor consideration was given to off-design operation. The more recent applications for turbotip fans require good performance during V/STOL, cruise and loiter operation, including both full or partial turbine arcs of admission. This wide range of operating conditions establishes the need for good off-design performance and turbine tip clearance control in contrast to fans which operate at or near design point only. The performance of an impulse turbine at design point is not influenced appreciably by the amount of tip turbine clearance, and thus clearances of greater than 0.63 cm (0.25 inches) were permitted. Indeed, performance of a large clearance impulse turbine is very poor at off-design conditions.

Good tip clearance control was considered during the design selection of the LCF459 fan system. Impingement cooling of the fan casings was employed to maintain frame temperatures consistent with acceptable running clearances. Mounting and attachment of the hot scroll, with its large thermal growth migrations, was established for isolation of the seal running surfaces, both at the fan inlet tip and the turbine tip. A secondary benefit exists for a fan turbine with good clearance control. For an impulse turbine, the level of exit swirl is directly related to the turbine tangential speed. The speeds for low swirl, where turbine outlet guide vanes are not required, are usually lower than the speeds desirable for an aerodynamically and mechanically optimized fan. With good clearance control, a small amount of turbine reaction can be used to reduce the swirl levels to the case where exit guide vanes are no longer required. A high level of tip speed can then be maintained consistent with the fan requirements. This desirable feature led to the selection of a turbine with about 15 percent average reaction and a fan tip speed of 343 m/sec (1125 ft/sec).

As part of the design studies, the expected turbine clearance for a few of the critical fan operating conditions was determined to evaluate the adequacy of the selected configuration. The running clearance at a particular operating point for the turbine is established by the sum of three conditions:

Radial growth of the fan casing as established by the impingement cooling system.

Radial growth of the fan and turbine rotor due to centrifugal forces and metal temperature effects.

Relative deflection of the rotor and frame during maneuver loadings experienced during flight.

The conditions selected for the study were idle, short take-off, vertical landing, design point, cruise and loiter. At each of the conditions, a typical set of flight maneuvers was assumed based on aircraft flying experience. Pitch precession is by far the most critical maneuver for establishment of required clearances for maneuvers. The relative growth of the rotor and fan casing, which supports the tip seal, was evaluated by determining the frame temperatures and growth at each condition along with the growth of the fan rotor due to centrifugal and thermal effects. The frame thermal growth during the take-off and landing conditions required a transient evaluation of the frame temperatures due to the short operating times involved. Figure 5.6 shows the estimated transient growth experienced by the frame for these conditions.

Table 5.5 gives a listing of the rotor/stator relative motions calculated for each condition with the take-off clearances estimated after 20 seconds of operation and the landing at one minute. The maximum total relative motion, including thermal, centrifugal and maneuver effects, occurs during the landing condition where a radial clearance of 0.14 cm (0.056 in) is required to just prevent turbine tip seal run-in. Including an allowance of 0.05 cm (0.020 in) clearance for maximum assembly tolerance, a build-up clearance was established at 0.19 cm (0.076 in). Using this clearance as a base point, the running clearance for each flight condition was determined as listed in the table. These clearances were used to establish the changes in turbine efficiency as described in Section 4.1 of this report.

5.3 Weights and Inertias

5.3.1 Fan Weight

The base point fan weight is 386 kg (850 lbs). This includes the single circular scroll cross-section with dual inlets, one feeding a 240 degree arc and the other feeding the remaining 120 degree arc. The fan configuration is shown in Figure 5.1. The fan weight includes all fan components between the fan inlet and exhaust planes. Items not included in the weight are scroll insulation and the fan exhaust tailcone, both of which are aircraft dependent. Table 5.6 gives a weight breakdown of the fan assembly by major components.

Other optional configurations of the LCF459 fan with scroll configurations tailored to meet specific aircraft installations include:

A double inlet scroll, similar to the base point fan, with a multilobe scroll bubble for minimized fan frontal area, Figure 5.7.

A circular scroll with two scroll inlets, each feeding a 180 degree turbine arc.

A multilobe scroll with a single canted circular inlet. The single inlet is split with each inlet feeding either 120 or 240 degrees of turbine arc. A blocker plate located in the scroll arms at 120 degrees can be changed between two locations to provide left-to-right fan commonality.

The estimated weights of these three alternate fan configurations are given in Table 5.7.

5.3.2 Engine Weights

The YJ97-GE-100 engine is an existing engine configuration with a weight of 335 kg (739 lbs). This engine weight includes a discharge nozzle of an estimated weight of 9 kg (20 lbs), which is not required when used as a gas generator for a lift/cruise fan system. As a gas generator, the weight of the YJ97-GE-100 is 326 kg (719 lbs).

As part of this study, combustor water injection was considered as an option for increased thrust during emergency operation. The added weight of the engine mounted components for water injection is 9.5 kg (21 lbs). This weight includes the spray bars, manifolds and bypass control valve.

The Growth J97 engine weight was estimated on a preliminary basis by evaluating the changes between the YJ97-GE-100 and Growth engines. The estimated weight is 379 kg (835 lbs) with an exhaust nozzle and 370 kg (815 lbs) as a gas generator for lift/cruise fans.

The engine weights as specified above, do not include the following engine/aircraft installation items:

Starter

Engine inlet noise fairing

Engine/aircraft connection fittings and lines

Engine rotor speed sensor

Engine oil pressure sensor

Actuator for main fuel control lever

Engine/aircraft electrical wiring

Oil tank

5.3.3 Inertias

The inertias of the rotating components of the LCF459 and J97 engines are listed in Table 5.8. Design rotational speeds (100 percent) are also tabulated to aid in calculating forces during angular precession.

5.4 Installation

The installation of a lift/cruise fan system is strongly aircraft dependent. The inlets, ducting and exhaust systems are tailored to fit within the confines of the aircraft. For this reason, the propulsion furnished components are the gas generator and the lift/cruise fan accessories.

5.4.1 Gas Generator Mounting System

The YJ97-GE-100 engine employs a determinant mounting system when installed as a gas generator. Figure 5.8 shows a schematic of the most common mounting arrangement. Main trunnion mounts are located on each side of the main frame and resist vertical and axial forces. A forward vertical mount is located on the compressor front frame with a side drag-link located on the aft flange of the compressor case. Details of the engine mounting provisions are given in Reference 4 and the applicable J97 installation drawing.

The mounting provisions for the Growth J97 are the same as for the YJ97-GE-100. The design changes in the compressor amount to a 5.1 cm (2.00 in) increase in engine length and a 3.8 cm (1.50 in) increase in compressor inlet diameter. The remaining engine envelope remains the same as for the YJ97-GE-100 engine.

5.4.2 Lift/Cruise Fan Mounting System

The installation envelope of the lift/cruise fan is strongly dependent on the scroll geometry as established for the particular aircraft installation. Installation dimensions for two typical scroll systems employed with the LCF459 fan are given in Figures 5.9 and 5.10. Figure 5.9 shows the single inlet multilobe scroll arrangement and Figure 5.10 is for a double inlet circular scroll. Both systems employ a determinant three point mounting arrangement. The three mounts are located on the fan frame, and resist loads as shown in Figure 5.8. Each fan mount resists axial or thrust loads. One of the mounts adjacent to the scroll inlet also resists vertical and side loads and serves as the hard-point mount. A vertical restraint is also required on the mount opposite the scroll inlets.

The mounting systems described above employ separate mounting of

an evaluation relative to the frame capability.

Service lines to the accessory package cannot be routed through the fan frame because of size restrictions. A separate service strut is assumed to be aircraft-furnished to provide an access path to the accessories in the fan tailcone.

5.4.5 Heat Rejection and Cooling

The cooling requirements and heat rejection of the J97 engine are given in Reference 4. Engine compartment cooling is required to maintain the engine surface temperatures within the limits given in Table 5.9. In addition, all controls and accessories are limited to temperatures of 163 - 177°C (325 - 350°F). Each particular aircraft installation must be evaluated to determine cooling flow requirements to maintain the required structural temperatures.

The LCF459 is designed to minimize nacelle cooling requirements. Cooling air is extracted from the fan discharge and distributed through manifolds for impingement cooling of the fan frames. At design point, about 0.68 kg/sec (1.5 lb/sec) frame cooling air is required to maintain a frame case temperature of 232°C (450°F). This impingement cooling air performs a secondary function of purging the nacelle cavities. The fan design also employs buffer air, extracted from the fan discharge stream, for pressurization of the scroll sliding seals. Leakage from these seals will be cool air, less than 24°C (75°F) above ambient total temperature. This buffer air is also used to pressurize the fan inlet air seal and is recouped into the fan inlet airstream.

The inlet scoops for the buffer air must be mounted in the flowpath of the airframe-furnished exhaust nozzle. Figure 4.60 shows a sketch of a typical air inlet scoop. The external piping for routing this air to the scroll outer collector manifold is not illustrated on the fan installation drawing. Weight estimates for the air inlet and piping are included in the fan weight. The same is true for the impingement cooling air manifolds; the weight is included in the fan weight but the routing is not shown on the installation drawing.

5.4.6 Lubrication

Each lift/cruise fan incorporates a self-contained lubrication system. The lubrication and scavenge pumps are driven by the fan shaft. An integral lube tank is contained in the stator frame hub. A separate oil cooler will be placed in the fan exhaust stream, if required, to maintain acceptable oil temperatures. Use of integral fan lubrication systems eliminates the

the lift/cruise fan and the gas generator. Integral installations of a composite engine/fan system are also possible if mounting redundancies are avoided. A typical installation of this type is shown in Figure 5.11. This arrangement couples the engine and fan together through a ball joint flange arrangement. The aircraft-furnished joint must be designed to resist relative rotation of the fan and engine without restraint to angular misalignment. A vertical and side restraint are required on the engine with three thrust mounts and a vertical restraint located on the fan frame. Side restraint of the fan is provided by a mount located on the scroll inlet ducting. This arrangement is similar to that employed in helicopters for mounting engines to the gearbox.

Details of each particular installation and mounting arrangement must be evaluated to determine forces and moments transferred into the engine and fan components.

5.4.3 Inlet and Exhaust Attachments

The lift/cruise fan is designed to be isolated from the aircraft inlet and exhaust system installations. The attachments to the fan shall transmit only those small forces associated with slip-joints and bellows type attachments at the inlet and exhaust planes. The pressure-area or piston force associated with free-bellows systems shall not be transmitted to the fan scroll. Pressure compensated or tied bellow arrangements are required to minimize these forces.

The engine installation has similar restraints in that the inlet attachment to the engine shall not transmit aircraft induced forces into the compressor front frame.

5.4.4 Accessory Packages

Provisions for mounting aircraft accessories are provided on both the J97 gas generator and the lift/cruise fan. The capability of the YJ97-GE-100 engine is given in the engine model specification, Reference 4. Power extraction for this engine is limited to 18.6 kw (25 horsepower) because of the gearbox torque capability.

The lift/cruise fan incorporates the capability of mounting aircraft accessories in the exhaust tailcone envelope. A direct drive to the fan shaft is provided for power extraction to a present limit of 111.8 kw (150 horsepower). The fan frame is designed to accept the accessory mounting loads at the frame flange adjacent to the inner flowpath as identified in the sketch of a typical accessory package shown in Figure 2.7. The weight of this aircraft accessory package is 79 kg (175 lbs) with an overhung moment of 28.8 kg-m (2500 in-lbs) for the present design study. Other accessory packages require

dependency on the engine systems and the need for interconnect to cover single engine or engine-out operation.

The J97 engine contains an integral lubrication system. However, the lube tank and associated hardware are aircraft-furnished and not included in the engine weight. The lube tank requirements are defined in the engine model specification.

5.5 Performance

The LCF459 lift/cruise fan has been designed for operation with a Growth J97 gas generator. Operation is also possible with the existing YJ97-GE-100 engine. A comparison of the design point engine discharge gas conditions is given in Table 5.10. For operation with the YJ97-GE-100 engine, the fan turbine must be modified to accept the 10 percent lower flow function. This change could be accomplished through partial arc (325 degree) scroll operation, reorientation of turbine stators for reduced area, or reduction of turbine annulus area. The second case, reorientation of stators, is the most probable method which would be used due to simplicity of design changes. This case was assumed during the development of LCF459 performance with the existing YJ97-GE-100 engine.

The complementary aircraft studies have identified several combinations of numbers of fan/engines and the conditions where engine combustor water injection is required during emergency operation. Table 5.11 lists the results of these studies and identifies two prime systems:

> Three fans with two Growth J97 engines. In cruise, the system operates one-on-one, and in VTOL the three fans are powered by two gas generators.
>
> Equal numbers of fans and YJ97-GE-100 engines. Cruise and VTOL operation are with equal numbers of fans and engines.

Some of the arrangements consider water injection as a means of increasing take-off thrust, either during normal or emergency operation. Performance data have been determined for these numerous propulsion combinations.

5.5.1 Component Performance

The component performance of the LCF459 fan was based on estimated component maps for the fan and turbine. Figure 5.12 shows the estimated fan map and Figure 5.13 shows the estimated turbine map. These two maps are based on a fan design point efficiency of 85 percent and a turbine design point efficiency of 86 percent. Table 5.12 lists the other

significant design point parameters, including the turbine exit diffusion and ducting total pressure losses.

During partial arc operation, the performance of the fan system was corrected for windage and end losses existing in the inactive portion of the turbine annulus as defined in Section 4.1 of this report.

5.5.2 VTOL Performance

Performance during VTOL operation, sea level static, 32°C (90°F) day, was determined for the two engine/fan combinations. This static performance not only includes normal operation on the design operating line, but also includes operation during maximum control excursions and engine-out emergency operation.

The VTOL performance was determined for the typical installation assumptions as given in Table 5.13 which are considered representative of a lift/cruise installation operating in the lift mode. Comparable engine installation assumptions are given in Table 3.7. VTOL performance of the LCF459 with the Growth J97 engine is given in Table 5.14 and with the YJ97-GE-100 engine in Table 5.15. This performance data was generated at a fan stall margin of 25 percent to yield maximum thrust in conjunction with maximum distortion tolerance.

5.5.3 Cruise Performance

Cruise performance was determined for the LCF459 powered by either the Growth J97 or the YJ97-GE-100 engine. In cruise, both systems incorporate a single gas generator driving a single lift/cruise fan. The installation assumptions used during generation of the cruise data are given in Table 5.16. The performance was determined at a constant fan stall margin of 18 percent, which infers a continuously variable and controllable nozzle area. Operation of the fan system with a two position or step changing nozzle area is possible, but at some reduction in fan performance.

Detailed cruise performance is presented in Reference 5. Specific fuel consumption characteristics extracted from that reference are presented in Figure 5.14 for both the Growth J97 and YJ97-GE-100 cycles. The characteristics are shown using ambient pressure and temperature corrections which remove the effects of altitude. A comparison of the two cycles shows that the Growth engine has slightly lower fuel consumption, by virtue of the higher compressor pressure ratio.

5.6 Control Response

Control of the aircraft attitude during V/STOL flight must be obtained through modulation of the thrust of the lifting units or by use of additional reaction control devices, such as nozzles or control fans. For aircraft using lift or lift/cruise fans for propulsion, modulation of the fan thrust has been identified as an efficient method of control. Previous fan thrust control systems have employed thrust spoiling using exhaust louvers, as in the XV-5A aircraft; variable area scrolls (VAS), Reference 8; and turbine energy modulation (TEM), Reference 9. Each of these systems had particular undesirable features. The most recent and effective control system developed employs a method of energy transfer between pairs of interconnected engines. This Energy Transfer for Attitude Control (ETAC) concept has been subjected to analysis and development testing by both the McDonnell Aircraft Corporation and the General Electric Company. Under contract with NASA, McDonnell has performed tests of a typical ETAC interconnect system using two YJ97-GE-100 engines. The results of these tests are reported in References 10 and 11. These tests demonstrated the feasibility of the control system to yield the required levels of thrust control without distress to the engine system and at a rate fast enough to meet the response criteria for V/STOL flight operation. The LCF459 was designed to operate as the lifting device with a control system using the ETAC concept for thrust modulation. Operation of fan systems in the environment of ETAC has been described in detail in References 1 and 12. These requirements and criteria were applied to the LCF459 fan design.

The scope of this design study did not require a detailed transient analysis of the J97 engine and LCF459 fan during operation with the ETAC system. The analysis was limited to scaling of previous response analyses to reflect the design features of the LCF459, particularly the rotor inertia. The following discussion will be limited to a general description of the engine and fan transient operation, and an estimate of the fan and system time constants for the LCF459 propulsion system.

5.6.1 Engine Operation

Operation of the ETAC system is not limited to systems incorporating lift/cruise fans. Two interconnected gas generators are all that is required for operation of this control system. Figure 5.15 shows a schematic of two interconnected engines. A valve, located in the cross-duct, is provided for engine isolation during starting. Two ETAC valves are located in the fan duct, downstream of the cross-duct and upstream of the exhaust nozzles. The exhaust nozzles are shown to simulate the fan turbine nozzle in the fan configuration.

As the ETAC valve for Engine 1 is closed to produce a pressure drop, the Engine 1 is throttled and yields an increase in discharge pressure and temperature. The higher pressure at Engine 1 then causes a flow to occur in the cross-duct. The cross-duct flow in turn throttles Engine 2. For an ideal, no loss, cross-duct, the discharge conditions from each engine will stabilize at the same exhaust gas conditions. Figure 5.16 shows the variation of engine parameters as the ETAC valve is closed to a condition as established by a limiting temperature of 1144°K (2060°R) at the nozzles. The changes of pressure and temperature are shown for both engines. The difference of flow between the two engines represents the level of cross-flow, 6.9 percent maximum. The variation of gas power at the nozzles shows a 28 percent increase on the high side engine with only small changes on the low side. This change of power, when delivered to a fan turbine, produces changes of fan thrust for aircraft control. For power transfer in the opposite direction, Engine 2 valve is used with Engine 1 valve in the minimum loss position.

Transient operation of the J97 engine during ETAC control inputs was demonstrated during the tests described in Reference 10. Figure 5.17 shows a typical engine transient during a step input of control. The transient is initiated by a rapid motion of the ETAC valve which is completed within 0.1 seconds, as limited by the electro-hydraulic controls on the valve. The sequence of events which occur in the engine following the initiation of the ETAC Valve 1 motion is as follows:

> The engine discharge pressure increases directly with valve motion due to the decreased engine effective area and the associated increase in engine operating conditions. During the initial part of the transient, there is little or no change of engine fuel flow because engine speed has not had time to change. The engine fuel control requires a change of engine speed to produce a change of fuel flow.
>
> The pressure at Engine 1, downstream of the ETAC valve drops slightly because the rise in engine discharge pressure is not adequate to overcome the pressure drop across the valve.
>
> Following the control valve motion, there is a deficiency of engine turbine torque and the engine speed begins to drop. The fuel control senses this speed drop and produces an increase in fuel flow.
>
> The increase in fuel flow causes an increase in engine discharge temperature and small increases in pressure until a stabilized speed-fuel flow condition is achieved. This total transient takes about 0.5 seconds to stabilize

This type of engine response to control inputs has been demonstrated to be stable and predictable based on the test programs. The time required for the transient to occur appears to be adequate to meet the aircraft control

requirements. A fuel flow anticipation system could very easily be incorporated in the engine system to improve the response time. This anticipation system would be designed to produce an engine fuel flow change proportional to the control valve position. The fuel flow change required for stabilized engine operation would then occur within the first 0.1 second of the transient, and would not require an engine speed change as previously described. With anticipation, the complete engine transient time could be reduced to about 0.2 seconds for a typical step control input.

5.6.2 Fan Operation

The previous discussion has shown that a change of power occurs at the fan turbine with motion of the ETAC valve. The fan systems convert this change of power into lift as shown in Figure 5.18. The fan thrust variation with control indicates an increase for the high side fan with little change for the opposite. Thrust spoiling is provided to maintain a constant two fan total thrust with control input. This thrust spoiling feature is desirable for fast thrust response as discussed below.

The transient operation of the two fan system is based on the fan response to the power variations produced by the engines during control inputs. Figure 5.19 shows a typical fan estimated thrust transient including the effects of engine, fan and thrust spoiling systems. The time variation of fan thrust is determined by the rapid thrust spoiling function on the low side fan and a longer transient on the high side as established by the fan speed change and inertial effects. The variation of control moments and system total lift is established by the differential and sum of the two fan thrust levels. Typical control moment transients show a time constant of about 0.2 seconds, where time constant is defined as the time required for the moments to achieve 63 percent of the total steady state moment change. A small short duration decrease in fan total thrust is shown to occur during the initial part of the transient. The lift deficiency will cause a very small but acceptable coupling of height with attitude control.

The transient variation of control forces is related to the combined effects of the engine and fan systems. For an overall control time constant of about 0.2 seconds, the fan alone time constant should be less than 0.3 seconds. This fan time constant is directly related to the fan moment of inertia, since a fan speed change is required to produce a fan thrust change.

A detailed transient analysis of the LCF459 fan was not conducted during this study. Comparison of this fan with the LF460 fan, Reference 1, should give fairly accurate time estimates because of the similarity of the two designs. Table 5.17 compares the fan aerodynamic design parameters and rotor inertia of the two fan systems. Using the results of transient

analysis of the LF460, with corrections for rotor inertias, the estimated time constants for the LCF459 are shown in Figure 5.20. This simplified analysis indicates that the LCF459 should be capable of meeting or exceeding the 0.3 second time constant criteria at fan speeds in excess of about 80 percent.

CONCLUSIONS

Preliminary design studies of a turbotip lift/cruise fan for the Navy multimission aircraft have identified a configuration which has a high degree of assurance for meeting the propulsion system goals and requirements. The J97 turbojet engine was selected as the gas source for powering the fan system. Conclusions derived based on these studies are:

1. A 1.5 meter (59.0 inch) diameter turbotip lift/cruise fan can be designed to meet modified requirements of MIL-E-5007D (Reference 2) and FAR-33-1B (Reference 3) with a fan weight of 386 kg (850 lbs). Operational capabilities include the ability to ingest a 1 kg (2.2 lb) bird and withstand maneuver loads including angular precession rate of 2.0 radians per second and 10 g vertical down-load.

2. A 6000 hour life lift/cruise fan configuration has been designed which will provide a design point thrust-to-weight ratio of 0.195 N/g (19.9 lb/lb).

3. Maintainability features have been included to provide on-wing component removal.

4. The rotor system incorporating 52 titanium blades and a conventional web disk, meets the design requirements and exhibits a rotor moment of inertia adequate to meet the transient response requirements for a time constant of less than 0.3 seconds.

5. The fan system is capable of operation as a lift/cruise fan or a lift fan, either as a right or left-hand installation, through proper consideration of lubrication and ducting system design.

6. An engine with 20 percent gas power growth over the YJ97-GE-100 can be obtained through modifications of Stages 1 through 5 of the compressor and turbine changes, primarily through material substitution. The growth engine weight was estimated to be 379 kg (835 lbs).

7. A low risk water system, using pre-combustor injection, was defined to provide increased thrust, if desired, during V/STOL and Emergency operation.

8. Good tip clearance control is required to maintain high efficiency levels for the required wide range of operation. The use of case impingement cooling provides a means to achieve close running clearances while maintaining flexibility for system development.

9. A fan system for installation in a multimission aircraft will require large distortion tolerance. A design point stall margin of 18 percent has been achieved. Operation with increased nozzle area during takeoff and landing will increase the estimated stall margin to 25 percent.

NOMENCLATURE

Symbol	Definition	Units
A	Area	m^2 (ft^2)
A_B	Turbine Bucket Projected Area, Length X Chord	m^2 (ft^2)
b	Blade Chord	m (ft)
EMERG	A One-Minute Emergency Rating for Use During Engine-Out Operation	-
F	Fraction of Admission Arc Durin Partial Arc Operation	-
F_N	Net Thrust	kN (lb)
g	Gravitational Constant	m/sec^2 (ft/sec^2)
h	Turbine Bucke. Height	cm (in)
H	Enthalpy	J/g °R (BTU/lb °F)
INTER	A 30-Minute Engine Rating	-
I_p	Rotor Polar Moment of Inertia	kg-m-sec^2 (lb-ft-sec^2)
J	Mechanical Equivalent of Heat	Nm/sec J (ft-lb/sec BTU)
K_F	Windage Loss Constant	-
MAX	A Three Second Rating which Establishes Maximum Control for V/STOL Take-Off and Landing	-
N	Fan Rotational Speed	rpm (rpm)
N_b	Number of Fan Blades	- (-)
P	Pressure	kN/m^2 (psia)
PCNG	Gas Generator Rotational Speed	pct (pct)
PCNF	Fan Rotational Speed	pct (pct)
P_{EL}	Partial Arc End Loss Power	kw (hp)
P_{WL}	Partial Arc Windage Power Loss	kw (hp)
S. L.	Sidewards Maneuver Acceleration	g's (g's)
$t_{m/c}$	Blade Thickness to Chord Ratio	- (-)
T	Temperature	°K (°R)

NOMENCLATURE

Symbol	Definition	Units
u_p	Turbine Pitch Tangential Velocity	m/sec (ft/sec)
I	Rotor Blade Relative Air Velocity	m/sec (ft/sec)
Vo	Turbine Nozzle Ideal Velocity	m/sec (ft/sec)
VTO	A One-Minute Engine Rating for V/STOL Take-Off	-
W	Gas Flow Rate	kg/sec (lb/sec)
WFM	Engine Fuel Flow Rate	kg/hr (lb/hr)
WWL	Combustor Water Flow Rate	kg/sec (lb/sec)
WXFR	Flow Transfer	pct (pct)
β_1	Turbine Bucket Inlet Air Angle	rad (deg)
β_2	Turbine Bucket Exit Air Angle	rad (deg)
δ	Turbine Tip Clearance	cm (in)
δ_o	Ambient Pressure Correction Relative to Standard Pressure	- (-)
η	Efficiency	pct (pct)
θ	Ambient Temperature Correction Relative to Standard Day	- (-)
$\dot{\theta}$	Roll Maneuver Angular Rate	rad/sec (rad/sec)
$\ddot{\theta}$	Roll Maneuver Angular Acceleration	rad/sec^2 (rad/sec^2)
ρ	Fluid Density	kg/m^3 (lb/ft^3)
$\dot{\psi}$	Pitch Maneuver Angular Rate	rad/sec (rad/sec)
$\ddot{\psi}$	Pitch Maneuver Angular Acceleration	rad/sec (rad/sec)
ω	Blade Torsional Frequency	rad/sec (rad/sec)

Subscripts

4	Engine Turbine Inlet
22	Fan Inlet
51	Engine Turbine Discharge
54	Fan Turbine Inlet

REFERENCES

1. General Electric Company, Aircraft Engine Group, Cincinnati, Ohio: LF460 Detail Design, NASA Contractor Report CR-120787, September, 1971.

2. Military Specification: Engines, Aircraft, Turbojet and Turbofan, General Specification for MIL-E-5007D, October, 1973.

3. Federal Aviation Agency: Turbine Engine Foreign Object Ingestion and Rotor Blade Containment Type Certification Procedures, FAR 33-IB, April, 1970.

4. General Electric Company, Aircraft Engine Group, Lynn, Massachusetts: Engine, Aircraft, Turbojet YJ97-GE-100, Model Specification E-1155, October 15, 1969.

5. General Electric Company, Aircraft Engine Group, Cincinnati, Ohio: LCF450/J97 Estimated Performance, Report Number R75AEG413, July, 1975.

6. General Electric Company, Aircraft Engine Group, Cincinnati, Ohio: Air Force Advanced Lift Fan and Lift/Cruise Fan Demonstrator Program, Technical Report AFAPL-TR-69-7, February, 1969.

7. General Electric Company, Gas Turbine Department, Schenectady, New York: Rotation Loss Test for MARAD Reversing Turbine Study Contract, Report Number DF-63-GTD-21, December, 1963.

8. General Electric Company, Aircraft Engine Group, Cincinnati, Ohio: Investigations of a Variable Area Scroll for Power Transfer in Tip Turbine Lift Fan Systems, U.S. Army Aviation Material Laboratories Technical Report 67-26, 1967.

9. General Electric Company, Aircraft Engine Group, Cincinnati, Ohio: Demonstration of Turbine Energy Modulation (TEM) Method of Lift Fan Thrust Control, General Electric Report R69AEG391, September, 1969.

10. McDonnell Douglas Corporation, St. Louis, Missouri: A Full Scale Test of a New V/STOL Control System, Energy Transfer Control (ETC), Report MDCA1588, June, 1972.

11. McDonnell Douglas Corporation, St. Louis, Missouri: A Full Scale Test of a New V/STOL Control System, Energy Transfer Control (ETC),

Phase II - Engine Out Operation, Report MDCA1588, Supplement 1, April, 1973.

12. General Electric Company, Aircraft Engine Group, Cincinnati, Ohio: Conceptual Design Studies of Lift/Cruise Fans for Military Transports, NASA Contractor Report CR-134636, May, 1974.

13. Marshal, R. and Rogo C. : Experimental Investigation of Low Aspect Ratio and Tip Clearance on Turbine Performance and Aerodynamic Design, Continental Aviation Report Number 1043, May, 1968.

14. Kofskey, Milton G.: Experimental Investigation of Three Tip-Clearance Configurations Over a Range of Tip Clearance Using a Single-Stage Turbine of High Hub-to-Tip Radius Ratio; NASA TMX-472, May, 1961.

15. Holeski, Donald E., and Futral, Samuel M.: Effect of Rotor Tip Clearance on the Performance of a 5-Inch Single-Stage Axial-Flow Turbine, NASA TMX-1757, March, 1969.

TABLE 2.1

GAS CONDITIONS AT FAN DESIGN POINT

3-on-2 Growth J97, Intermediate Power, Sea Level Static, Standard Day

Gas Flow, kg/sec (lb/sec)	37.31	(82.25)
Pressure, kN/m^2 (lb/in^2) *	374.0	(54.25)
Temperature, °K (°R)	1028	(1851)
Power, kw (hp)	12,183	(16,338)
Throat Area, sq meters (sq in)	0.0782	(121.2)

2-on-2 J97-GE-100, Maximum Power Transfer, Sea Level Static, 32°C (90°F) Day

Gas Flow, kg/sec (lb/sec)	30.95	(68.24)
Pressure, kN/m^2 (lb/in^2) *	386.3	(56.03)
Temperature, °K (°R)	1144	(2060)
Power, kw (hp)	11,518	(15,447)
Throat Area, sq meters (sq in)	0.0663	(102.7)

* Gas Conditions are Given at the Inlet Flange to the Fan Scroll and Included 3.1 and 2.7 Percent Pressure Loss for the Growth and -100 Engines Respectively.

TABLE 2.2

GROWTH J97 GAS CONDITIONS USED IN FAN DESIGN POINT STUDIES

Gas Flow, kg/sec (lb/sec)	37.14	(81.87)
Pressure, kN/m^2 (lb/in^2)	369.9	(53.57)
Temperature, °K (°R)	1019	(1835)
Power, kw (hp)	11,960	(16,039)

(Scroll Inlet Gas Conditions, Including 3.1 Percent Pressure Loss, Used in Studies Prior to Definition of Growth Engine as Defined in Tables 2.1 and 3.6)

TABLE 2.3

BASE POINT FAN DESIGN PARAMETERS

ESTABLISHED FOR AERODYNAMIC DESIGN STUDIES

Tip Diameter, meters (in)	1.499	(59.0)
Tip Speed, meters/sec (ft/sec)	343	(1125)
Specific Flow, $kg/sec\text{-}m^2$ ($lb/sec\text{-}ft^2$)	195	(40.0)
Fan Exit Mach Number	0.55	
Turbine Exit Mach Number	0.55	
Fan Hub Loading Parameter	2.14	

TABLE 2.4

BASE POINT FAN

Tip Diameter, meters (inches)	1.50 (59.0)
Pressure Ratio	1.31
Turbine Pressure Ratio	1.34
Tip Speed, meters/sec (ft/sec)	343 (1125)
Specific Flow, kg/sec-m^2 (lb/sec-ft^2)	195 (40.0)
Fan Exit Mach Number	0.55
Turbine Blade Exit Mach Number	0.55
Turbine Stator Exit Mach Number	0.59
Inlet Radius Ratio	0.418
Fan Airflow, kg/sec (lb/sec)	284 (626)
Ideal Thrust, kn (lb)	73.08 (16,430)

(Initial Configuration Selected Prior to Aerodynamic Design Studies)

TABLE 2.5 EFFECTS OF DESIGN VARIABLES ON FAN THRUST

Variable	Tip Speed meter/sec	Tip Speed ft/sec	Specific Flow kg/sec-m^2	Specific Flow lb/sec-ft^2	Fan Exit Mach Number	Turbine Exit Mach Number	Fan Diameter meters	Fan Diameter inches	Fan Pressure Ratio	Turbine Pressure Ratio	Flow kg/sec	Flow lb/sec	Thrust kN	Thrust lb	Δ Thrust percent
Basepoint	343	1125	195	40	0.55	0.55	1.50	59	1.31	1.34	284	626	73.08	16,430	-
Tip Speed	320	1050	195	40	0.55	0.55	1.50	59	1.30	1.42	277	610	72.01	16,190	-1.5
Specific Flow	343	1125	203	41.5	0.55	0.55	1.50	59	1.30	1.32	297	654	74.55	16,760	+2.0
Fan Exit Mach No	343	1125	195	40	0.45	0.55	1.50	59	1.30	1.38	286	630	72.99	16,410	-0.1
Turbine Exit Mach No	343	1125	195	40	0.55	0.45	1.50	59	1.315	1.32	283	623	73.08	16,436	0.0
Fan Diameter	343	1125	195	40	0.55	0.55	1.52	60	1.30	1.34	296	653	74.37	16,720	+1.8

TABLE 2.6

LCF459 AERODYNAMIC PARAMETERS

SELECTED AFTER AERODYNAMIC DESIGN STUDIES

AND USED IN MECHANICAL STUDIES

Tip Diameter, meters (inches)	1.50	(59)
Pressure Ratio	1.319	
Gas Flow, kg/sec (lb/sec)	37.14	(81.87)
Pressure, kN/m^2 (lb/in^2)	369.4	(53.57)
Temperature, °K (°R)	1019	(1835)
Turbine Pressure Ratio	1.270	
Tip Speed, meter/sec (ft/sec)	343	(1125)
Specific Flow, $kg/sec\text{-}m^2$ ($lb/sec\text{-}ft^2$)	203	(41.5)
Fan Exit Mach Number	0.50	
Turbine Blade Exit Mach Number	0.55	
Turbine Stator Exit Mach Number	0.45	
Inlet Radius Ratio	0.424	
Airflow, kg/sec (lb/sec)	293	(646)
Ideal Thrust, kN (lb)	74.46	(16,740)

TABLE 2.7

COMPONENT DESIGN LIFE

(Without Repair)

	Hours
Turbine Blades and Vanes	3,000
Fan Blades	6,000
Disk	6,000
Scroll	3,000
Frame	6,000
Bearings	6,000

Low Cycle Fatigue - 6,000 Missions with 3 Flight Cycles/Mission

TABLE 2.8

TYPICAL DUTY CYCLE FOR ASW MISSION WITH GROWTH J97 ENGINES

Mission Segment	Altitide		Speed	Time	Thrust
	Meters	Feet	Mach	Secs	% of Int *
STOL Take-Off	0 0	0 0	0 0.25	2.0 0.5	VTO 100%
Climb	0 10970	0 36000	0.25 0.70	11.0	100%
Cruise	10970	36000	0.70	12.0	75%
Descend	10970 3040	36000 10000	0.70 0.35	0	Idle
Loiter	3040	10000	0.35	240	25%
Climb	3040 10970	10000 36000	0.35 0.70	11.0	Int
Cruise	10970	36000	0.7	12.0	75%
Descend	10970 1524	36000 5000	0.70 0.25	0	Idle
Loiter	1524	5000	0.25	10.0	25%
VTO Landing	1524 0	5000 0	0.25 0	1.0	80% VTO

* Thrust Levels Given in Percent of Intermediate Thrust at the Flight Altitude and Mach Number

TABLE 3.1 COMPARISON OF GROWTH AND YJ97-GE-100 DESIGN POINTS

(Sea Level Static, Standard Day)

Parameter	YJ97-GE-100	Growth J97
Speed, percent	100	100
Speed, rpm	13650	14231
Compressor Airflow, kg/sec (lb/sec)	31.15 (68.66)	36.30 (80.03)
Compressor Pressure Ratio	13.80	16.69
Compressor Efficiency, percent	84.6	83.6
Stall Margin	22.42	22.15
Turbine Inlet Temperature, °K (°R)	1352 (2433)	1396 (2513)
Turbine Discharge Temperature, °K (°R)	996 (1793	1005 (1809)
Turbine Discharge Pressure, kN/M^2 (psia)	358.0 (51.92)	378.0 (54.83)
Turbine Discharge Flow, kg/sec (lb/sec)	31.73 (69.95)	36.99 (81.55)
Ideal Gas Power, kw (hp)	9810 (12890)	11950 (15700)

TABLE 3.2 GROWTH ENGINE WEIGHT ESTIMATES

	YJ97-GE-100	Growth J97
Weight, kg (lbs)	335 (739)	379 (835)

Weight Includes 9.1 kg (20 lbs) Convergent Exhaust Nozzle.

TABLE 3.3 SHORT-TIME RATING LIMITS

WITHOUT WATER	YJ97-GE-100	Growth J97
● INTER	T4 = 1382°K (2487°R)	T4 = 1426°K (2567°R)
● VTO	T4 = 1433°K (2580°R)	T4 = 1467°K (2640°R)
● MAX *	T5 = 1144°K (2060°R)	T5 = 1144°K (2060°R)
● EMERG	T5 = 1144°K (2060°R)	T5 = 1144°K (2060°R)

WITH 4% COMBUSTOR WATER		
● VTO	T4 = 1433°K (2580°R)	T4 = 1467°K (2640°R)
● MAX *	T5 = 1144°K (2060°R)	T5 = 1144°K (2060°R)
● EMERG	PCNG = 110%	PCNG = 110%

* At MAX Power Rating, Engine Speed is Unchanged from VTO Rating. Increase in Operating Point is achieved through Power Transfer Between Pairs of Engines.

TABLE 3.4 GAS GENERATOR INSTALLATION PARAMETERS

Inlet Recovery	0.985
Compressor Bleed	0.5 Percent
Power Extraction	19 kw (25 hp)

TABLE 3.5 J97-GE-100 SHORT-TIME RATINGS (UNINSTALLED)

DAY	RATING	PCNG pct	WFM kg/hr	WFM lb/hr	WWL kg/sec	WWL lb/sec	T4 °K	T4 °R	P51 kN/m²	P51 psia	T51 °K	T51 °R	W51 kg/sec	W51 lb/sec	WXFR pct	W54 kg/sec	W54 lb/sec
STD	INTER	101.5	2188	4824	0	0	1382	2488	365.3	52.98	1019	1835	32.00	70.54	0	32.00	70.54
	VTO	103.8	2341	5162	0	0	1433	2580	375.4	54.49	1059	1907	32.27	71.14	0	32.27	71.14
	MAX	103.8	2639	5817	0	0	1521	2738	417.2	60.51	1144	2060	32.35	71.31	6.42	34.43	75.89
	EMERG	109.0	2645	5831	0	0	1541	2773	393.2	57.02	1144	2060	32.41	71.49	0	32.41	71.49
32°C (90°F)	INTER	101.5	2084	4595	0	0	1403	2525	349.2	50.65	1037	1867	30.32	66.85	0	30.32	66.85
	VTO	103.1	2199	4848	0	0	1433	2580	359.6	52.16	1061	1909	30.89	68.09	0	30.89	68.09
	MAX	103.1	2478	5464	0	0	1521	2737	397.2	57.60	1144	2060	30.95	68.24	5.85	32.76	72.23
	EMERG	107.8	2517	5549	0	0	1539	2770	381.2	55.28	1144	2060	31.43	69.30	0	31.43	69.30
STD	INTER	101.5	2422	5340	1.16	2.57	1306	2351	370.7	53.77	970	1746	33.23	73.25	0	33.23	73.25
	VTO	107.6	2814	6204	1.17	2.59	1433	2580	394.1	57.16	1070	1926	33.64	74.16	0	33.64	74.16
	MAX	107.6	3097	6827	1.17	2.59	1510	2718	433.4	62.85	1144	2060	33.71	74.32	5.91	35.70	78.71
	EMERG	110.0	2918	6433	1.17	2.59	1467	2640	400.7	58.12	1097	1975	33.68	74.26	0	33.68	74.26
32°C (90°F)	INTER	101.5	2307	5086	1.10	2.43	1327	2388	354.3	51.39	987	1777	31.48	69.39	0	31.48	69.39
	VTO	107.0	2684	5918	1.14	2.51	1433	2580	382.2	55.43	1071	1928	32.60	71.87	0	32.60	71.87
	MAX	107.0	2955	6514	1.14	2.51	1509	2716	419.9	60.90	1144	2060	32.68	72.04	5.87	34.59	76.27
	EMERG	110.0	2889	6370	1.15	2.52	1501	2702	394.1	57.16	1126	2026	32.71	72.11	0	32.71	72.11

TABLE 3.6 GROWTH J97 SHORT-TIME RATINGS (UNINSTALLED)

DAY	RATING	PCNG pct	WFM kg/hr	WFM lb/hr	WWL kg/sec	WWL lb/sec	T4 °K	T4 °R	P51 kN/m²	P51 psia	T51 °K	T51 °R	W51 kg/sec	W51 lb/sec	WXFR pct	W54 kg/sec	W54 lb/sec
STD	INTER	101.5	2586	5701	0	0	1426	2567	385.9	55.97	1028	1851	37.31	82.25	0	37.31	82.25
	VTO	103.3	2726	6009	0	0	1467	2640	394.5	57.21	1059	1907	37.56	82.81	0	37.56	82.81
	MAX	103.3	3071	6771	0	0	1554	2797	444.0	64.40	1144	2060	37.65	83.01	7.59	40.43	89.31
	EMERG	107.9	3082	6795	0	0	1575	2836	413.3	59.95	1144	2060	37.79	83.31	0	37.79	83.31
32°C (90°F)	INTER	101.5	2468	5442	0	0	1450	2610	369.2	53.55	1048	1886	35.34	77.92	0	35.34	77.92
	VTO	102.4	2543	5607	0	0	1467	2640	375.5	54.46	1061	1909	35.73	78.78	0	35.37	78.78
	MAX	102.4	2867	6320	0	0	1554	2797	419.8	60.98	1144	2060	35.80	78.93	7.16	38.36	84.58
	EMERG	107.3	2933	6467	0	0	1574	2834	400.7	58.12	1144	2060	36.63	80.76	0	36.63	80.76
STD	INTER	101.5	2866	6320	1.36	2.99	1350	2430	391.9	56.84	980	1764	38.74	85.41	0	38.74	85.41
	VTO	107.0	3283	7238	1.37	3.02	1467	2640	414.5	60.12	1071	1928	39.20	86.42	0	39.20	86.42
	MAX	107.0	3608	7955	1.37	3.02	1542	2775	460.0	66.72	1144	2060	39.29	86.61	6.69	41.91	92.40
	EMERG	110.0	3445	7595	1.37	3.02	1512	2722	423.3	61.40	1107	1993	39.28	86.59	0	39.28	86.59
32°C (90°F)	INTER	101.5	2737	6035	1.29	2.84	1373	2472	374.9	54.38	999	1799	36.69	80.89	0	36.69	80.89
	VTO	103.3	3127	6896	1.33	2.93	1467	2640	401.4	58.22	1072	1929	37.95	83.67	0	37.95	83.67
	MAX	103.3	3439	7582	1.33	2.93	1541	2774	444.9	64.52	1144	2060	38.03	83.85	6.60	40.54	89.38
	EMERG	110.0	3412	7524	1.33	2.93	1548	2787	416.4	60.40	1136	2045	38.14	84.08	0	38.14	84.08

TABLE 3.7 J97-GE-100 SHORT-TIME RATINGS (INSTALLED)

DAY	RATING	PCNG pct	WGM kg/hr	WGM lb/hr	WWL kg/sec	WWL lb/sec	T4 °K	T4 °R	P51 kN/m²	P51 psia	T51 °K	T51 °R	W51 kg/sec	W51 lb/sec	WXFR pct	W54 kg/sec	W54 lb/sec
STD	INTER	101.5	2071	4786	0	0	1389	2501	359.0	52.07	1026	1846	31.36	69.15	0	31.36	69.15
	VTO	103.5	2300	5070	0	0	1433	2580	367.6	53.32	1059	1907	31.60	69.66	0	31.60	69.66
	MAX	103.5	2591	5712	0	0	1521	2738	408.2	59.21	1144	2060	31.67	69.83	7.11	33.93	74.80
	EMERG	108.6	2600	5732	0	0	1541	2774	384.4	55.75	1144	2060	31.78	70.06	0	31.78	70.06
32°C (90°F)	INTER	101.5	2068	4560	0	0	1411	2539	343.2	49.78	1043	1877	29.73	65.54	0	29.73	65.54
	VTO	102.7	2154	4749	0	0	1433	2580	351.1	50.93	1061	1909	30.16	66.49	0	30.16	66.49
	MAX	102.7	2427	5351	0	0	1521	2738	387.4	56.19	1144	2060	30.22	66.63	6.48	32.18	70.94
	EMERG	107.6	2474	5455	0	0	1540	2772	372.6	54.04	1144	2060	30.81	67.92	0	30.81	67.92
STD	INTER	101.5	2403	5297	1.14	2.52	1314	2365	364.8	52.91	976	1757	32.57	71.81	0	32.57	71.81
	VTO	107.2	2766	6097	1.15	2.54	1433	2580	386.6	56.07	1070	1926	32.96	72.67	0	32.96	72.67
	MAX	107.2	3042	6706	1.15	2.54	1509	2717	425.2	61.67	1144	2060	33.03	72.83	6.12	35.05	77.28
	EMERG	110.0	2877	6342	1.15	2.54	1471	2647	392.1	56.87	1099	1979	33.02	72.79	0	33.02	72.79
32°C (90°F)	INTER	101.5	2288	5045	1.12	2.46	1334	2402	348.7	50.57	993	1787	30.86	68.03	0	30.86	68.03
	VTO	106.6	3635	5810	1.12	2.46	1433	2580	374.5	54.32	1071	1928	31.92	70.38	0	31.92	70.38
	MAX	106.6	2900	6394	1.12	2.46	1509	2716	411.1	59.63	1144	2060	31.99	70.53	5.97	33.90	74.74
	EMERG	110.0	2850	6284	1.13	2.47	1506	2711	385.7	55.95	1128	2031	32.06	70.68	0	32.06	70.68

TABLE 3.8 GROWTH J97 SHORT-TIME RATINGS (INSTALLED)

DAY	RATING	PCNG pct	WFM kg/hr	WFM lb/hr	WWL kg/sec	WWL lb/sec	T4 °K	T4 °R	P51 kN/m²	P51 psia	T51 °K	T51 °R	W51 kg/sec	W51 lb/sec	WXFR pct	W54 kg/sec	W54 lb/sec
STD	INTER	101.5	2570	5665	0	0	1433	2581	397.5	55.04	1034	1862	36.57	80.63	0	36.57	80.63
	VTO	102.9	2678	5904	0	0	1467	2640	386.3	56.03	1059	1907	36.78	81.09	0	36.78	81.08
	MAX	102.9	3016	6651	0	0	1554	2798	434.9	63.07	1144	2060	36.87	81.28	9.26	40.28	88.81
	EMERG	107.7	3030	6680	0	0	1577	2838	404.3	58.64	1144	2060	37.04	81.65	0	37.04	81.65
32°C (90°F)	INTER	101.5	2452	5405	0	0	1458	2625	363.0	52.64	1054	1897	34.65	76.40	0	34.65	76.40
	VTO	101.9	2489	5487	0	0	1467	2640	366.1	53.10	1060	1909	34.84	76.82	0	34.83	76.82
	MAX	101.9	2805	6183	0	0	1554	2797	411.2	59.46	1144	2060	34.91	76.96	8.74	37.96	83.69
	EMERG	107.0	2884	6358	0	0	1575	2836	392.0	56.85	1144	2060	35.90	79.15	0	35.90	79.15
STD	INTER	10[illegible].5	2844	6270	1.33	2.93	1358	2444	385.4	55.90	986	1775	37.98	83.73	0	37.98	83.73
	VTO	106.6	3227	7115	1.34	2.96	1467	2640	406.3	58.93	1071	1927	38.54	84.69	0	38.54	84.69
	MAX	106.6	3546	7818	1.34	2.96	1542	2775	451.1	65.42	1144	2060	38.50	84.88	7.24	41.29	91.05
	EMERG	110.0	3411	7520	1.34	2.96	1519	2735	415.6	60.28	1112	2002	38.51	84.89	0	38.51	84.89
32°C (90°F)	INTER	101.5	2715	5985	1.26	2.78	1381	2486	388.6	53.46	1005	1809	35.97	79.30	0	35.97	79.30
	VTO	106.0	3072	6772	1.30	2.86	1467	2640	393.2	57.03	1072	1929	37.15	81.92	0	37.15	81.92
	MAX	106.0	3377	7446	1.30	2.86	1541	2774	435.6	63.17	1144	2060	37.24	82.10	7.05	39.86	87.88
	EMERG	110.0	3379	7450	1.30	2.87	1555	2800	408.9	59.30	1142	2055	37.39	82.43	0	37.39	82.43

TABLE 4.1 UNSHROUDED TURBINE TIP CLEARANCE EFFICIENCY PENALTIES

FLIGHT CONDITION	TIP CLEARANCE	EFFICIENCY CHANGE RELATIVE TO SHROUDED TURBINE
VTOL		
Take-Off	0.048	-2.0
Landing	0.056	-2.4
Design Point	0.045	-1.6
Cruise	0.035	-1.1
Loiter	0.070	-3.0

TABLE 4.2

FAN AERO DESIGN PARAMETERS

Selected at Conclusion of Aerodynamic and Mechanical Trade Studies

Total Pressure Ratio	1.319
Static Pressure Ratio	1.074
Corrected Airflow, kg/sec (lb/sec)	293 (646)
Adiabatic Efficiency	0.85
Corrected Tip Speed, m/sec (ft/sec)	342.9 (1125)
Tip Diameter, m (in)	1.499 (59.0)
Radius Ratio	0.407
Specific Flow, kg/sec m^2 (lb/sec ft^2)	199.2 (40.8)
Rotor Tip Relative Mach Number	1.19
Hub Work Coefficient, $2gJ\Delta H/u_h^2$	1.86
Number of Blades	52
Number of Vanes	27
Blade Aspect Ratio	3.77
Vane Aspect Ratio	2.33
Exit Mach Number	0.55

TABLE 4.3

TURBINE AERO DESIGN PARAMETERS

Selected at Conclusion of Aerodynamic and Mechanical Trade Studies

Inlet Temperature, °K (°R) *	1019 (1835)
Inlet Gas Flow, kg/sec (lb/sec) *	37.14 (81.87)
Inlet Pressure, kN/m^2 (lb/in^2) *	350.9 (50.89)
Total-to-Total Pressure Ratio	2.74
Exit Mach Number	0.55
Exit Total Temperature, °K (°R)	829 (1492)
Adiabatic Efficiency	0.86
Design Energy, J/g (BTU/lb)	210 (95.1)
Tip Diameter, m (in)	1.674 (65.89)
Radius Ratio	0.9347
Bucket Length, cm (in)	5.46 (2.15)
Number of Nozzle Vanes	157
Number of Buckets	364
Number of OGVs	9
Bucket Aspect Ratio	2.43
Pitch Wheel Speed, m/sec (ft/sec)	370.5 (1215)
Stage Work Coefficient, $H/2g\ Ju^2$	0.83
Stage Velocity Ratio, u/Vo	0.475
Admission Arc, degrees	360
Hub Reaction, percent	10
Tip Reaction, percent	20

* Scroll Inlet Pressure, Flow and Temperature Based on Estimated Growth Engine Discharge Conditions, and Include 3.1 Percent Ducting and 5.0 Percent Scroll Total Pressure Loss.

TABLE 4.4 TURBINE AERODYNAMIC DESIGN POINT

Location	Hub	Pitch	Tip
Radius, m (in)	1.212 (30.795)	1.255 (31.87)	1.297 (32.945)
P_{s1}/P_{am}	1.193	1.278	1.357
P_{s2}/P_{am}	-	1.036	-
V_1, m/s (ft/sec)	727 (2385)	705 (2314)	685 (2248)
M_1	1.321	1.281	1.245
R_1, m/s (ft/sec)	410 (1344)	382 (1253)	357 (1171)
M_{R1}	0.744	0.688	0.638
α_1, deg	20.1	20.7	21.4
β_1, deg	37.5	40.8	44.4
R_2, m/s (ft/sec)	432 (1417)	442 (1451)	453 (1485)
M_{R2}	0.789	0.808	0.827
V_2, m/s (ft/sec)	302 (992)	302 (991)	302 (990)
M_2	0.553	0.552	0.552
β_2, deg	43.8	42.5	41.3
Swirl Angle, deg	8.8	8.5	8.2
Reaction, percent	10	15	20

TABLE 4.5 PARTIAL ADMISSION LOSS ESTIMATES

	VTOL (2/3 Arc)	Engine Out (1/3 Arc)
Gas Generator Speed, percent	101.9	107.0
Fan Speed, percent	90.3	73.5
Windage Power Loss, kW (hp)	47.6 (64)	44.7 (60)
End Losses, kW (hp)	57.3 (77)	42.4 (57)
Total Losses, kW (hp)	105 (141)	87 (117)
Total Power Loss, percent	2.0	3.1

TABLE 4.6

SCROLL COMPARISON

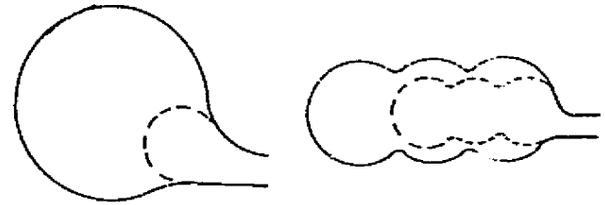

	CIRCULAR	MULTILOBE
Forming Dies Required	10	10
Length of Weld, m (ft)	18.3 (60)	22.9 (75)
Scroll Reference Section Height, cm (in)	28.7 (11.3)	12.2 (7.5)
Minimum Section Height, cm (in)	15.2 (6.0)	12.2 (4.8)
Scroll Performance Loss (Percent of P)	4.30	5.35
Scroll and Casing Weight, kg (lb)	111 (245)	117 (258)
Fan Frontal Area, m^2 (ft^2)	3.14 (33.9)	2.58 (27.8)

TABLE 4.7 SCROLL PRESSURE LOSS ESTIMATES

	Circular	Multilobe
Entrance and Turning Loss	1.20	1.20
Skin Friction	0.70	1.00
Diffusion Loss	1.50	1.50
Strut Loss	0.90	0.90
Tie Rods	0.00	0.75
Total	4.30%	5.35%

TABLE 4.8 SCROLL LIFE ANALYSIS, ASW MISSION

Flight Condition	Temperature °K	Temperature °F	Pressure kN/m²	Pressure lb/in²	Stress kN/m²	Stress lb/in²	Time Hours	Percent Life Used 0.2% Creep	Percent Life Used Rupture	Number of Cycles	Number of Life Cycles
VTO	842	1515	387	56.2	207,000	30,000	5	72.1	16.7	1	600
Transition	778	1400	351	50.9	172,000	25,000	20	4.7	1.0	1	600
Climb	766	1380	195	28.4	37,000	5,400	231	1.9	0.3	2	1200
Loiter	493	887	154	22.4	14,000	2,000	2489	-	-	2	1200
Cruise	447	805	75	10.9	27,000	3,900	245	-	-	2	1200
Landing	806	1450	315	45.7	172,000	25,000	10	21.3	4.5	1	600
							3000	100.0	22.5		

TABLE 4.9

SCROLL DEFECT TOLERANCE

	Maximum Defect Size	
	cm	in
Partial Mission (Landing)	2.03	0.80
One Mission (Takeoff-Landing)	1.47	0.58
Full Service Life (600 Missions)	0.46	0.18

TABLE 4.10

FAN DISK COMPARISON

	Number of Blades	Conventional Disk	Twin-Web Disk
Weight	52 or 56	Equal	
2/Rev Margin (Percent)	56	6.5	0
	52	11	4
3/Rev Cross-Over (Percent Speed)	56	59	51.5
	52	67.5	60

TABLE 4.11

EFFECTS OF LEAN ON FRAME THERMAL STRESSES

	10° Lean				20° Lean				25° Lean			
Outer Ring Temperature	290°C	554°F	230°C	446°F	290°C	554°F	230°C	446°F	290°C	554°F	230°C	446°F
Mid Ring Temperature	290°C	554°F	150°C	302 F	290°C	554°F	190°C	302°F	290°C	554°F	150°C	302°F
Inner Ring Temperature	40°C	104°F	40°C	104°F	40°C	104°F	40°C	104°F	40°C	104°F	40°C	104°F
Stress Locations	kN/m^2	ksi	kN/m^2	ksi	kN/m^2	ksi	kN/m^2	ksi	kN/m^2	ksi	kN/m^2	ksi
Inner Strut	896	130	496	72	731	106	386	56	648	94	352	51
Outer Strut	124	18	90	13	83	12	76	11	62	9	62	9
Mid Ring	1041	151	358	52	579	84	207	30	462	67	179	26
Outer Ring	614	89	614	89	241	35	407	59	152	22	365	53

TABLE 4.12

FRAME STRESSES, THERMAL AND GYRO PRECESSION

Configuration I

- 30 Inner Structural Stators
- 10 Outer Struts
- 20 Degrees Lean
- Temperatures

Inner Ring		Mid-Box		Outer Ring	
°C	°F	°C	°F	°C	°F
40	104	150	302	230	446

Configuration II

- 10 Inner Structural Stators
- 10 Outer Strust
- 20 Degrees Lean
- Temperatures - Same as Configuration I

Thermal Stresses

Member	Configuration I		Configuration II	
	kN/m^2	ksi	kN/m^2	ksi
Inner Ring	131	19	48	7
Mid-Box	345	50	179	26
Outer Ring	241	35	407	59
Inner Strut	607	88	386	56
Outer Strut	34	5	76	11

Gyroscopic Precession Stresses

	Configuration I		Configuration II	
	kN/m^2	ksi	kN/m^2	ksi
Inner Ring	124	18	145	21
Mid-Box	134	20	110	16
Outer Ring	14	2	34	5
Inner Strut	103	15	234	34
Outer Strut	96	14	96	14

TABLE 4.13 STRESSES FOR SELECTED FRAME CONFIGURATION

	Gyro Precession Moment		10g Down Maneuver		4g Side Maneuver		Rotor Thrust		Stator Airloads		Combined		Thermal Stress		Maneuver + Thermal		0.2% Yield		36,000 Cycle Limit			
																			Densified		Undensified	
	kN/m^2	ksi	kN/m^2	ksi	kN/m^2	ksi	kN/m^2	ksi	kN/m^2	ksi	kN/m^2	ksi	kN/m^2	ksi	kN/m^2	ksi	kN/m^2	ksi	kN/m^2	ksi	kN/m^2	ksi
Inner Ring	222.7	32.3	43.4	6.3	21.4	3.1	83.4	12.1	40.0	5.8	279.2	40.5	53.1	7.7	332.3	48.2	606.7	88	772.2	112	599.8	87
Outer Ring	55.8	8.1	283.7	41.1	69.6	10.1	107.5	15.6	159.9	23.2	370.2	53.7	518.5	60.7	788.8	114.4	930.8	135	N/A		1158.3	168
Inner Structural Vane	238.5	34.6	71.7	10.4	21.4	3.1	131.7	19.1	74.5	10.8	317.2	46.0	229.6	33.3	546.7	79.3	606.7	88	772.2	112	599.8	87
Outer Strut	102.0	14.8	75.8	11.0	19.3	2.8	48.9	7.1	73.8	10.7	132.4	19.2	120.6	17.5	253.0	36.7	524.0	76	772.2	112	599.8	87

TABLE 5.1

ROTOR MATERIALS

Structural Spinner	6061 Al
Fan Disk and Shaft	Ti 6-4
Fan Blades	Ti 17
Turbine Carriers and Blades	Rene 80 (Cast)
Bearings	M50
Bearing Support Cone	Ti 6-4

TABLE 5.2

SCROLL MATERIALS

Scroll Shell	Rene 41 (Sheet)
Nozzle Vanes	Rene 41 (Sheet)
Fan Casing	(Inco 718 (Bar/Sheet)
Seal Support Struts	Inco 718 (Cast)
Casing Seal	Inco 625 (Sheet)
Honeycomb Seal	Hastelloy X (Sheet)
Insulation *	Min-K

* Suggested Insulation, Insulation is Aircraft-Furnished

TABLE 5.3

FRAME MATERIALS

Hub	Inconel 718
Hub Liner	Nylon
Structural Vane	Inconel 718
Non-Structural Vane	7075 Aluminum
Mid Section Liners	Hastelloy X
Outer Case	Inconel 718
Outer Case Liner	Hastelloy X
Outer Strut	Inconel 718

TABLE 5.4

FRAME STRUT AND VANE GEOMETRY

	Inner Structural		Inner Non-Structural		Outer	
	Hub	Tip	Hub	Tip	Hub	Tip
Chord, m (in)	16.9 (6.67)					
t_m/c	0.08	0.08	0.04	0.04	0.12	0.12
Camber, degrees	37.1	30.5	37.1	30.5	0	0
Stagger, degrees	8.3	12.5	8.3	12.5	3	3
Airfoil Type	Double Circular Arc				NACA 65 A012	

TABLE 5.5 TURBINE TIP SHROUD RUNNING CLEARANCES

Flight Condition	Assumed Maneuvers	Rotor/Stator Relative Motion				Total		Running * Clearance	
		Maneuver Loading		Thermal/Centrifugal					
		(cm)	(in)	(cm)	(in)	(cm)	(in)	(cm)	(in)
Idle	0	0	0	-0.036	-0.014	-0.036	-0.014	0.228	0.090
VTO									
Takeoff	0.5 rad/sec; 3g	+0.048	+0.019	+0.071	+0.028	+0.119	+0.047	0.122	0.048
Landing	1.0 rad/sec; 5g	+0.096	+0.038	+0.071	+0.018	+0.142	+0.056	0.142	0.056
Design Point	0.3 rad/sec; 3g	+0.033	+0.013	+0.079	+0.031	+0.117	+0.046	0.114	0.045
Cruise	0.3 rad/sec; 3g	+0.033	+0.013	+0.104	+0.041	+0.137	+0.054	0.089	0.035
Loiter	0.5 rad/sec; 3g	+0.048	+0.019	+0.015	+0.006	+0.063	+0.025	0.178	0.070

Build-Up Clearance is Largest Relative Motion Plus 0.051 cm (0.020 in) for Assembly Build-Up = 0.142 cm (0.056 in) + 0.051 cm (0.020 in)
= 0.193 cm (0.076 in)

* Running Clearance is Build-Up Clearance Minus Thermal/Centrifugal Clearance

TABLE 5.6

LCF459 WEIGHT

	kg	lb
Rotor		
Turbine	19	(42)
Blades	67	(147)
Disk	55	(122)
Bearings and Sump	27	(59)
Frame	107	(235)
Scroll	111	(245)
	386	(850)

TABLE 5.7

WEIGHTS OF ALTERNATE LCF459 FANS

	kg	lb
Multilobe Scroll 120-240 Degree Inlets	391	(863)
Circular Scroll 180-180 Degree Inlets	386	(850)
Multilobe Scroll Single Inlet	395	(870)

TABLE 5.8

INERTIA OF ROTATING COMPONENTS

	Design RPM	Moment of Inertia kg-m-sec^2	Moment of Inertia lb-ft-sec^2
LCF459	4,370	2.97	21.5
YJ97-GE-100	13,650	0.239	1.73
Growth J97	14,230	0.265	1.92

TABLE 5.9

J97 COMPONENT SURFACE TEMPERATURE LIMITS

	Temperature °C	Temperature °F
Front Frame	177	350
Compressor Casing	343	650
Compressor Rear Frame	649	1200
Transfer Gearbox	177	350
Unibal Race, Thrust Mounting	316	600

TABLE 5.10

COMPARISON OF GROWTH J97 AND YJ97-GE-100 DISCHARGE CONDITIONS

	YJ97-GE-100 *		Growth J97 *	
Speed, percent	101.5		101.5	
Airflow, kg/sec (lb/sec)	32.00	(70.54)	37.31	(82.25)
Total Pressure, kN/m^2 (lb/in^2)	385.1	(55.98)	385.9	(55.97)
Turbine Inlet Temperature °K (°R)	1382	(2489)	1426	(2567)
Total Temperature, °K (°R)	1019	(1835)	1028	(1851)
Fuel Flow, kg/hr (lb/hr)	2188	(4824)	2586	(5701)
Ideal Gas Power, kw (hp)	10,231	(13,720)	12,475	(16,730)
Flow Function, $W\sqrt{T/P}$	2.797	(57.04)	3.090	(63.20)

* Uninstalled, Sea Level Static, Standard Day,
Total Pressure Given at Engine Turbine Discharge

TABLE 5.11

FAN/ENGINE COMBINATIONS

Mission	Fans/Engines	Engine	Water
ASW, CSAR SURV, SA	3/2	Growth	Yes
	2/2	YJ97-GE-100	No
VOD	3/3	Growth	No
	2/2	YJ97-GE-100	No
Technology Aircraft	3/3	YJ97-GE-100	No

TABLE 5.12

FAN AND TURBINE DESIGN POINT PARAMETERS

FAN	
Airflow, kg/sec (lb/sec)	293.0 (646)
Pressure Ratio	1.319
Speed, RPM	4370
Efficiency	0.850
Fan Exit Mach Number	0.55
TURBINE	
Corrected Speed, RPM/$\sqrt{°K}$ (RPM/$\sqrt{°R}$)	134.61 (101.59)
Energy Function, J/°K (BTU/°R)	0.2386 (0.05113)
Efficiency	0.860
Pressure Ratio	2.65
Turbine Exit Mach Number	0.55
MISCELLANEOUS	
Fan Mach Number at Mixing Station	0.50
Turbine Diffuser Loss Coefficient	0.13
Forward Air Seal Buffer Air, percent	0.23
Impingement Cooling Air, percent	0.23
Ducting Total Pressure Loss, percent	3.1
Scroll Total Pressure Loss, percent	5.0
Ducting Leakage, percent	0.0
Thrust (Uninstalled), kN (lb)	75.13 (16,890)

* Fan Turbine Performance Based on Growth Engine Gas Condition Given in Table 5.10

TABLE 5.13

INSTALLATION ASSUMPTIONS FOR VTOL OPERATION

Fan Inlet Recovery	0.985
Exhaust Nozzle Thrust Coefficient	0.940
Fan Shaft Power Extraction, kw (hp)	37.2 (50)
Ducting Total Pressure Loss, percent	3.1
Fan Stall Margin, percent *	27

* Fan Nominal Operating Line gives Stall Margin = 18%, VTO Operation at 25% gives Maximum Static Thrust.

TABLE 5.14 VTOL PERFORMANCE, THREE FANS WITH TWO GROWTH J97 ENGINES

(INSTALLED, SEA LEVEL STATIC, 32°C [90°F] DAY)

		NORMAL OPERATION (1)					ENGINE-OUT OPERATION (2)					ENGINE-OUT OPERATION (4% WATER) (2)				
PCNG pct	Condition	PCNF pct	W22 kg/sec	W22 lb/sec	F_N kN	F_N lb	PCNF pct	W22 kg/sec	W22 lb/sec	F_N kN	F_N lb	PCNF pct	W22 kg/sec	W22 lb/sec	F_N kN	F_N lb
92	NOM	65.9	189	417	23.89	5370	48.9	136	300	11.98	2693	49.5	138	304	12.11	2722
95	NOM	75.1	217	479	31.89	7171	56.2	158	349	16.56	3723	57.2	161	356	17.23	3874
	MAX	91.9	264	582	50.27	11301	71.8	207	457	28.95	6509	75.0	217	479	32.14	7225
98	NOM	83.1	241	531	40.00	8993	63.7	182	401	22.03	4953	64.5	185	407	22.74	5113
	MAX	94.8	271	597	53.89	12115	74.1	215	473	31.28	7032	77.3	224	494	34.67	7795
101.5	NOM	89.8	259	570	47.44	10664	69.8	202	445	27.21	6117	70.5	204	449	27.84	6258
	MAX	96.7	275	607	56.20	12634	75.5	219	482	32.71	7354	78.8	229	504	36.25	8150
101.9	NOM	90.3	260	573	48.45	10892	-	-	-	-	-	-	-	-	-	-
	MAX	96.7	275	607	56.21	12636	73.5	213	469	30.68	6897	-	-	-	-	-
107.0	MAX	-	-	-	-	-	-	-	-	-	-	-	-	-	-	-
110.0	MAX	-	-	-	-	-	-	-	-	-	-	75.4	219	482	32.64	7337

(1) Three Fans on Two Engines

(2) Three Fans on One Engine

TABLE 5.15 VTOL PERFORMANCE, EQUAL NUMBER OF FANS, YJ97-GE-100 ENGINES

(INSTALLED, SEA LEVEL STATIC, 32°C [90°F] DAY)

		NORMAL OPERATION (1)					ENGINE-OUT OPERATION (2)					ENGINE-OUT OPERATION (4% WATER) (2)				
PCNG pct	Condition	PCNF pct	W22 kg/sec	W22 lb/sec	F_N kN	F_N lb	PCNF pct	W22 kg/sec	W22 lb/sec	F_N kN	F_N lb	PCNF pct	W22 kg/sec	W22 lb/sec	F_N kN	F_N lb
92	NOM	69.3	200	441	27.35	6148	59.4	169	373	19.14	4303	60.0	171	377	19.62	4410
95	NOM	79.3	262	578	37.12	8344	68.6	198	436	26.40	5935	69.2	200	441	27.03	6076
	MAX	97.4	269	593	58.10	13061	85.5	247	545	43.49	9778	89.0	256	565	47.72	10727
98	NOM	88.2	254	560	47.04	10575	76.5	221	489	33.98	7640	77.0	223	492	34.56	7770
	MAX	100.5	283	623	61.47	13818	88.2	254	561	46.75	10510	92.0	264	582	51.49	11575
101.5	NOM	95.6	273	601	56.22	12638	83.6	242	534	41.24	9272	83.9	243	536	41.76	9388
	MAX	102.2	285	629	63.41	14255	90.0	259	571	48.91	10996	93.9	269	593	54.05	12152
102.7	NOM	97.1	276	609	58.76	13029	-	-	-	-	-	-	-	-	-	-
	MAX	102.3	286	630	63.56	14288	-	-	-	-	-	-	-	-	-	-
107.5	MAX	-	-	-	-	-	88.2	254	560	46.63	10483	-	-	-	-	-
110.0	MAX	-	-	-	-	-	-	-	-	-	-	90.0	259	571	48.97	11010

(1) Three Fans on Three Engines

(2) Three Fans on Two Engines

TABLE 5.16

INSTALLATION ASSUMPTIONS FOR CRUISE PERFORMANCE

Engine Power Extraction, kw (hp)	18.6 (25)
Fan Shaft Power Extraction, kw (hp)	18.6 (25)
Engine Compressor Bleed, percent	1.0
Ducting Pressure Loss, percent	3.1
Nozzle Thrust Coefficient	0.98
Fan Stall Margin, percent	20

Mach Number	Engine Inlet Recovery	Fan Inlet Recovery
0.0	0.985	0.985
0.2	0.989	0.993
0.4	0.990	0.995
0.6	0.990	0.994
0.8	0.987	0.980
0.9	0.984	0.970

TABLE 5.17

COMPARISON OF LCF459 AND LF460 FAN SYSTEMS

	LCF459	LF460
Diameter, m (in)	1.50 (59.0)	1.52 (59.95)
Tip Speed, m/sec (ft/sec)	343 (1125)	343 (1125)
Airflow, kg/sec (lb/sec)	293 (646)	280 (617)
Pressure Ratio	1.32	1.36
Thrust, kn (lb)	12640 (16950)	11230 (15060)
Rotor Inertia, kg-m-sec^2 (lb-ft-sec^2)	2.97 (21.5)	2.70 (19.5)

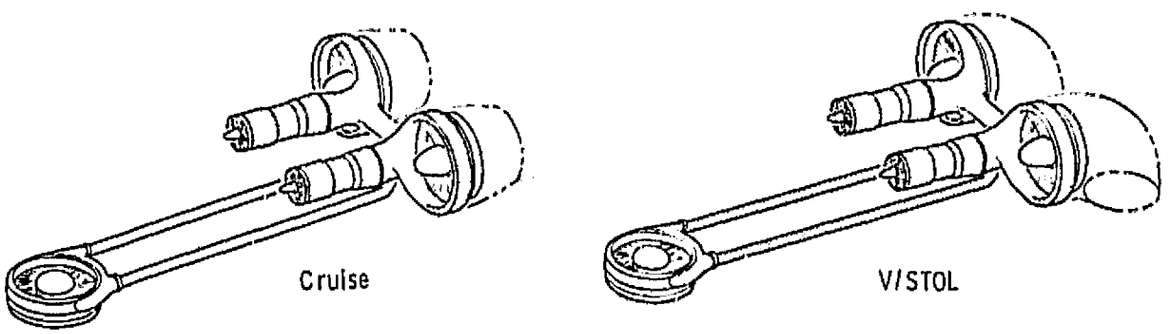

Figure 2.1 Schematic of Three-on-Two Arrangement.

Figure 2.2 Schematic of Two-on-Two Arrangement.

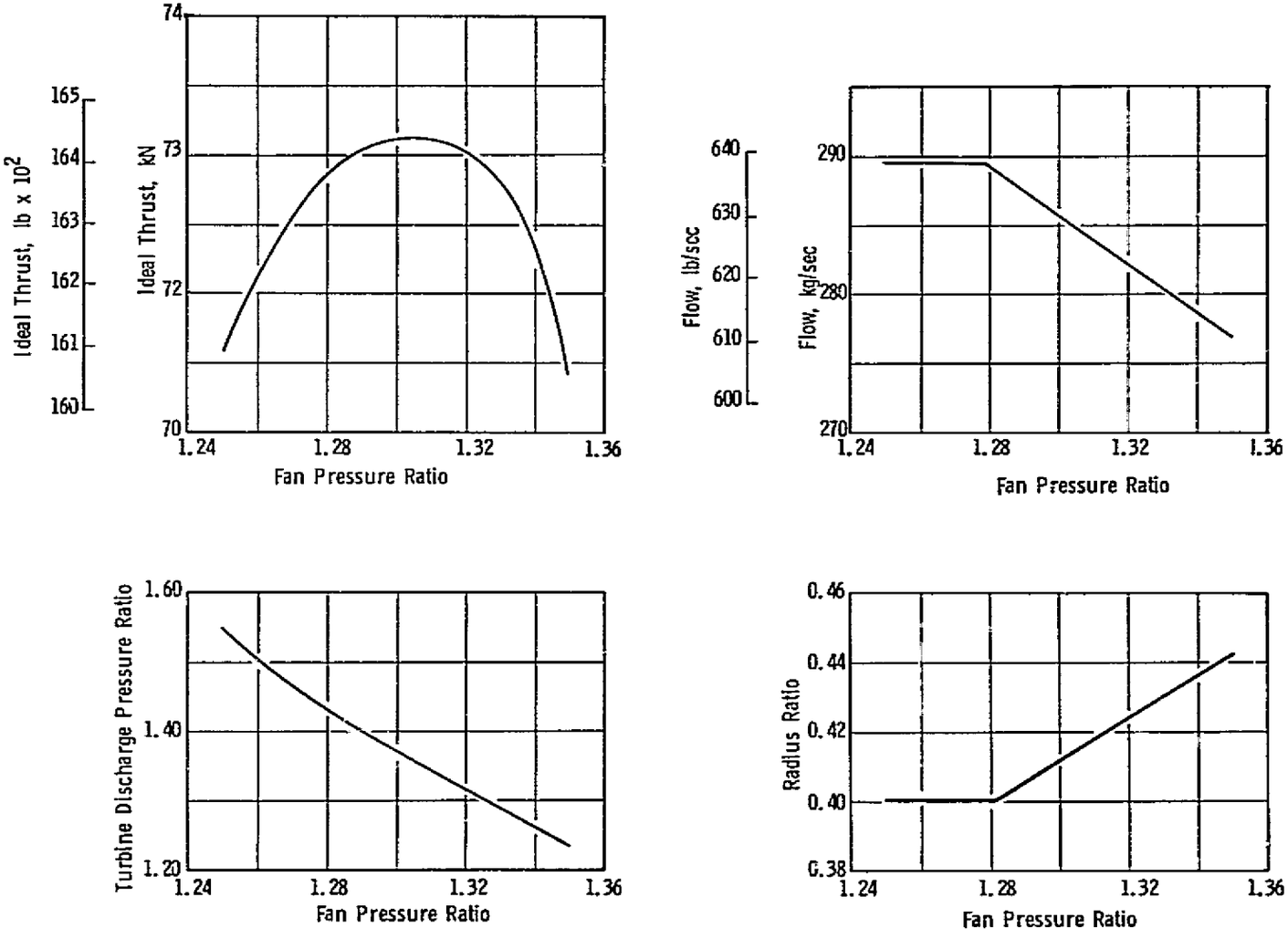

Figure 2.3 Effects of Parameters on Fan Design.

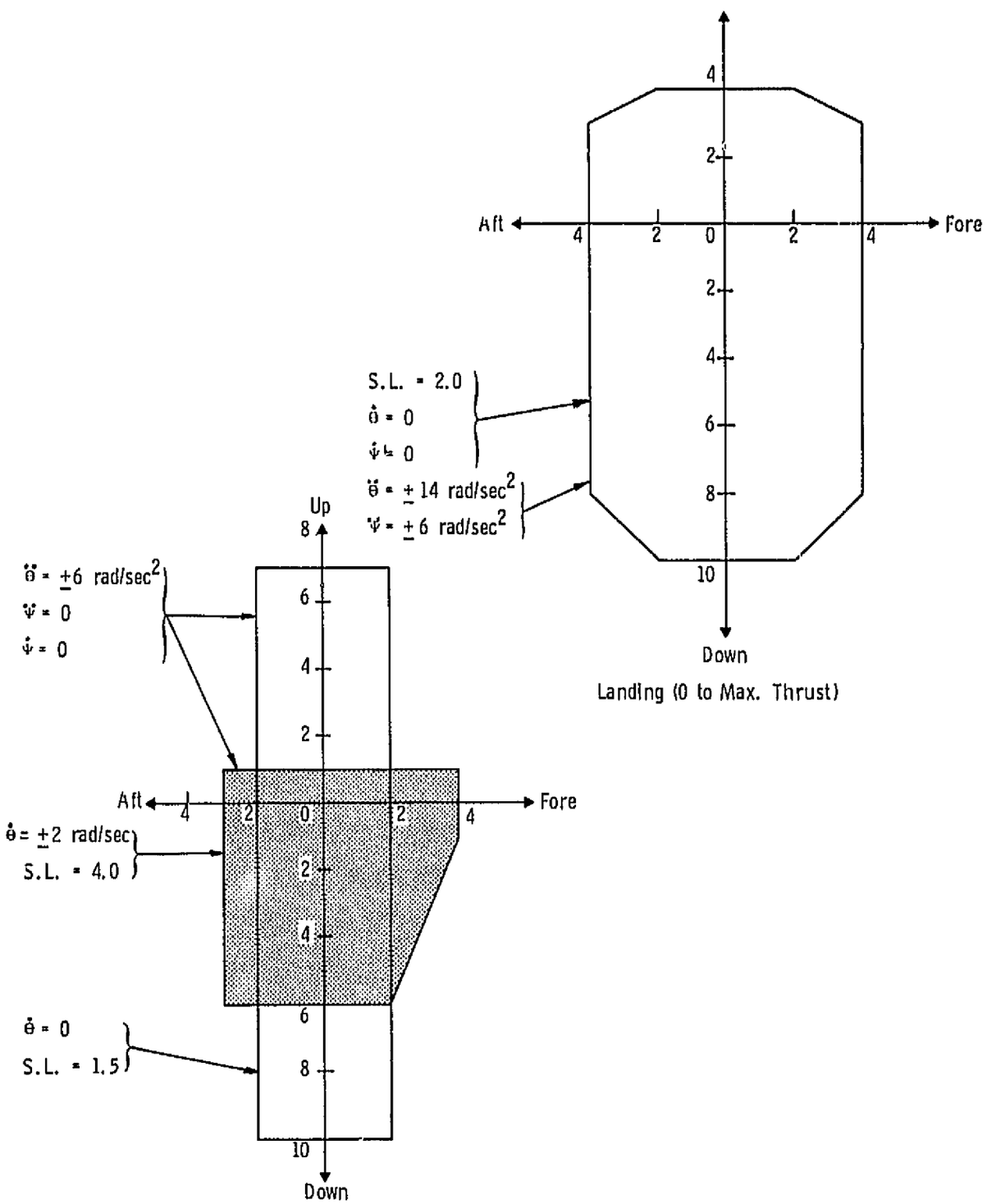

Figure 2.4 Maneuver Loading Criteria.

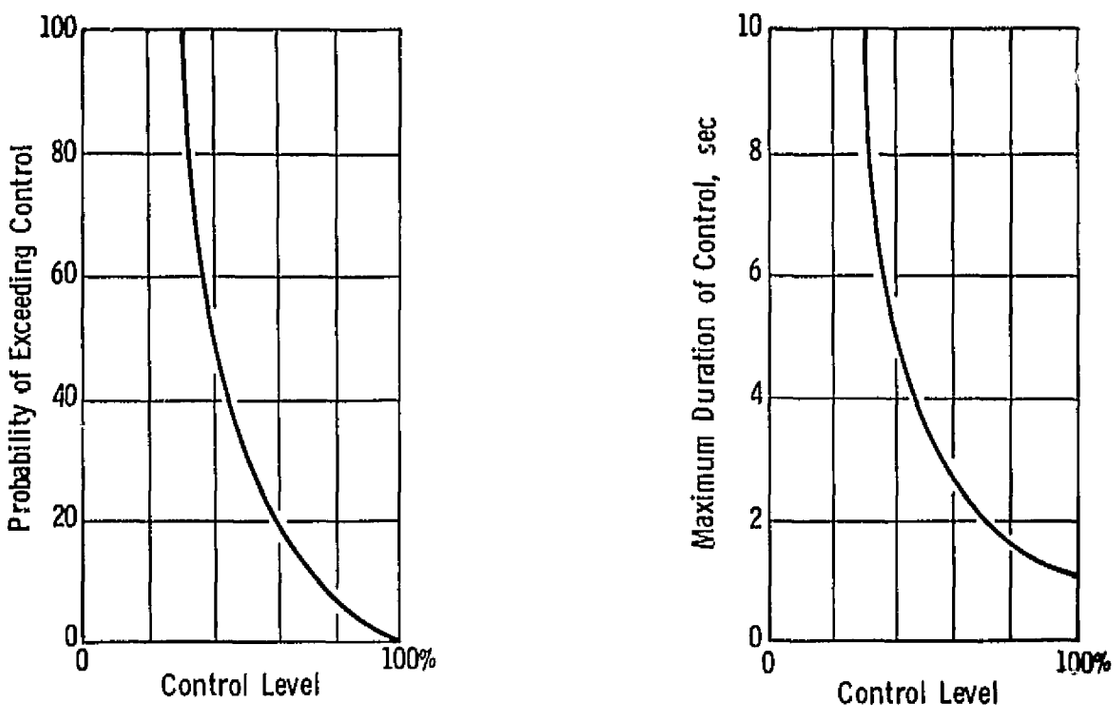

Figure 2.5 Control Duty Cycle.

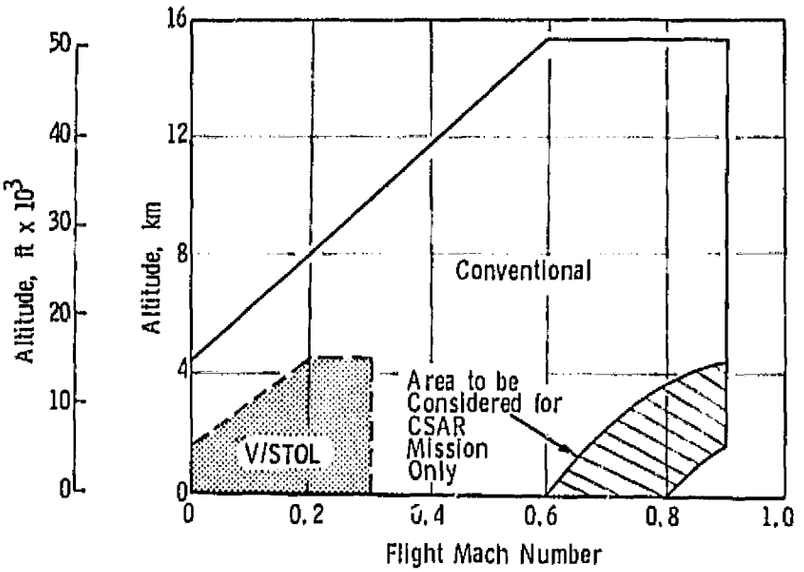

Figure 2.6 Flight Envelope.

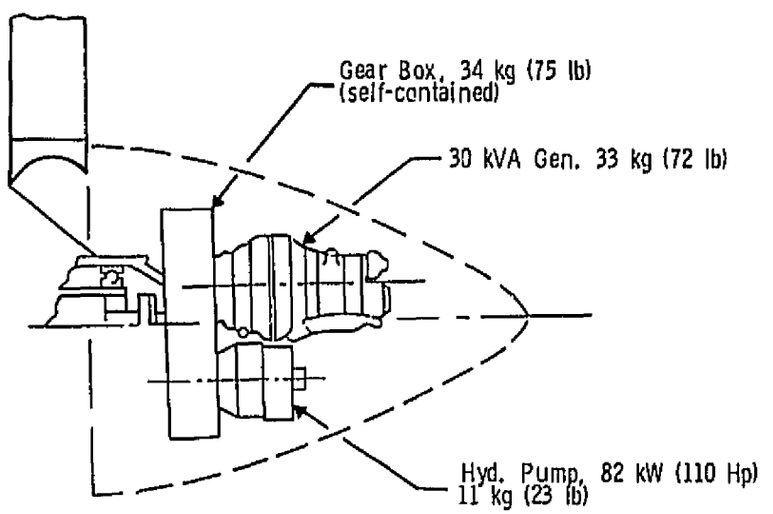

1g Loads
Shear - - - 77 kg (170 lb)
Overhung Moment - - - 283 N-m (2500 lb-in)

Figure 2.7 Typical Aircraft Accessory Package.

Anti-Submarine Warfare (ASW)

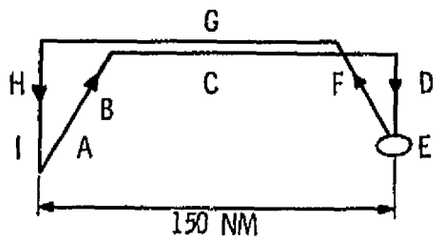

A) Warmup, TO Accel to Vcl	2 Min Int Thrust + 1/2 Min TO Thrust
B) Climb: Intermediate Thrust	SL to Opt Alt
C) Cruise Out: Altitude/Mach	Opt/Opt
D) Descend	-
E) Loiter 4 Hr: Altitude/Mach	10K/Opt
F) Climb: Intermediate Thrust	10K to Opt Alt
G) Cruise Return: Altitude/Mach	Opt/Opt
H) Descend	-
I) Reserves	5% Initial Fuel + 10 Min Loiter at SL

Vertical On-Board Delivery (VOD)

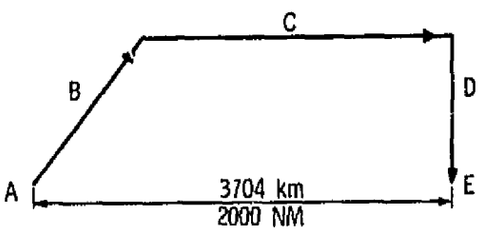

A) Warmup, TO Accel to Vcl	2 Min Int Thrust + 1/2 Min TO Thrust
B) Climb: Intermediate Thrust	SL to Opt Alt
C) Cruise: Altitude/Mach	Opt/Opt
D) Descend	-
E) Reserves	5% Initial Fuel + 20 Min Loiter at SL

Figure 2.8 Mission Definitions.

Surface Attack (SA)

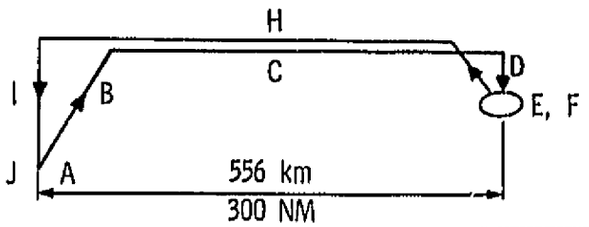

A) Warmup, TO, Accel to Vcl	2 Min Int Thrust + 1/2 Min TO Thrust
B) Climb: Intermediate Thrust	SL to Opt Alt
C) Cruise Out: Altitude/Mach	Opt/Opt
D) Descend	-
E) Loiter 2 Hr: Altitude/Mach	20K/Opt
F) Combat: Time/Altitude/Mach	5 Min/20K/0.8
G) Climb: Intermediate Thrust	20K to Opt Alt
H) Cruise Return: Altitude/Mach	Opt/Opt
I) Descend	-
J) Reserves	5% Initial Fuel + 10 Min Loiter at SL

Surveillance (SURV)

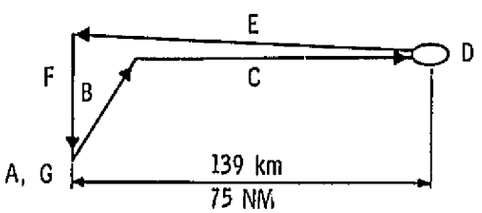

A) Warmup, TO Accel to Vcl	2 Min Int Thrust + 1/2 Min TO Thrust
B) Climb: Intermediate Thrust	SL to Opt Alt
C) Cruise Out: Altitude/Mach	Opt/Opt
D) Loiter 4 Hr: Altitude/Mach	25K +/Opt
E) Cruise Return: Altitude/Mach	Opt/Opt
F) Descend	-
G) Reserves	5% Initial Fuel + 10 Min Loiter at SL

Figure 2.8 Mission Definitions (Continued).

Combat (Strike) Search and Rescue (CSAR)

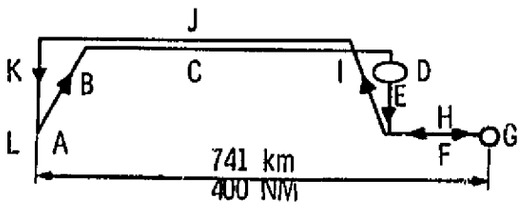

A) Warmup, TO Accel to Vcl	2 Min Int Thrust + 1/2 Min TO Thrust
B) Climb: Intermediate Thrust	SL to Opt Alt
C) Cruise Out: Altitude/Mach	Opt/Opt
D) Loiter: Altitude/Mach	Opt/Opt
E) Descend	-
F) Dash 50 NM: Altitude/Mach	SL/0.8
G) Hover, Rescue 2 Men	10 Min
H) Dash 50 NM: Altitude/Mach	SL/0.8
I) Climb: Intermediate Thrust	SL to Opt Alt
J) Cruise Return: Altitude/Mach	Opt/Opt
K) Descend	-
L) Reserves	5% Initial Fuel + 10 Min Loiter at SL

Figure 2.8 Mission Definitions (Concluded).

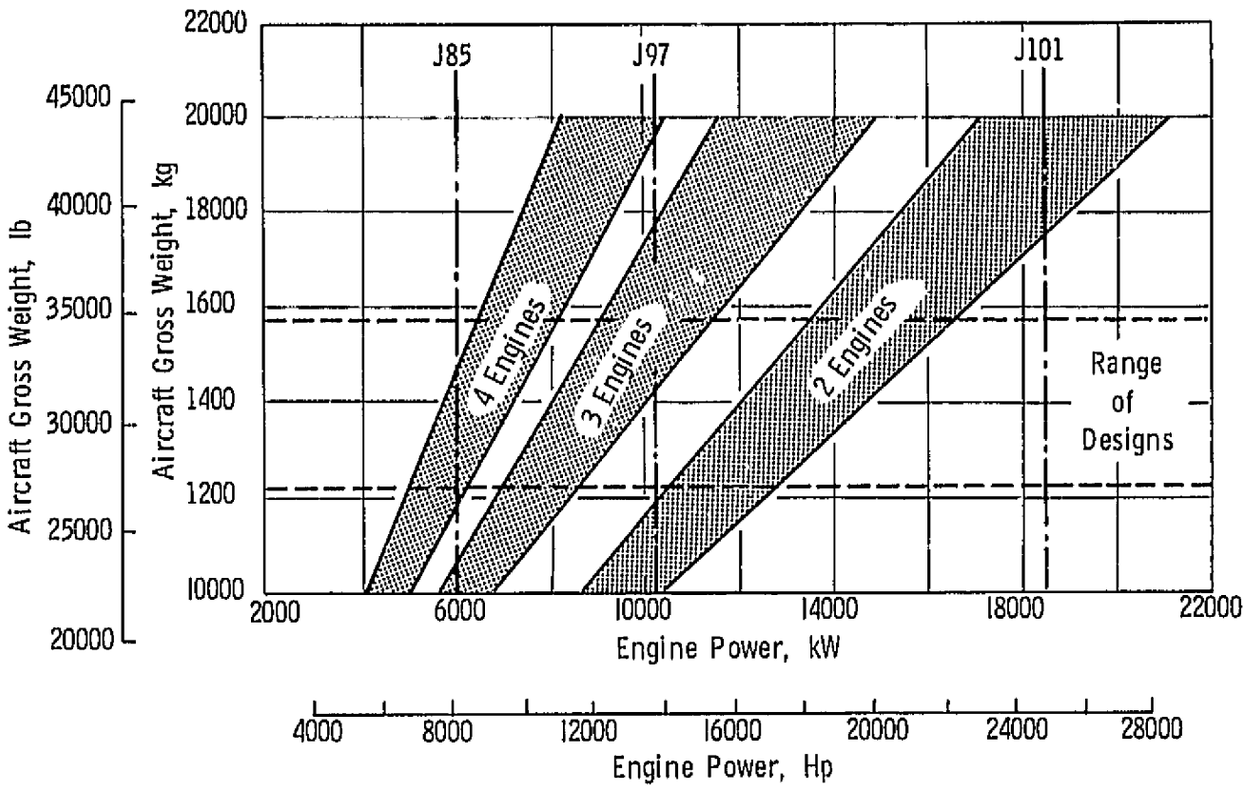

Figure 3.1 Engine Power - Aircraft Gross Weight Comparison.

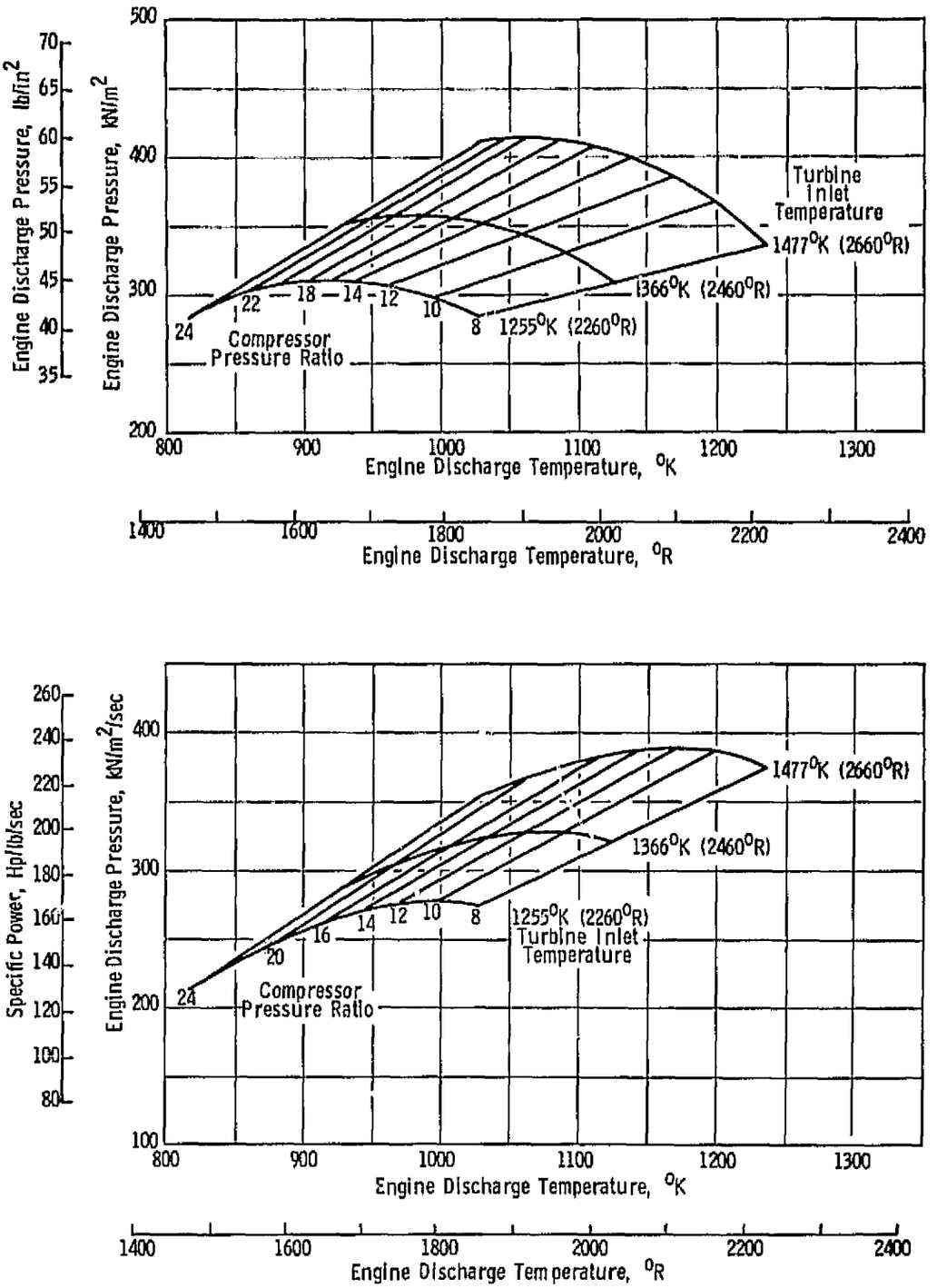

Figure 3.2 Turbojet Discharge Pressure - Gas Power Characteristics.

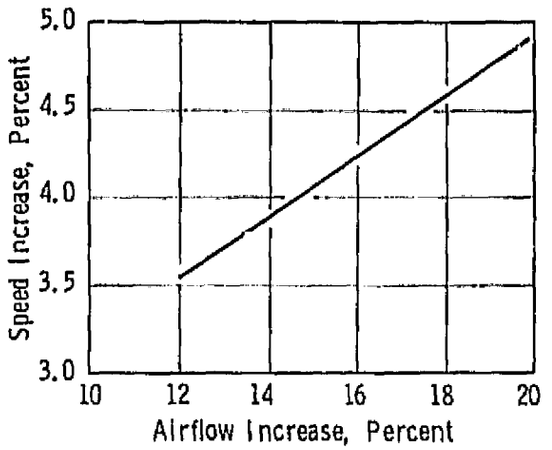

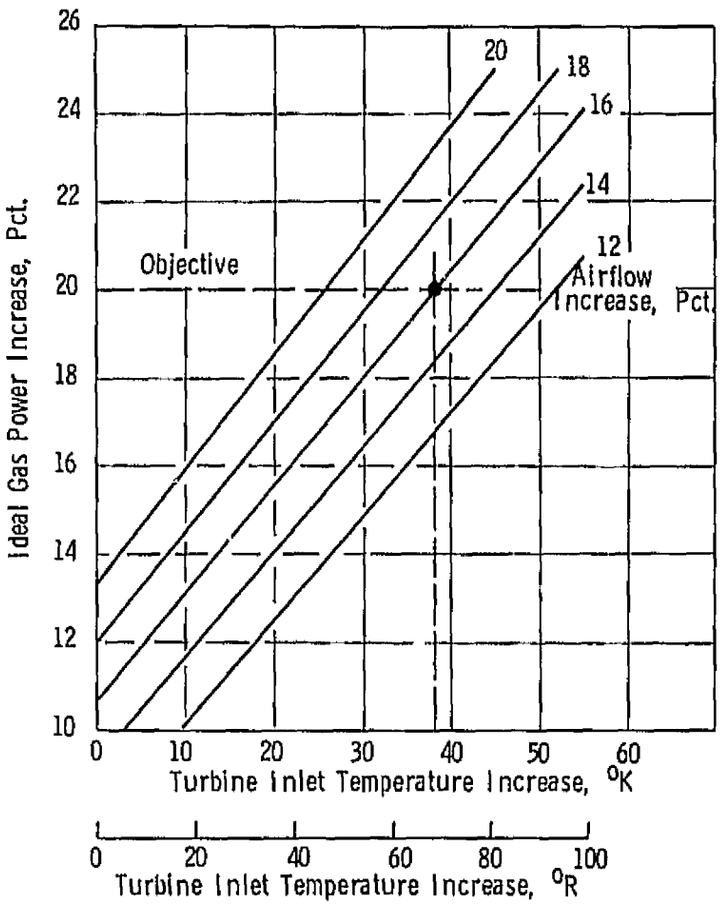

Figure 3.3 J97 Growth Characteristics.

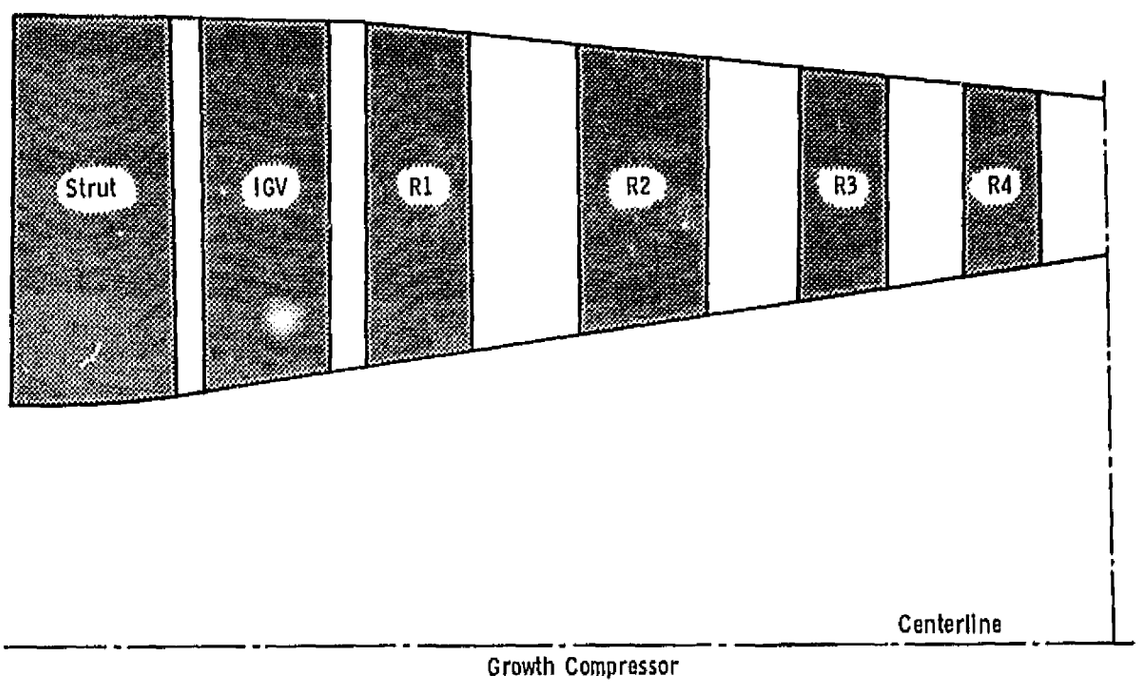

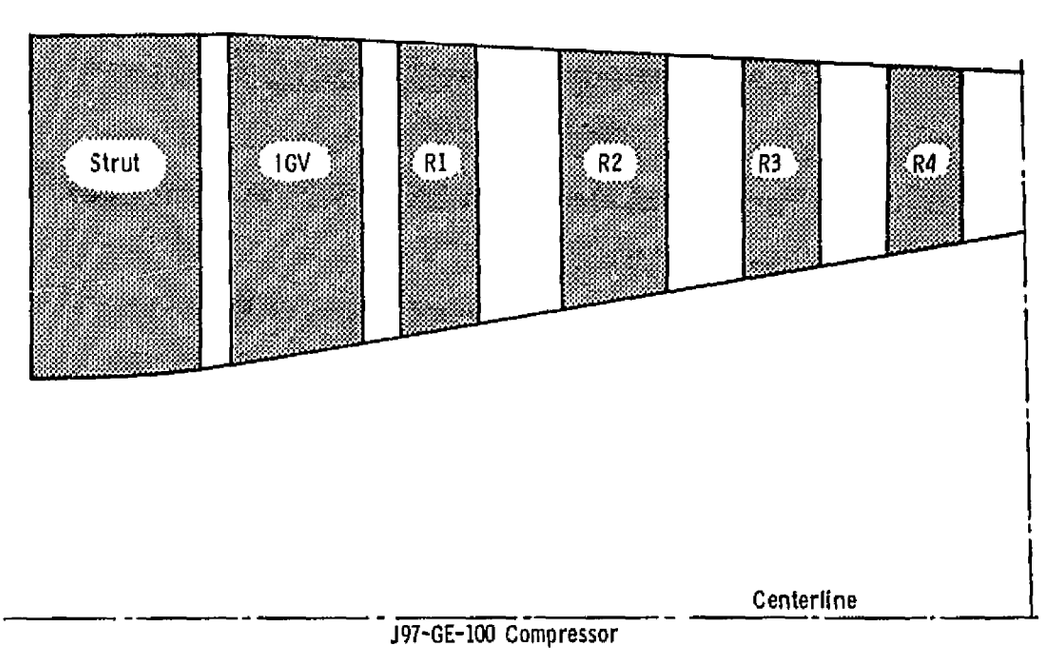

Figure 3.4 J97 Flowpath Comparison.

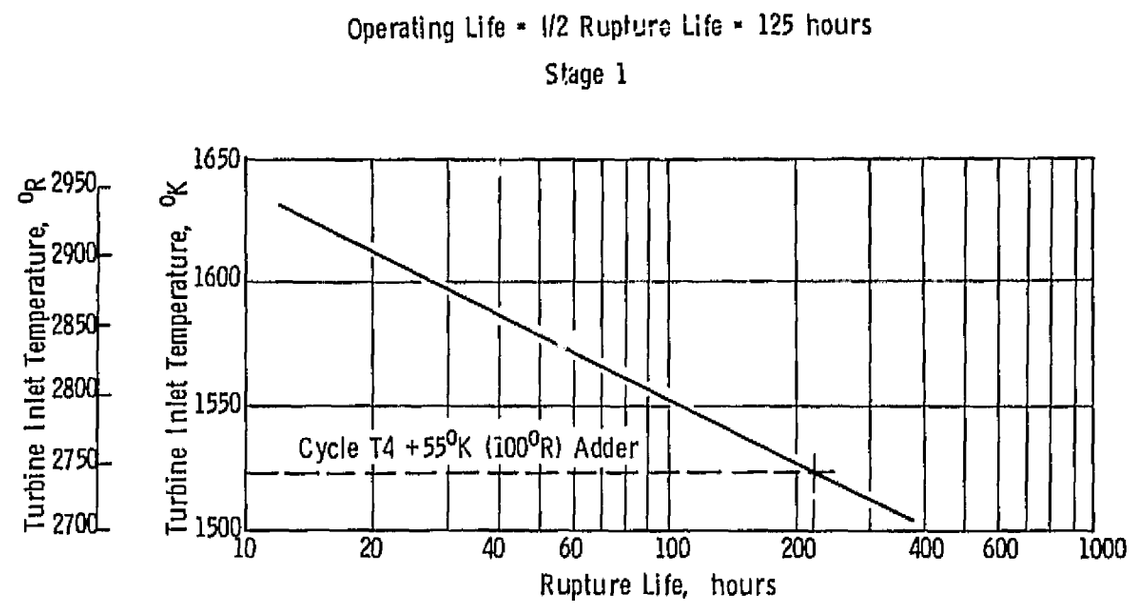

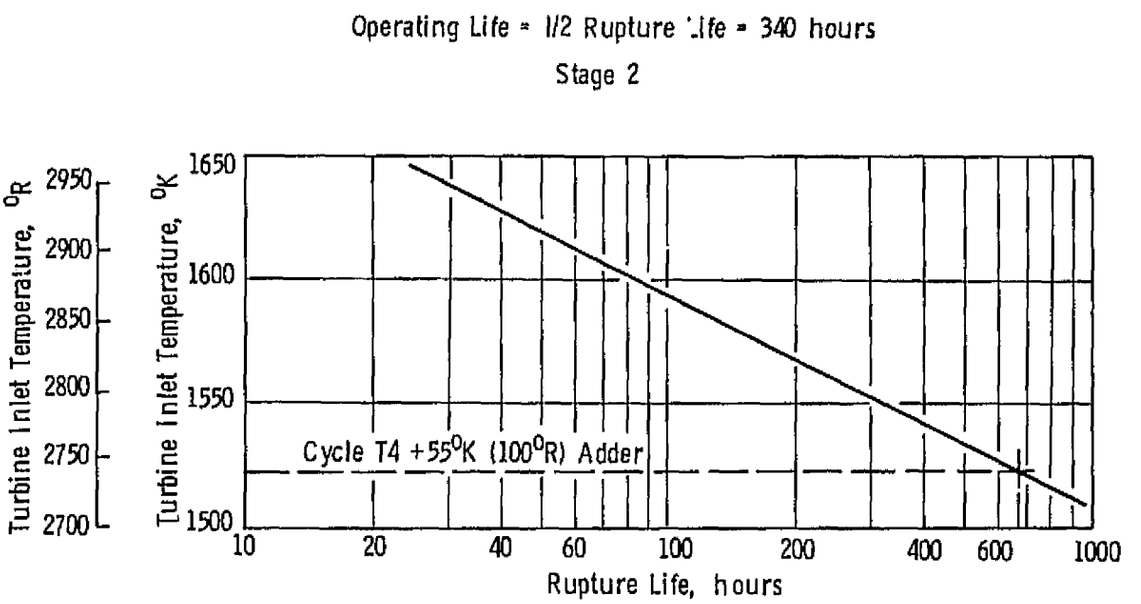

Figure 3.5 Growth J97 Turbine Life Analysis.

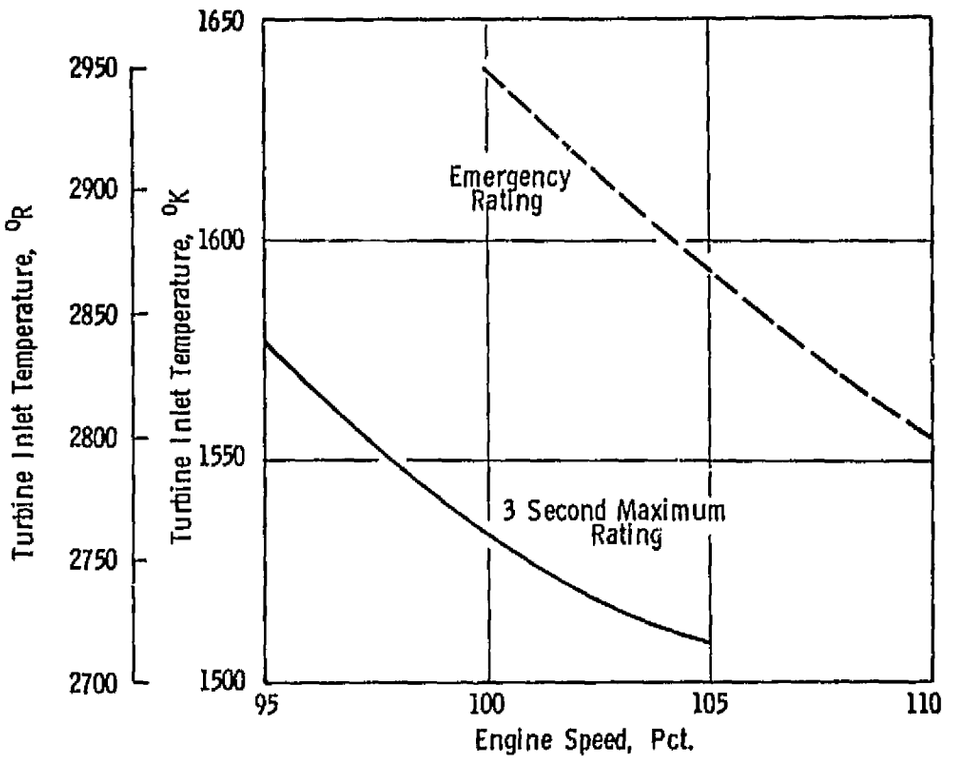

Figure 3.6 Engine Short-Time Limits.

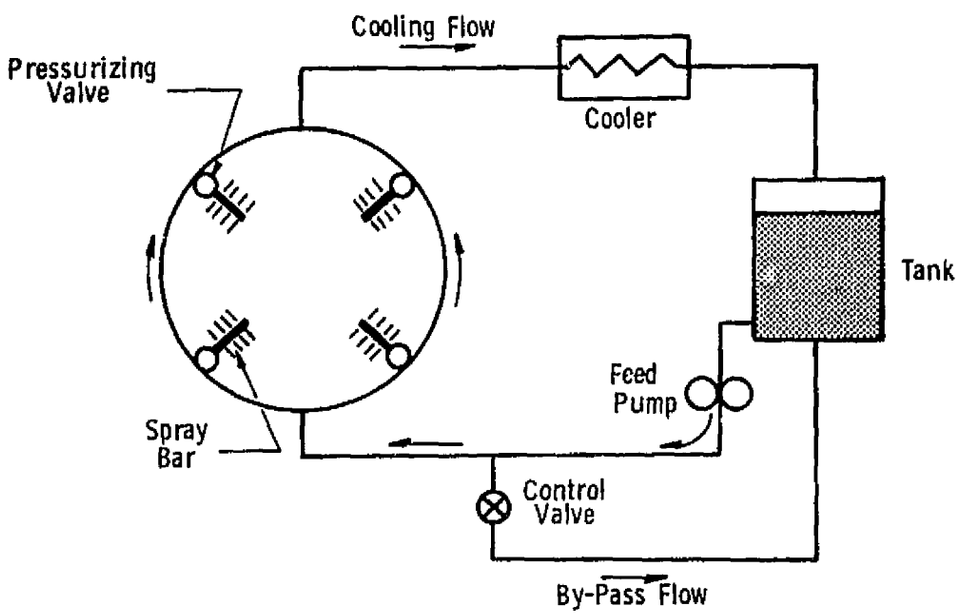

Figure 3.7 Water Injection System.

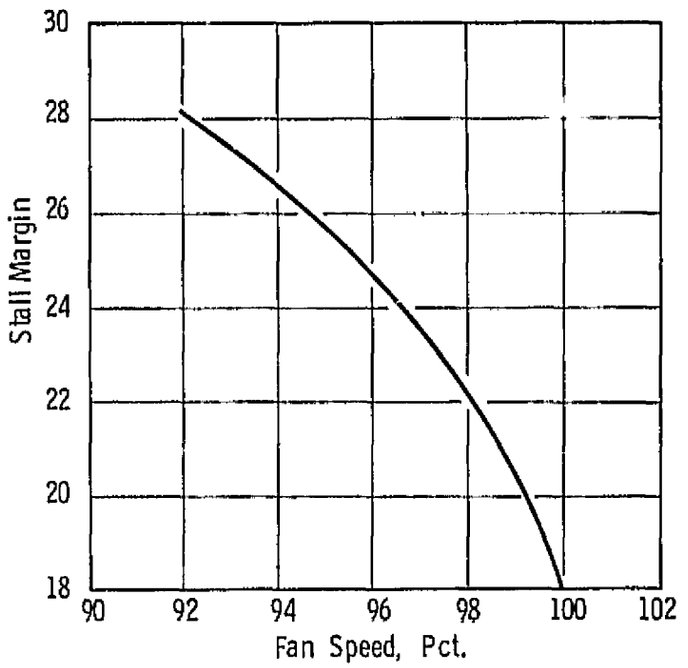

Figure 4.1 Stall Margin for Maximum Thrust.

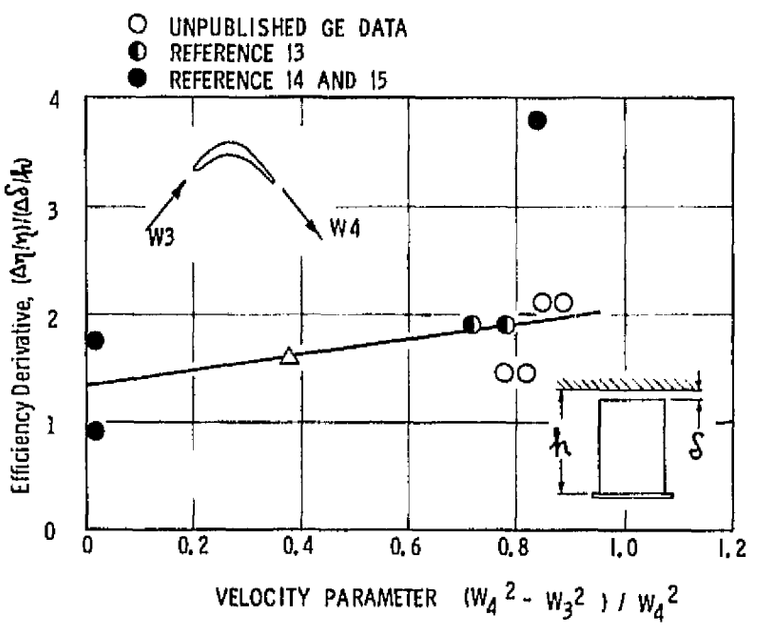

Figure 4.2 Effects of Tip Clearance on Unshrouded Turbine Efficiency.

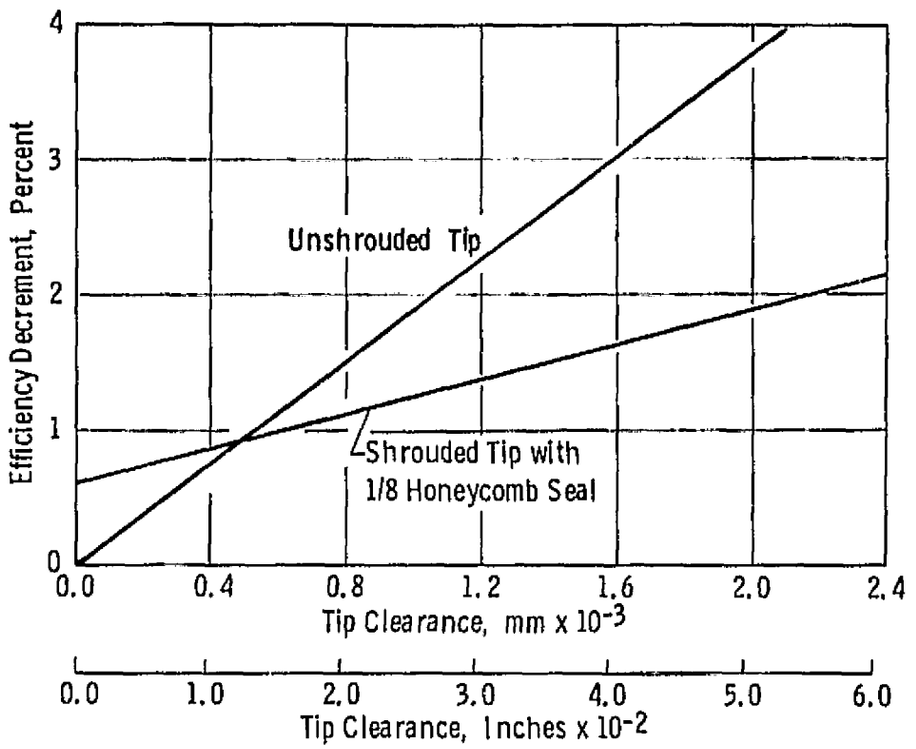

Figure 4.3 Tip Clearance Efficiency Derivatives.

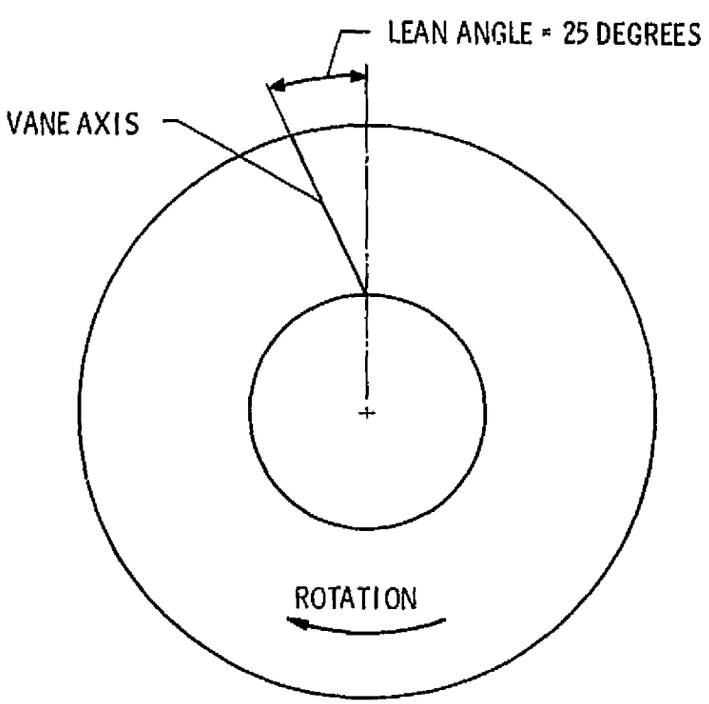

Figure 4.4 Stator Lean.

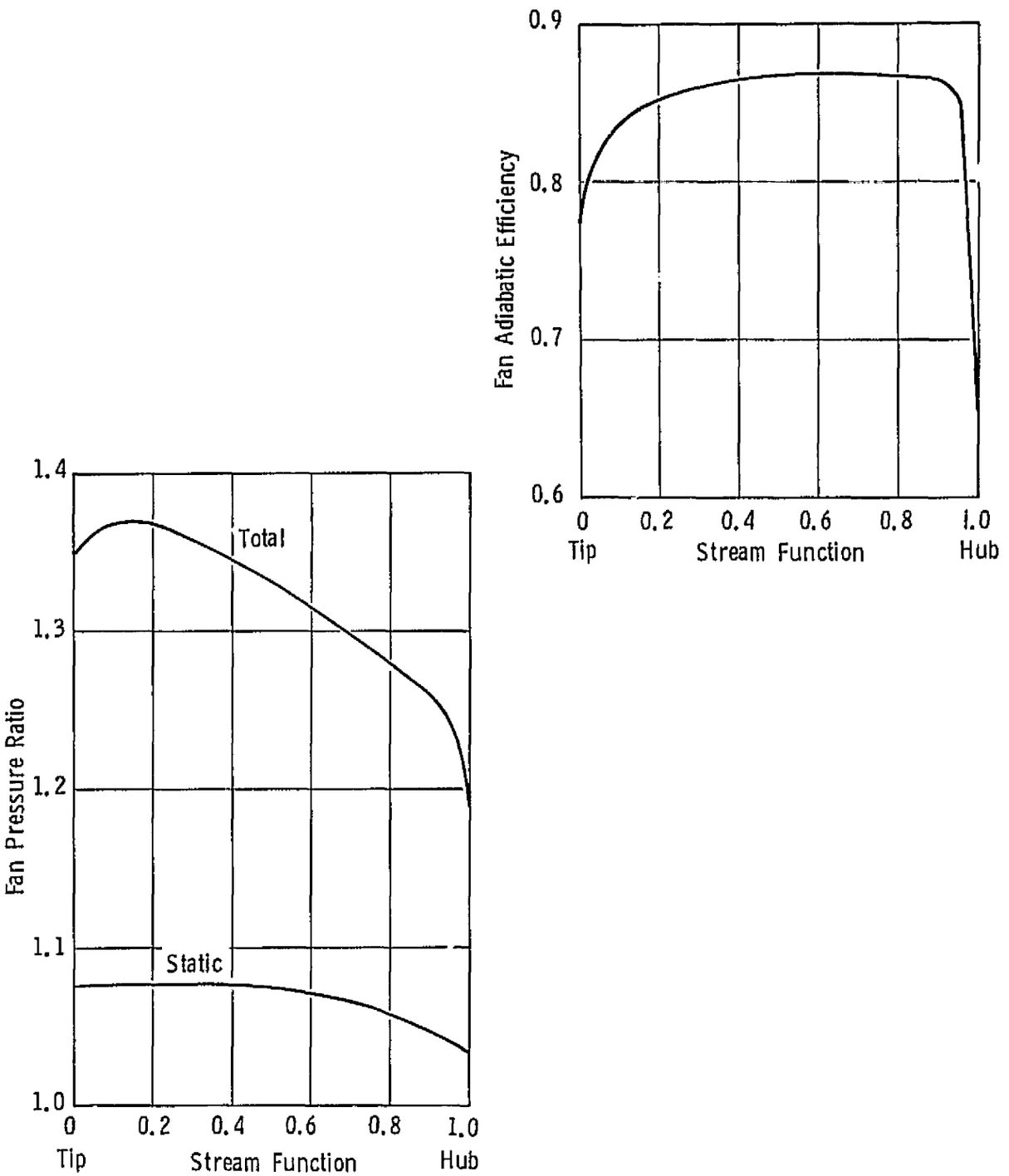

Figure 4.5 Fan Pressure Ratio and Efficiency.

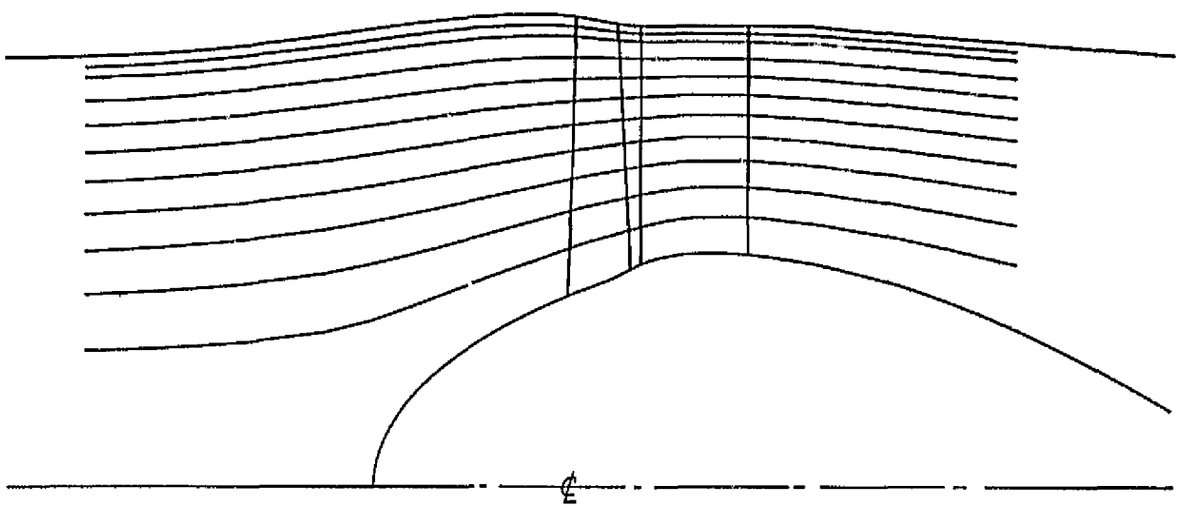

Figure 4.6 Fan Flowpath and Streamlines.

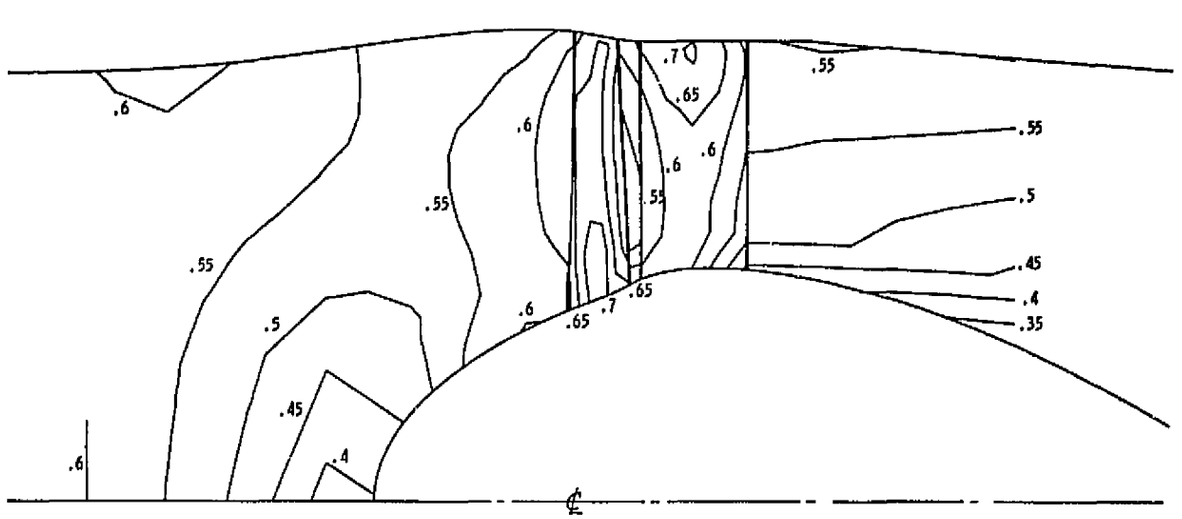

Figure 4.7 Meridional Mach Number Contours.

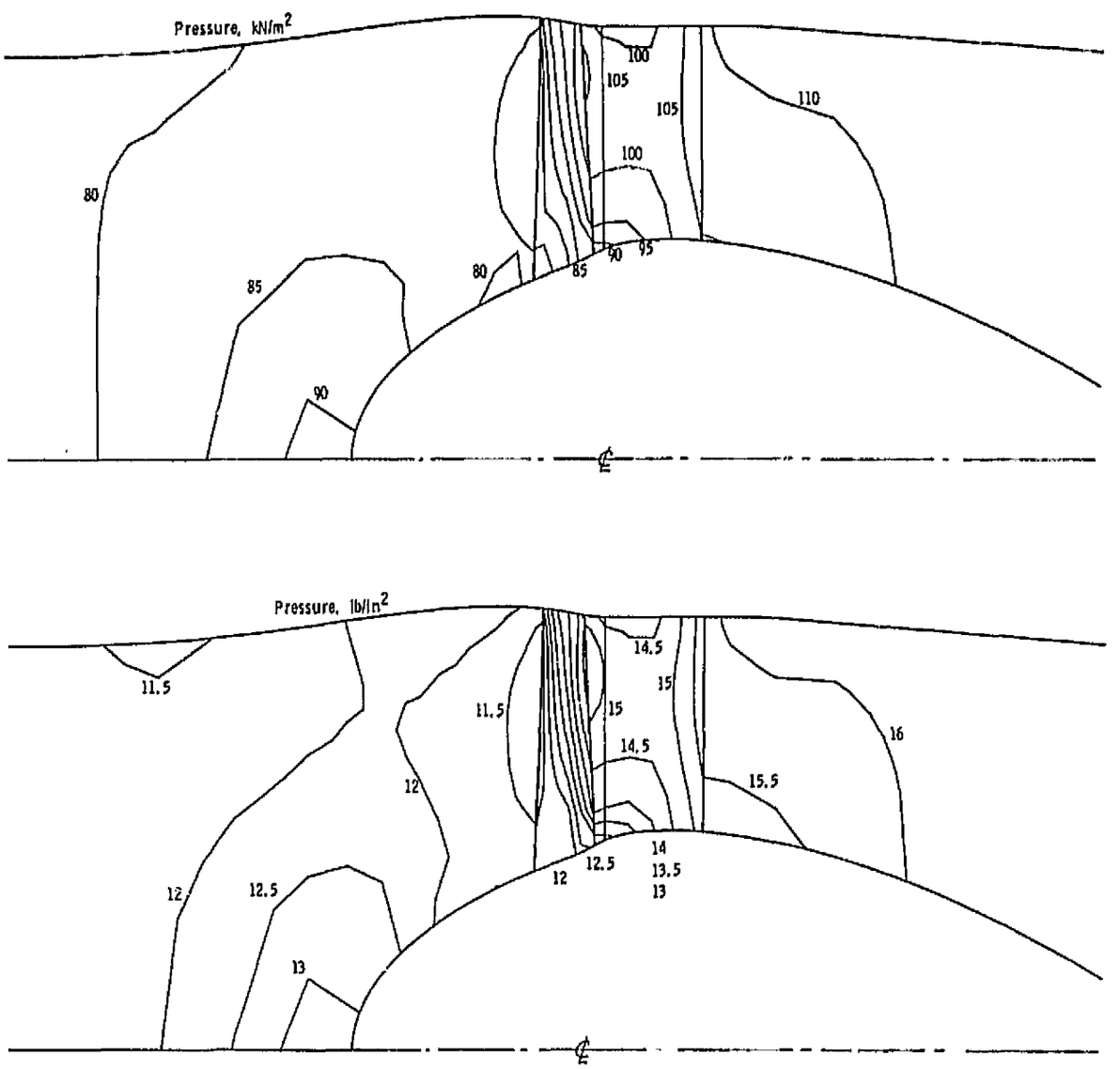

Figure 4.8 Static Pressure Contours.

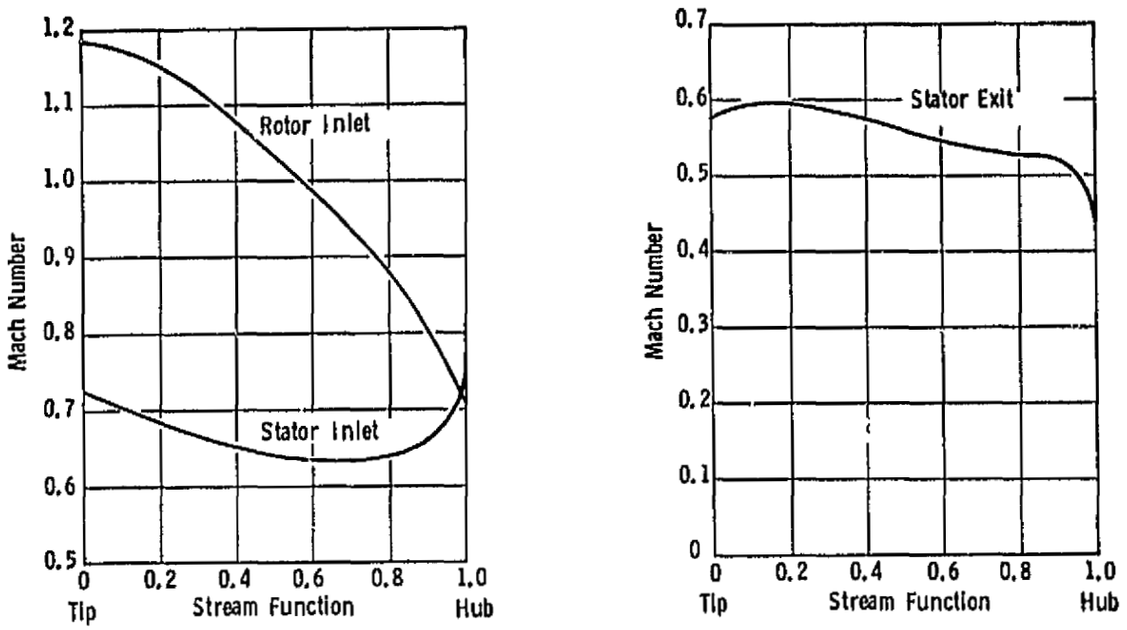

Figure 4.9 Blade Mach Numbers.

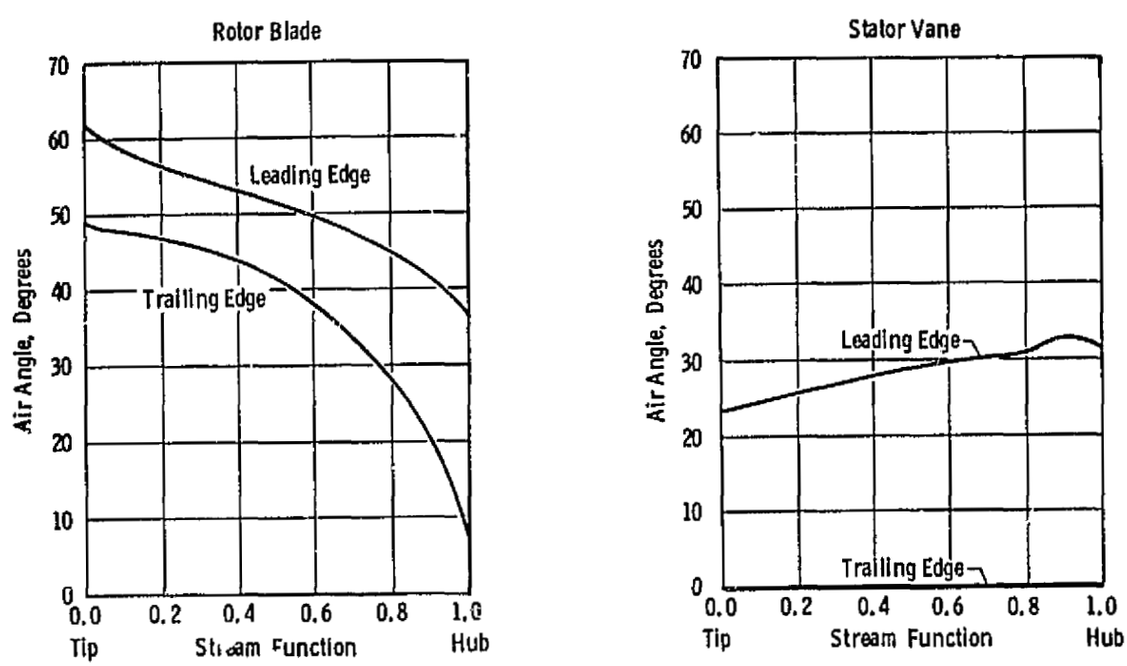

Figure 4.10 Air Angles.

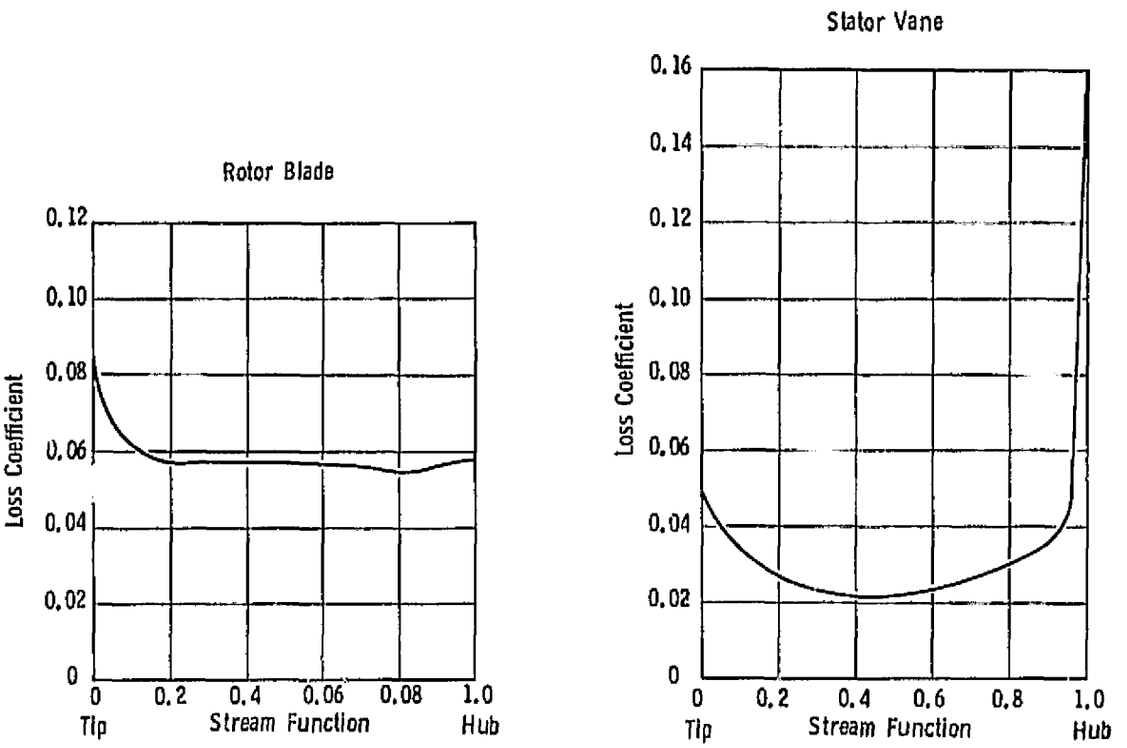

Figure 4.11 Loss Coefficients.

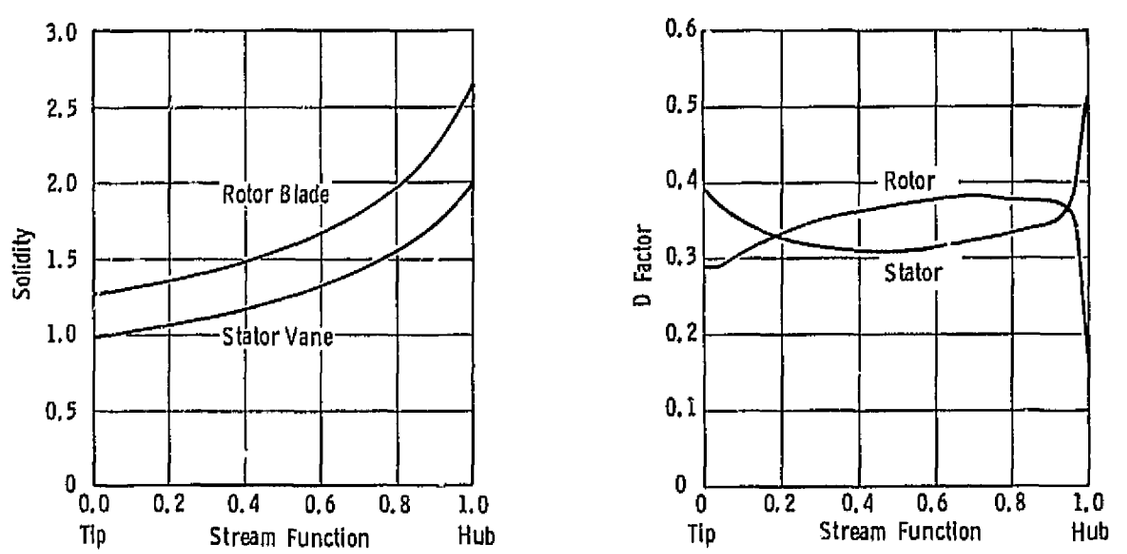

Figure 4.12 Solidities and D-Factors.

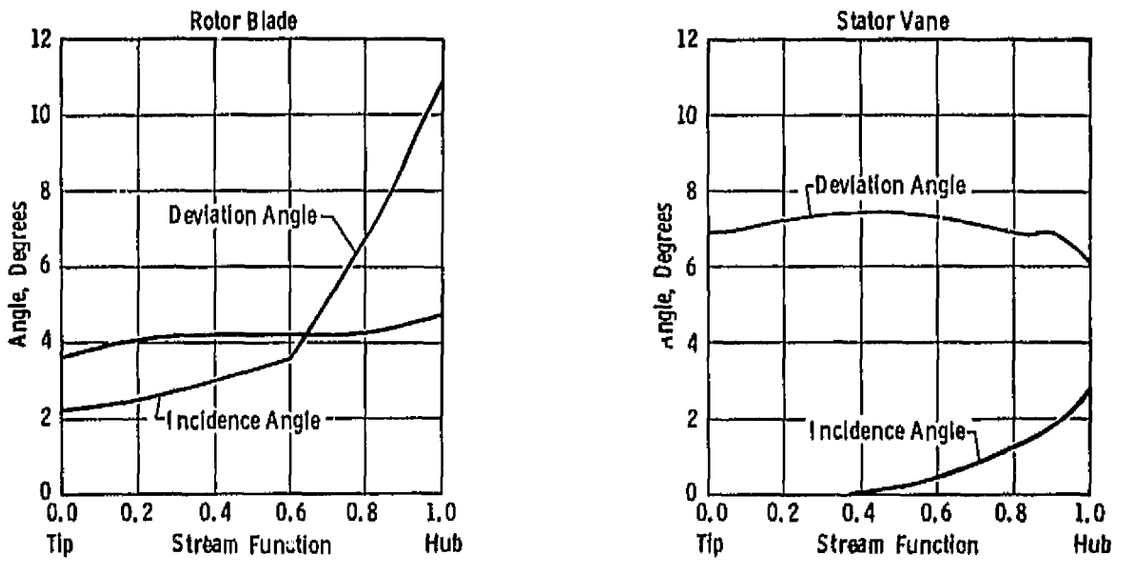

Figure 4.13 Deviation and Incidence Angles.

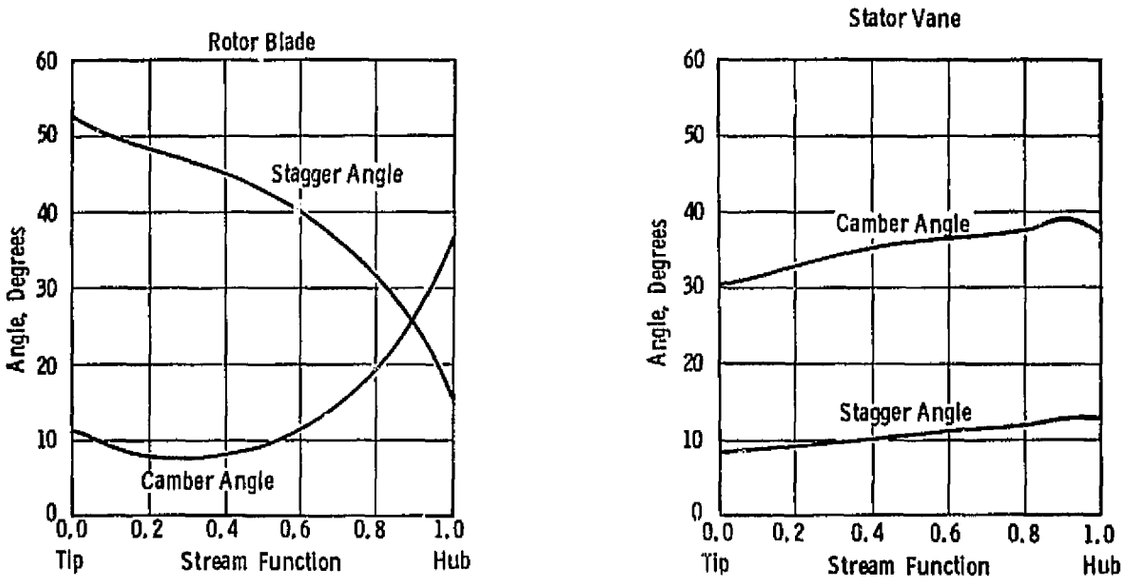

Figure 4.14 Stagger and Camber Angles.

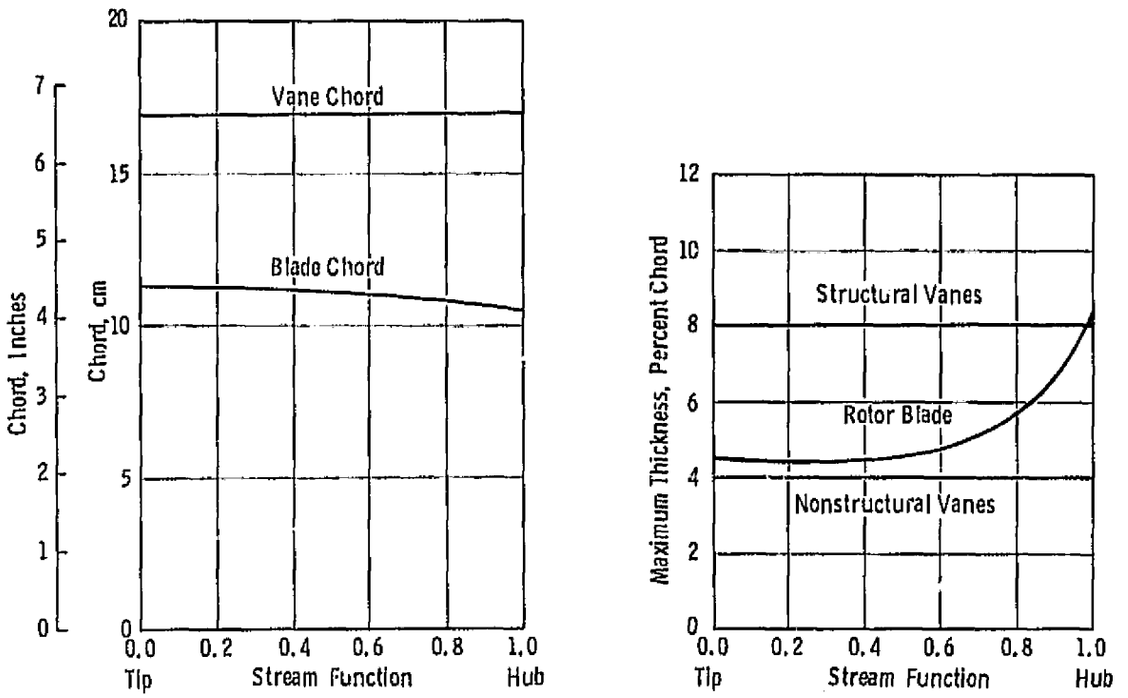

Figure 4.15 Thickness end Chord Distributions.

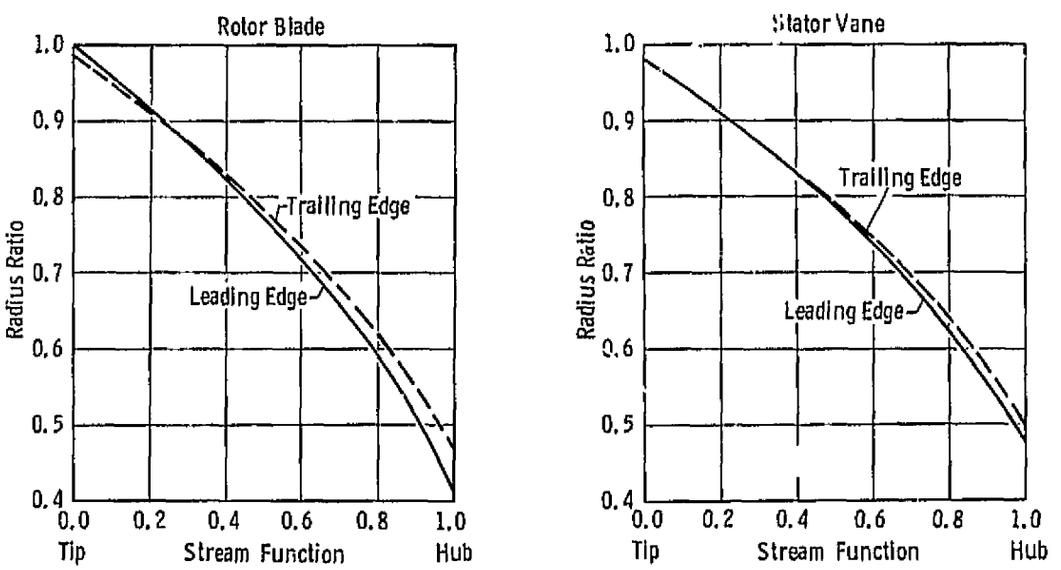

Figure 4.16 Stream Function Radial Location.

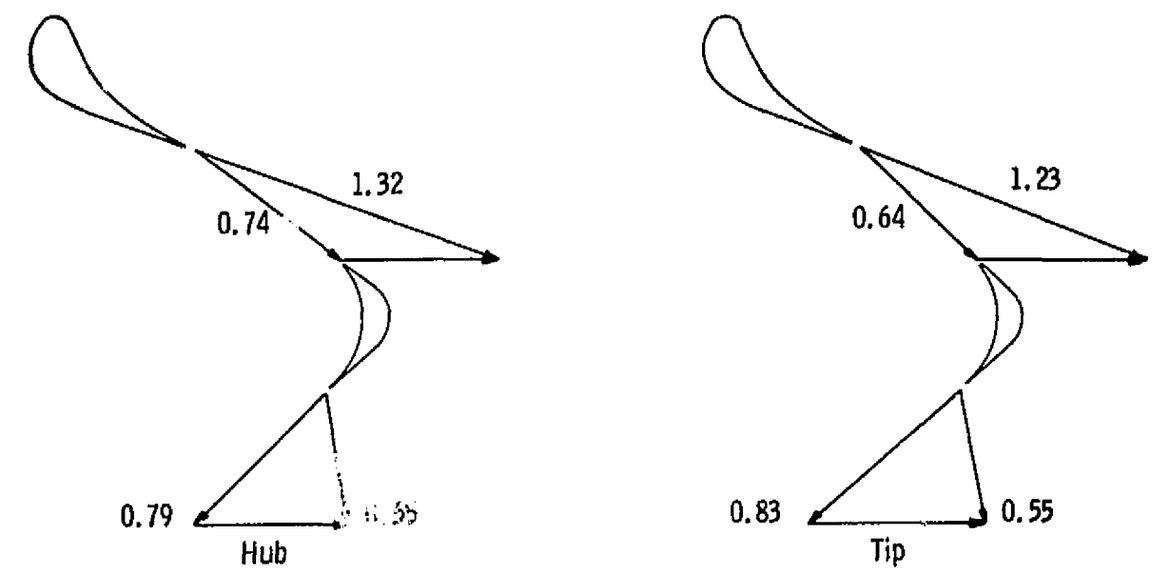

Figure 4.17 Turbine Vector Diagrams.

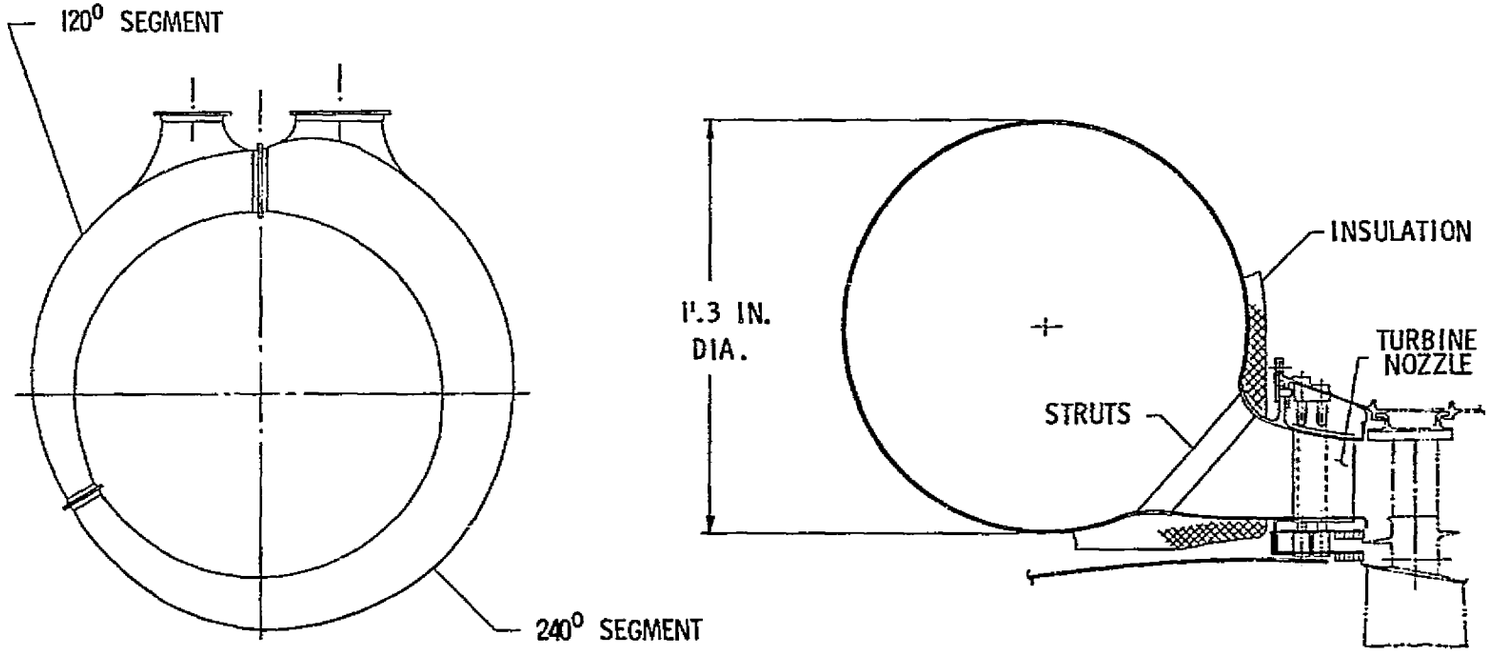

Figure 4.18 Circular Bubble Scroll.

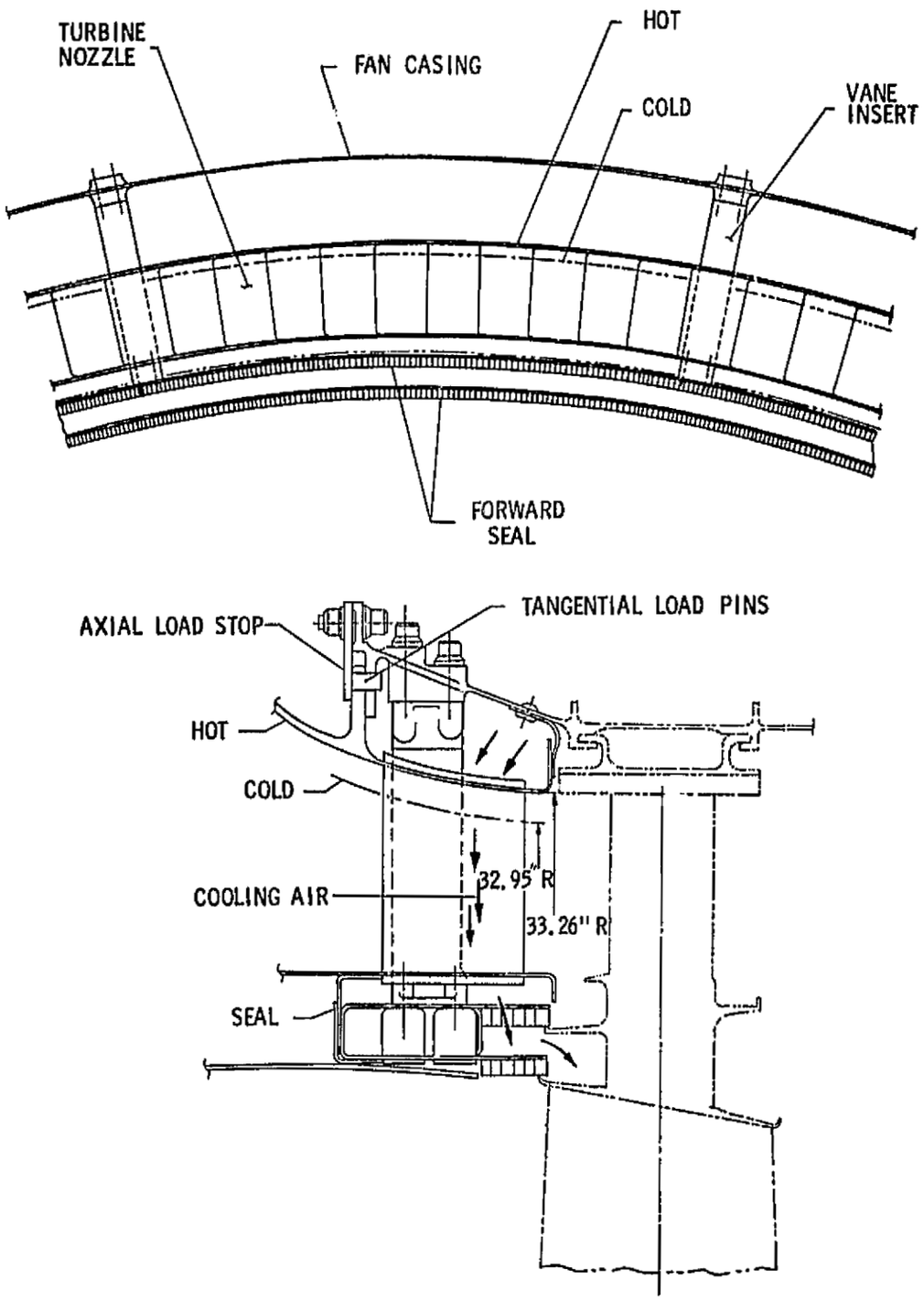

Figure 4.19 Scroll Mount and Seals.

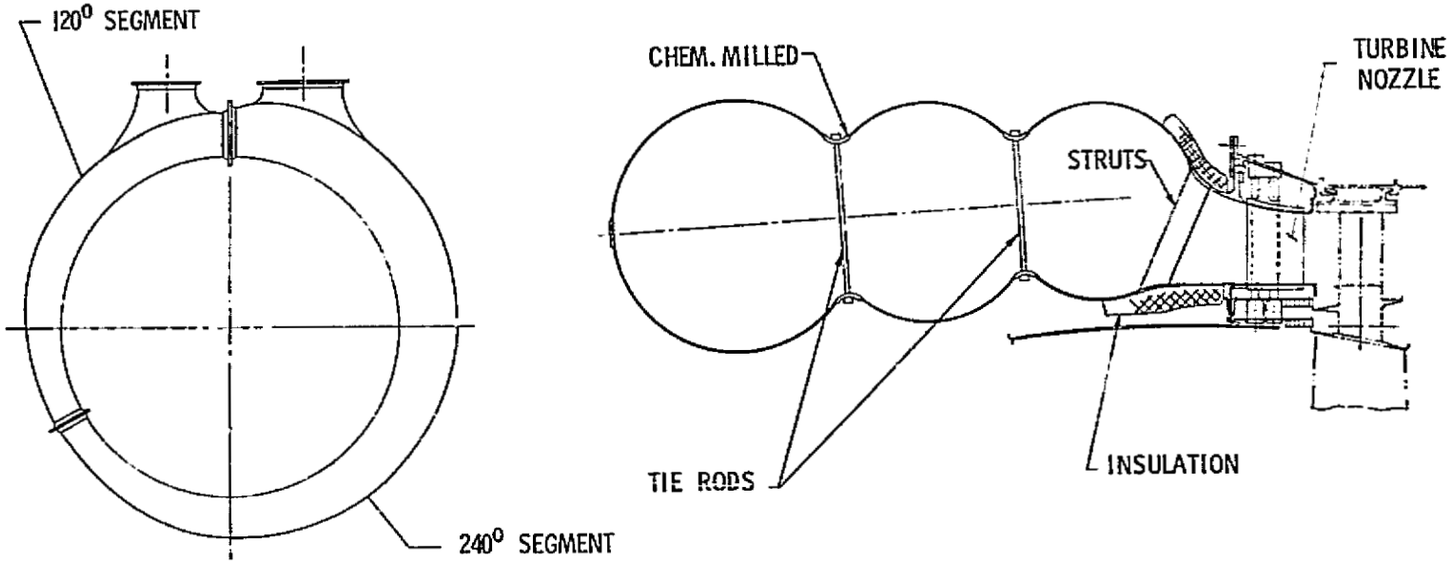

Figure 4.20 Multilobe Scroll.

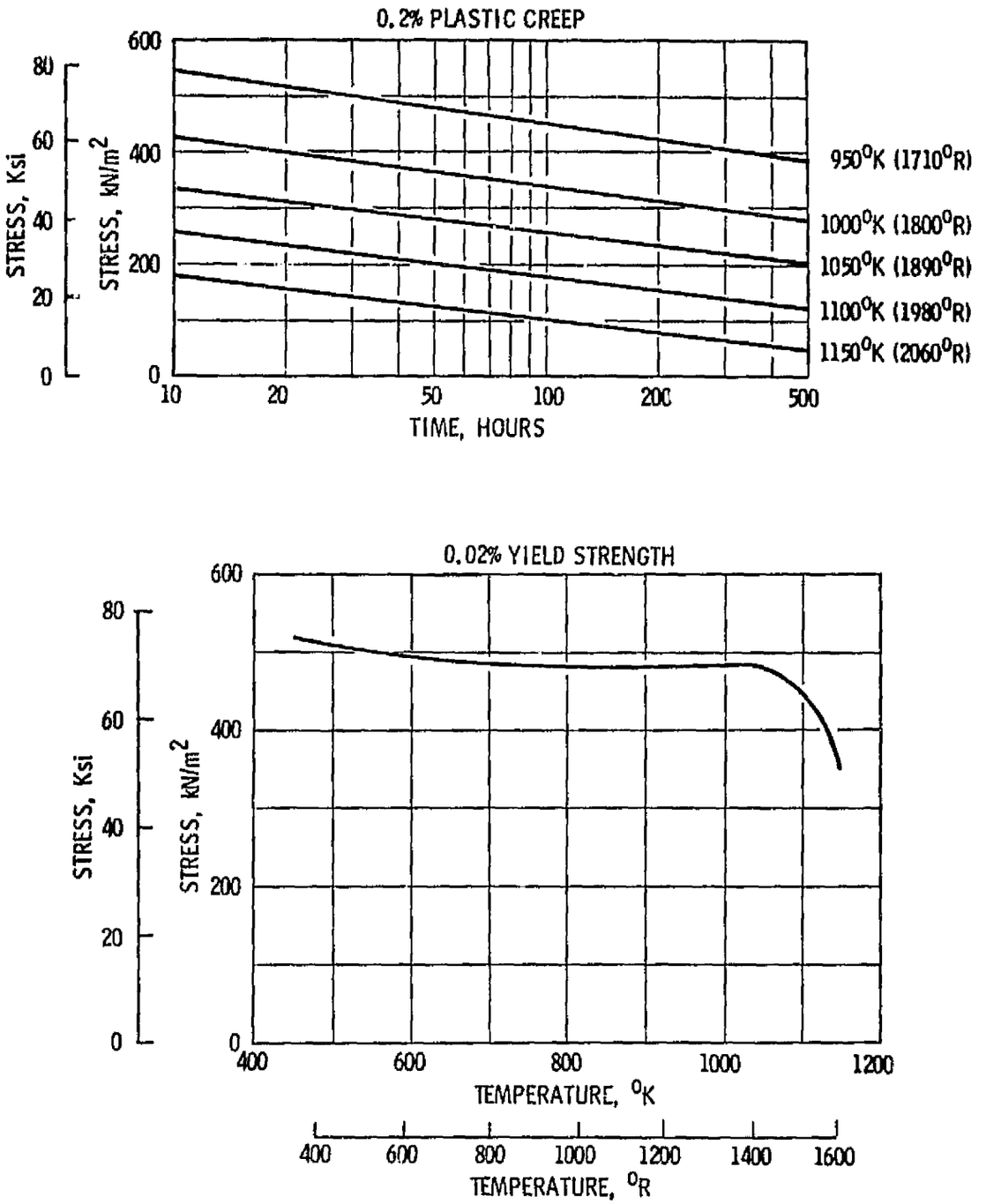

Figure 4.21 Scroll Material Stress Capability.

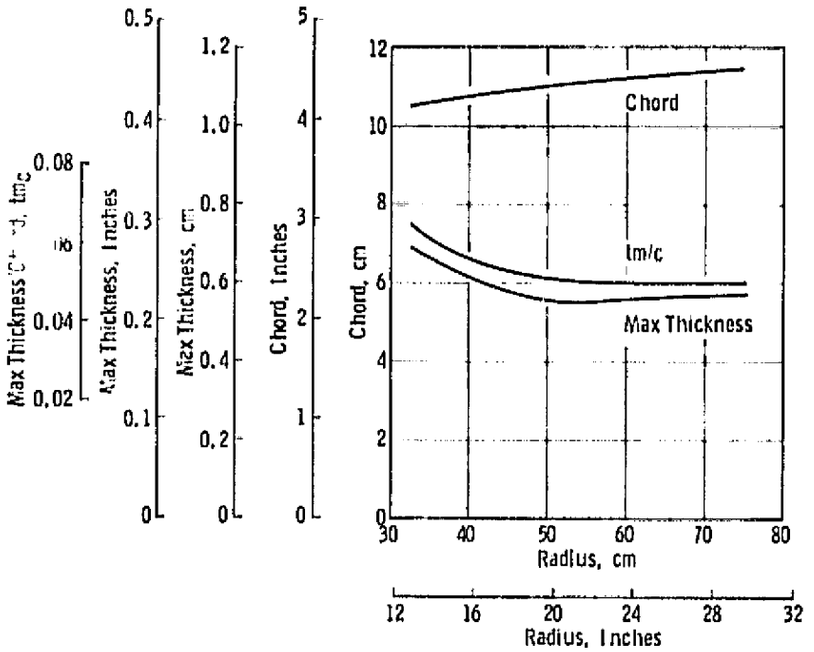

Figure 4.22 Initial Airfoil Geometery for Rotor Analysis.

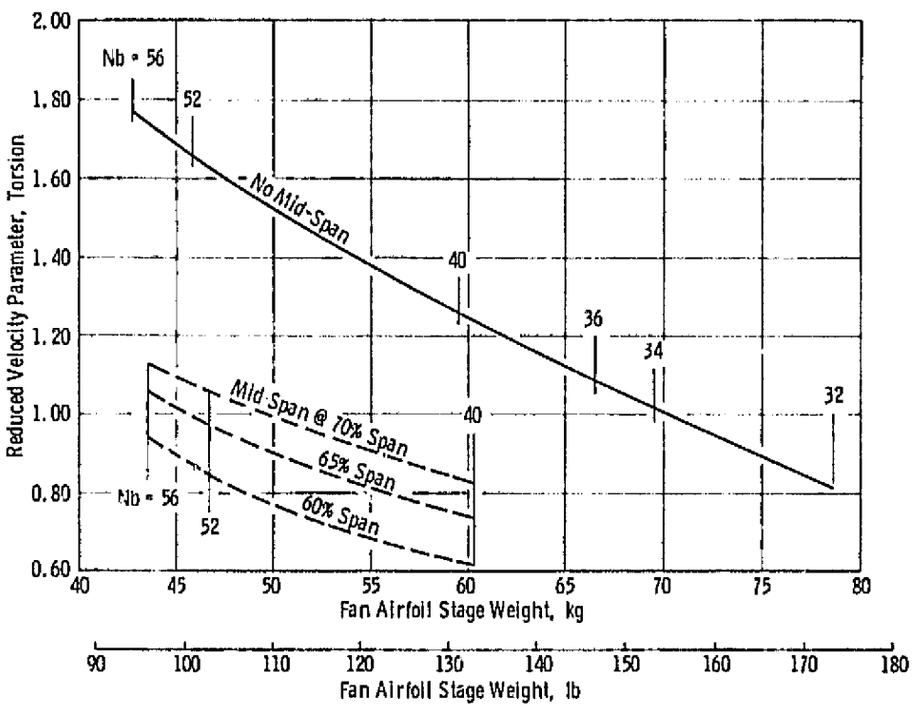

Figure 4.23 Effects of Mid-Spans and Blade Numbers on Torsional Stability.

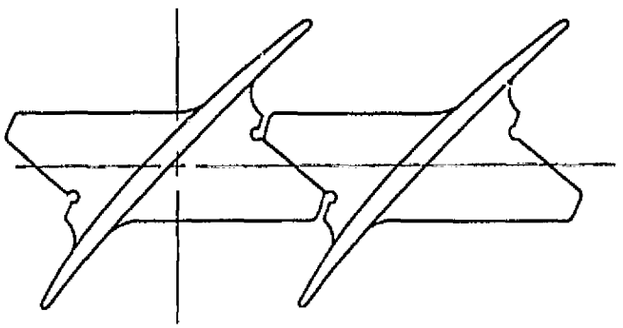

Figure 4.24 Mid-Span Shroud Geometry.

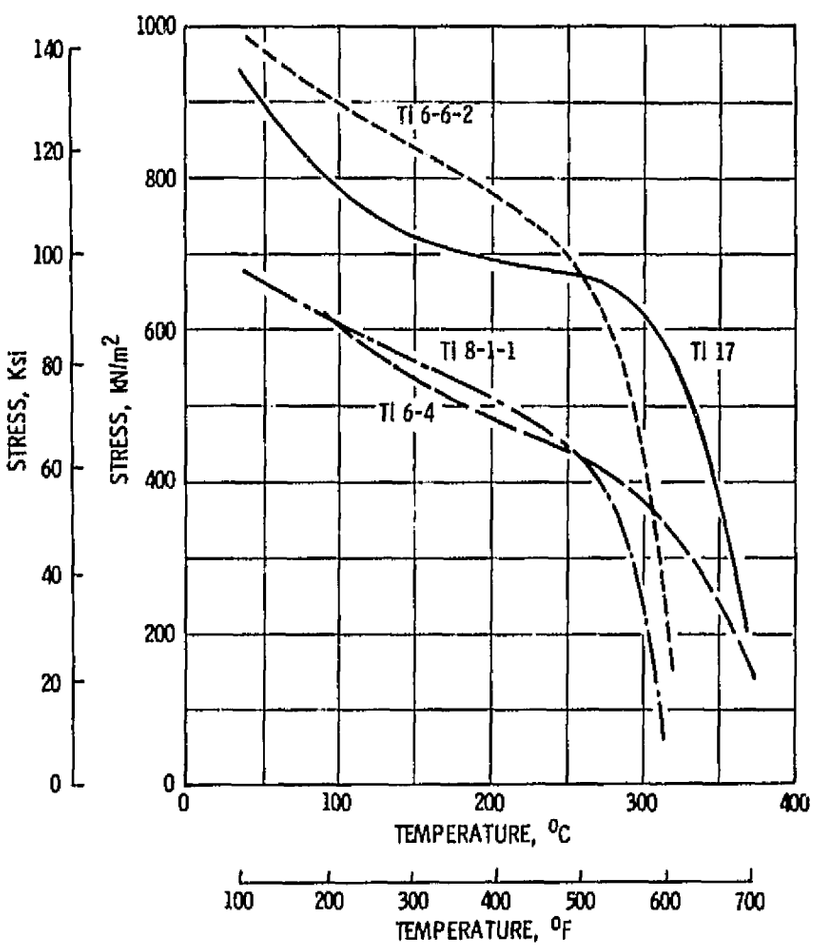

Figure 4.25 Comparison of Strength of Titanium Alloys.

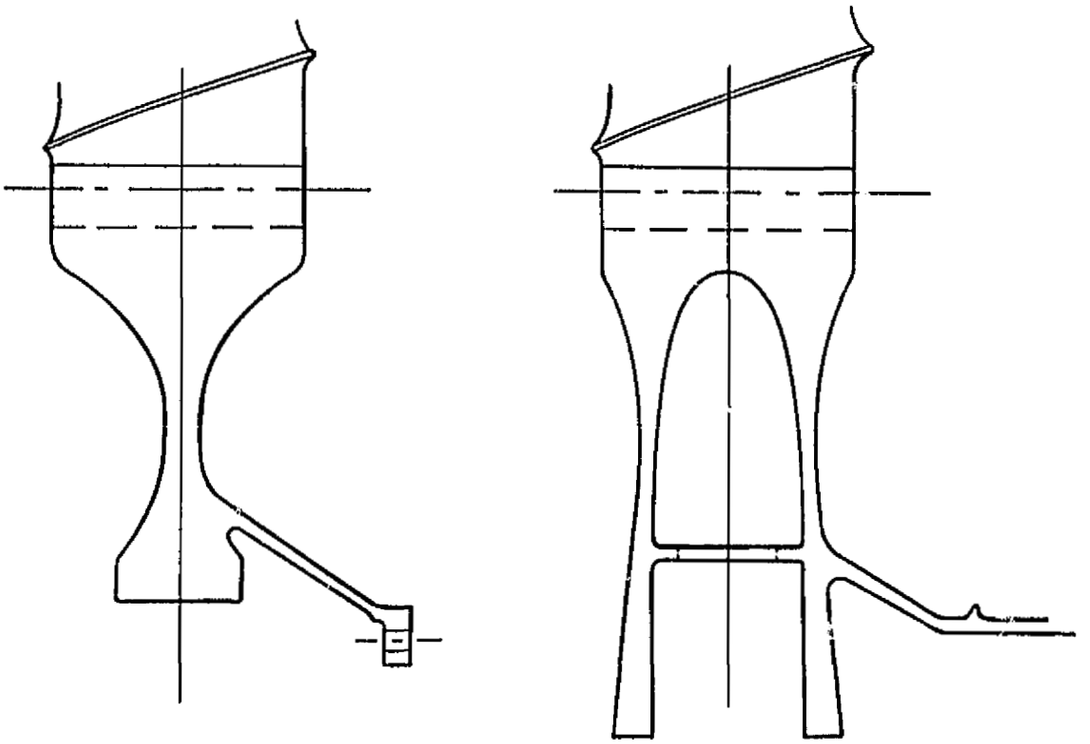

Figure 4.26 Disk Geometries.

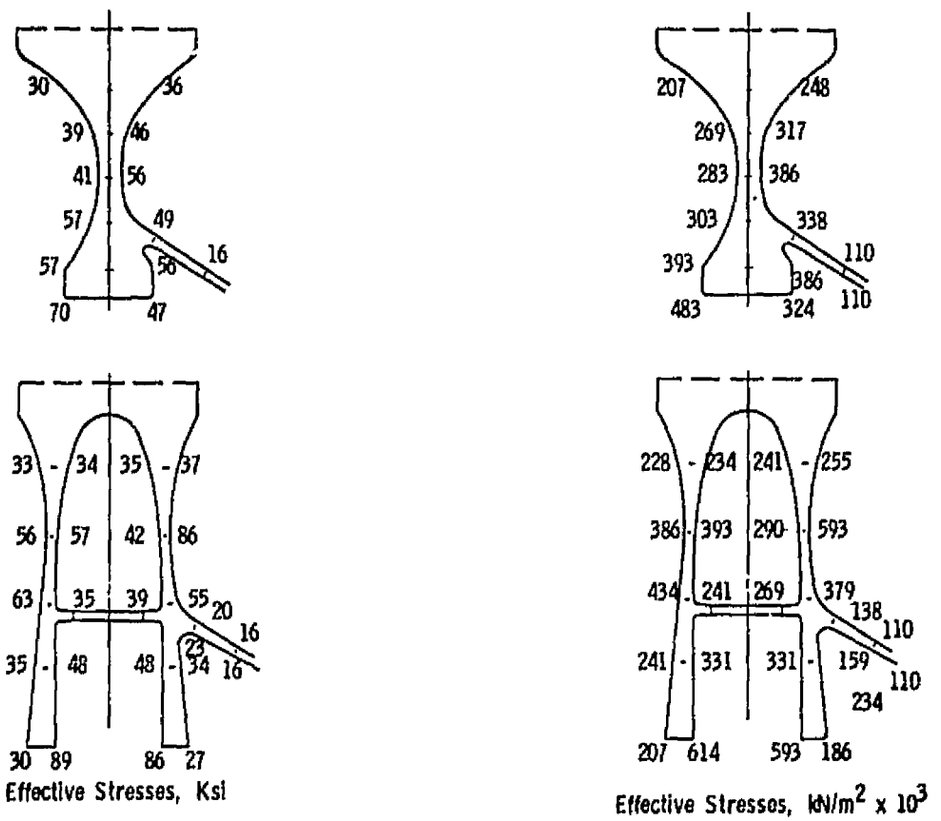

Figure 4.27 Twin-Web and Conventional Disk Stress Comparison.

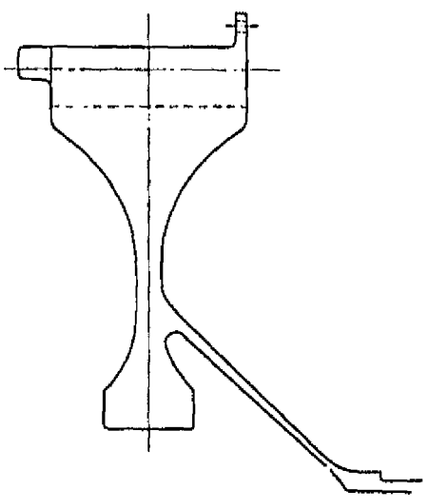

Figure 4.28 Final Disk Configuration.

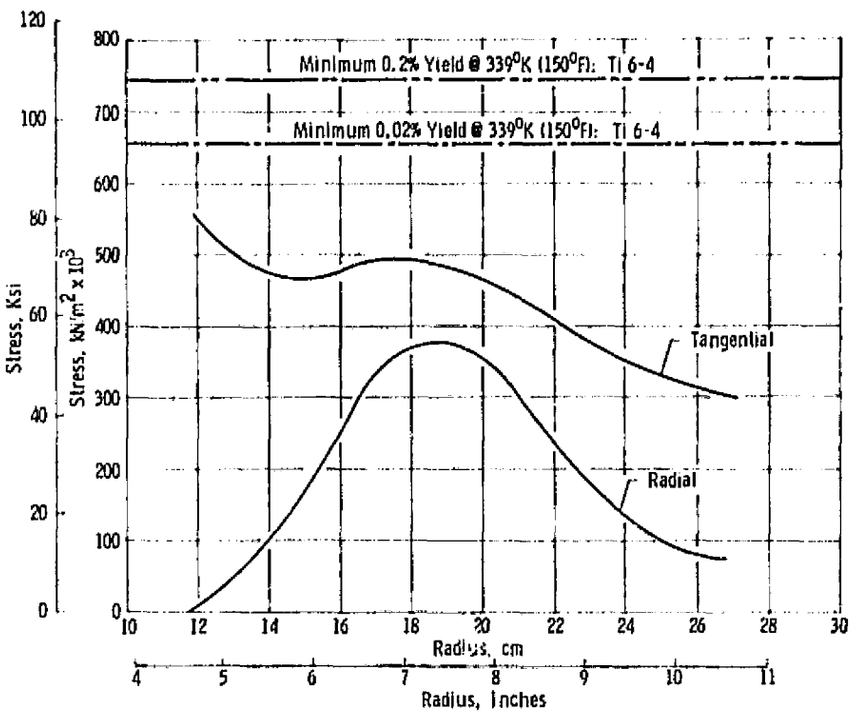

Figure 4.29 Disk Meanline Stress Distribution.

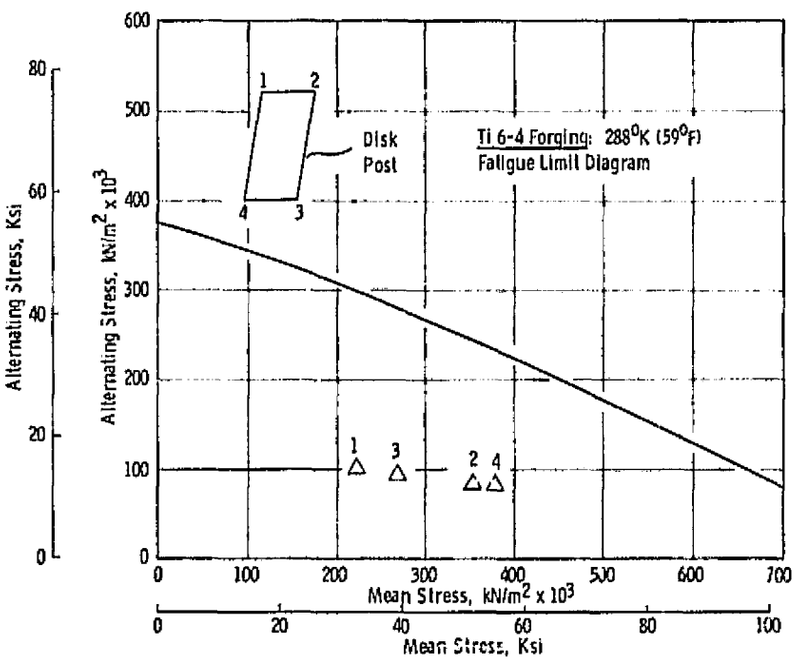

Figure 4.30 Disk Fatigue Strength.

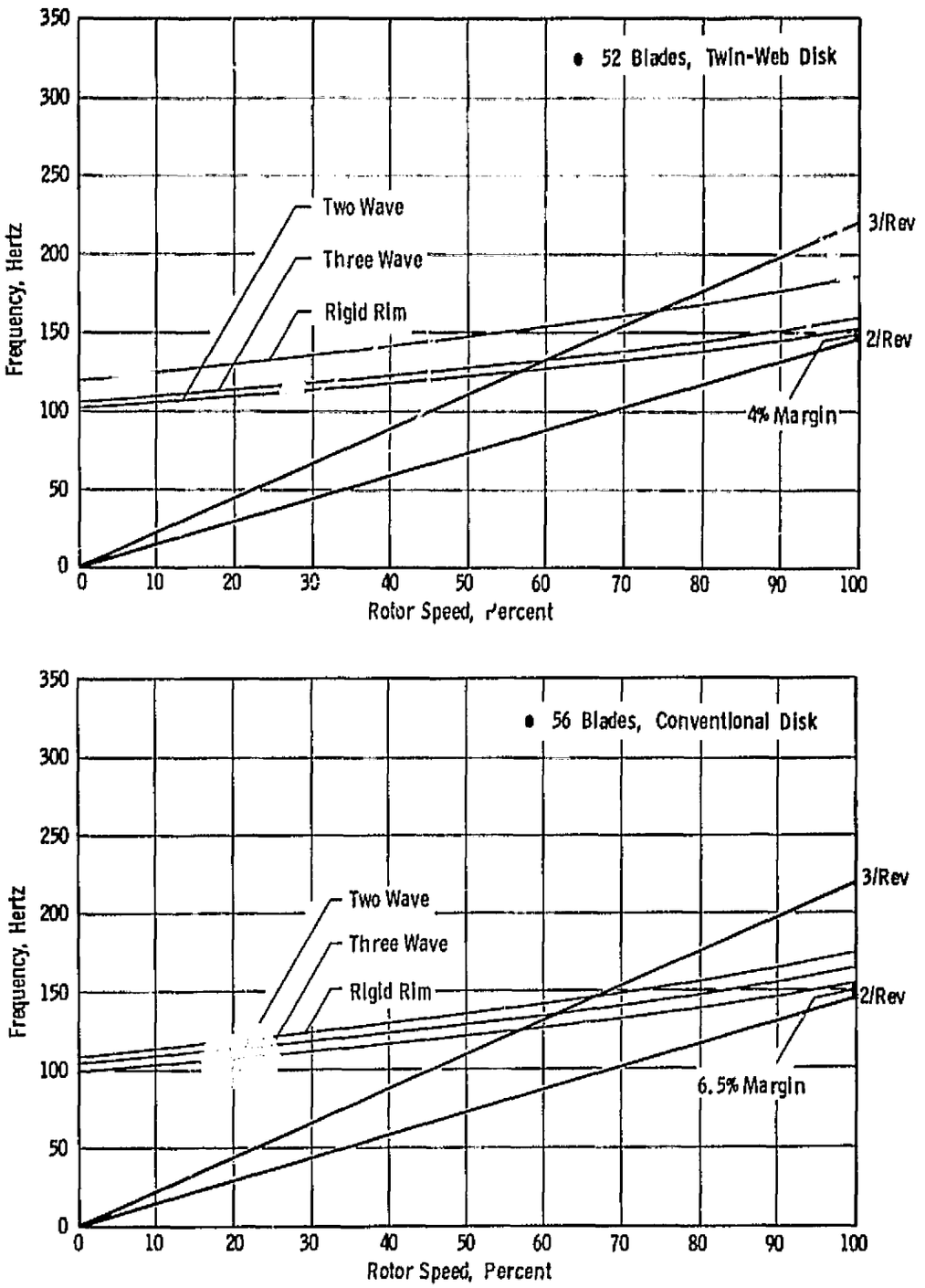

Figure 4.31 Rotor Blade-Disk Mode Frequency Diagrams.

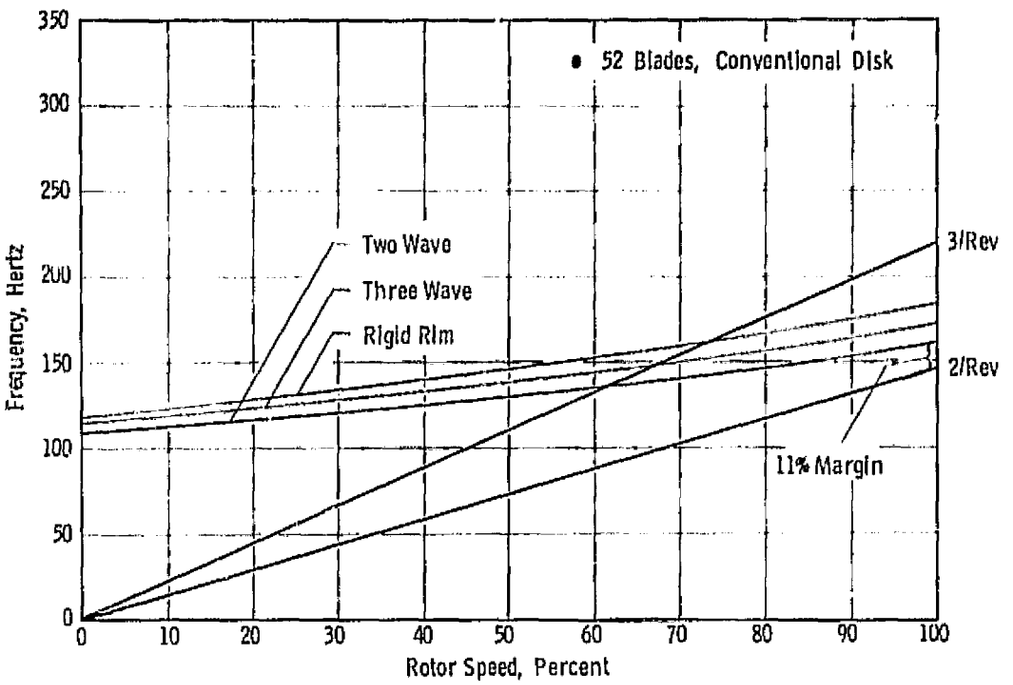

Figure 4.31 Rotor Blade-Disk Mode Frequency Diagrams (Concluded).

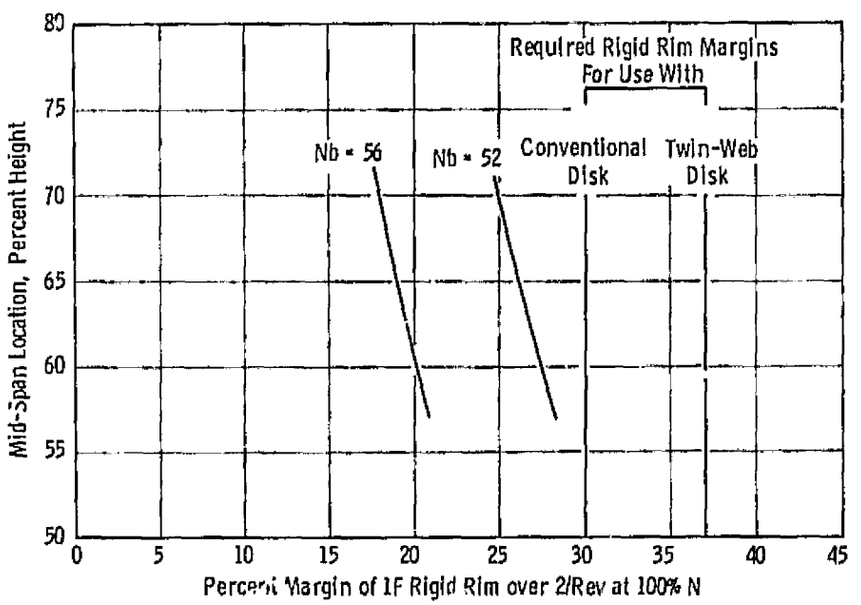

Figure 4.32 Effects of Mid-Span Location on Disk Frequency Margins.

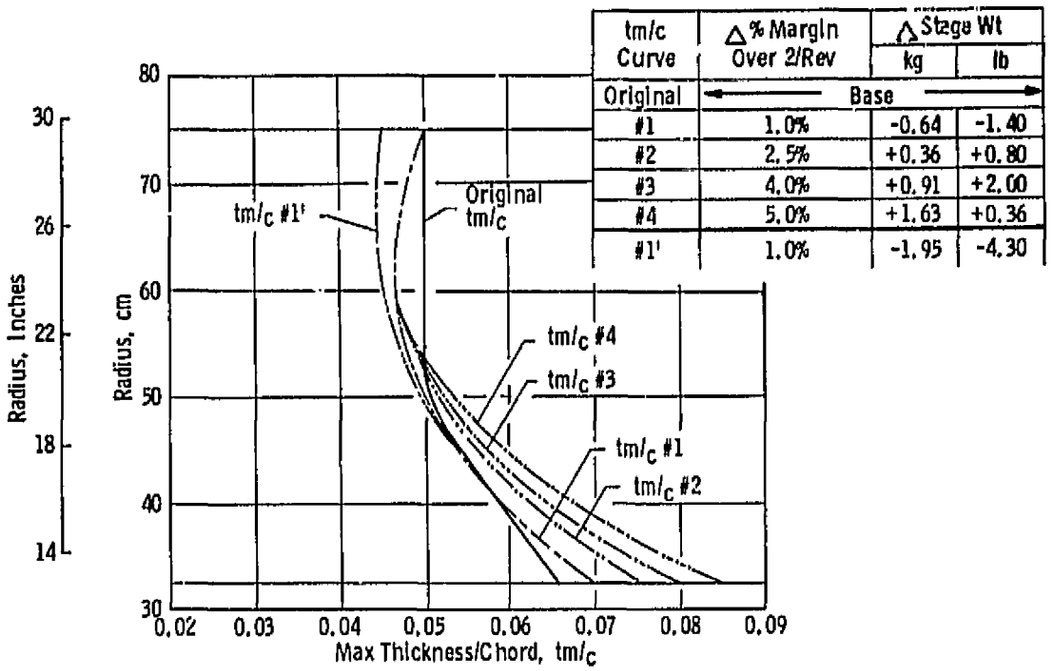

Figure 4.33 Effects of Blade Thickness Distribution on Rotor Weight and Stability Margin.

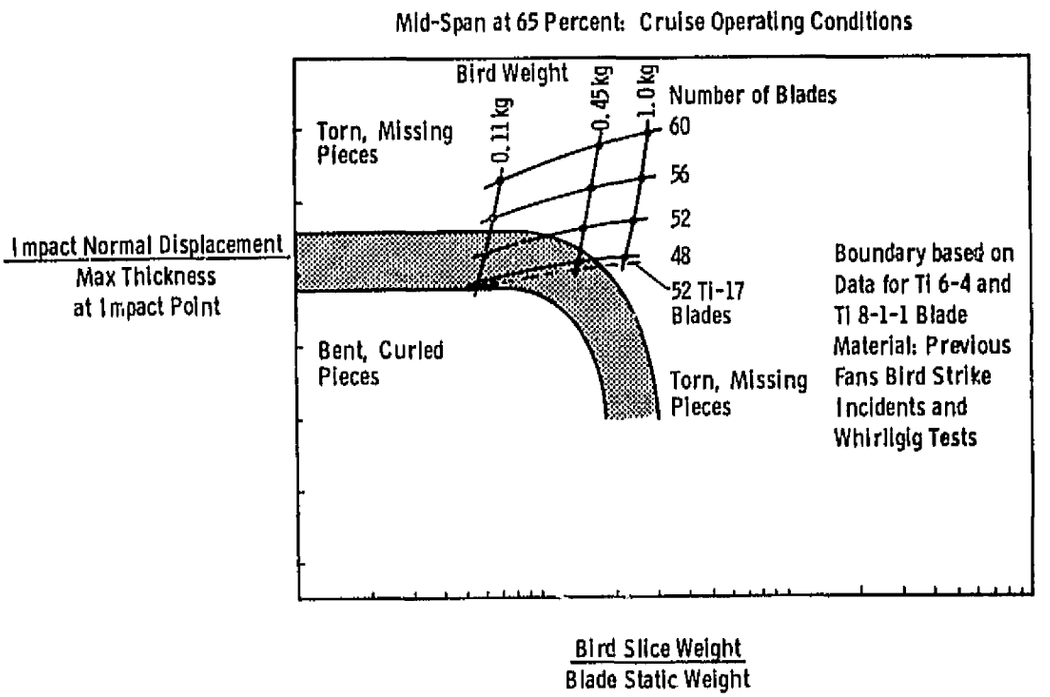

Figure 4.34 Rotor Bird Strike Capability.

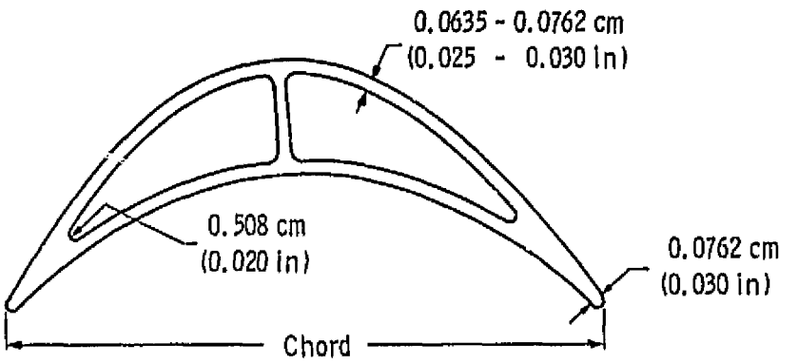

N_{Fan} Blades	$N_{Turbine}$ Blades	Constant Solidity Turbine Chord		△ Wt Turbine Airfoils		△ I_p Turbine Airfoils	
		cm	inches	kg	pounds	kg-m-sec^2	lb-ft-sec^2
52	208	3.94	1.550	Base		Base	
52	260	3.15	1.240	-1.40	-3.1	-0.094	-0.68
52	364	2.25	0.885	-3.04	-6.7	-0.202	-1.46

Figure 4.35 Effects of Turbine Blade Number on Weight.

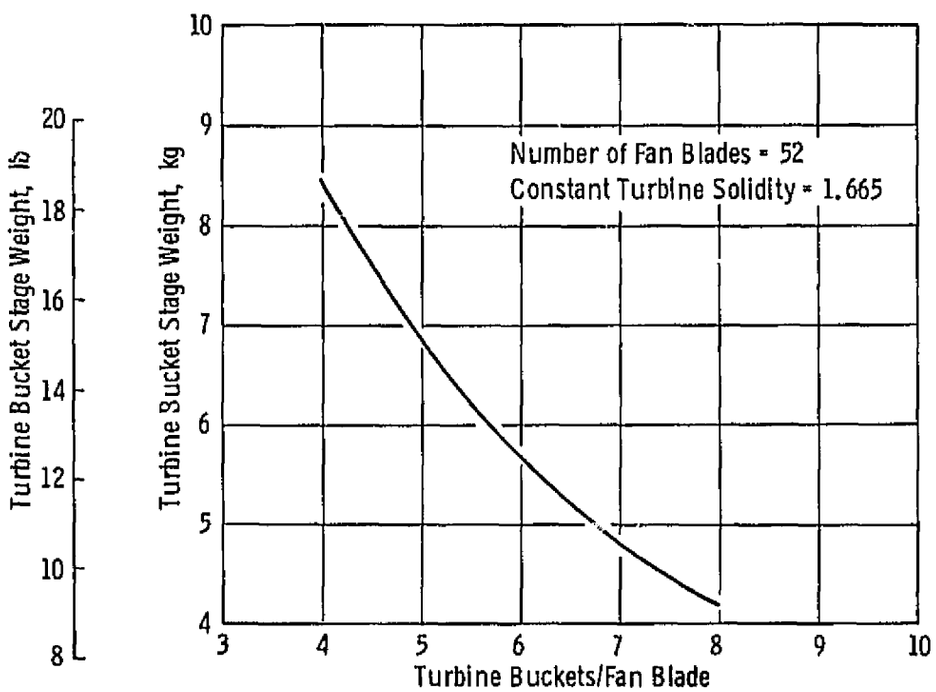

Figure 4.36 Turbine Blade Number Comparison.

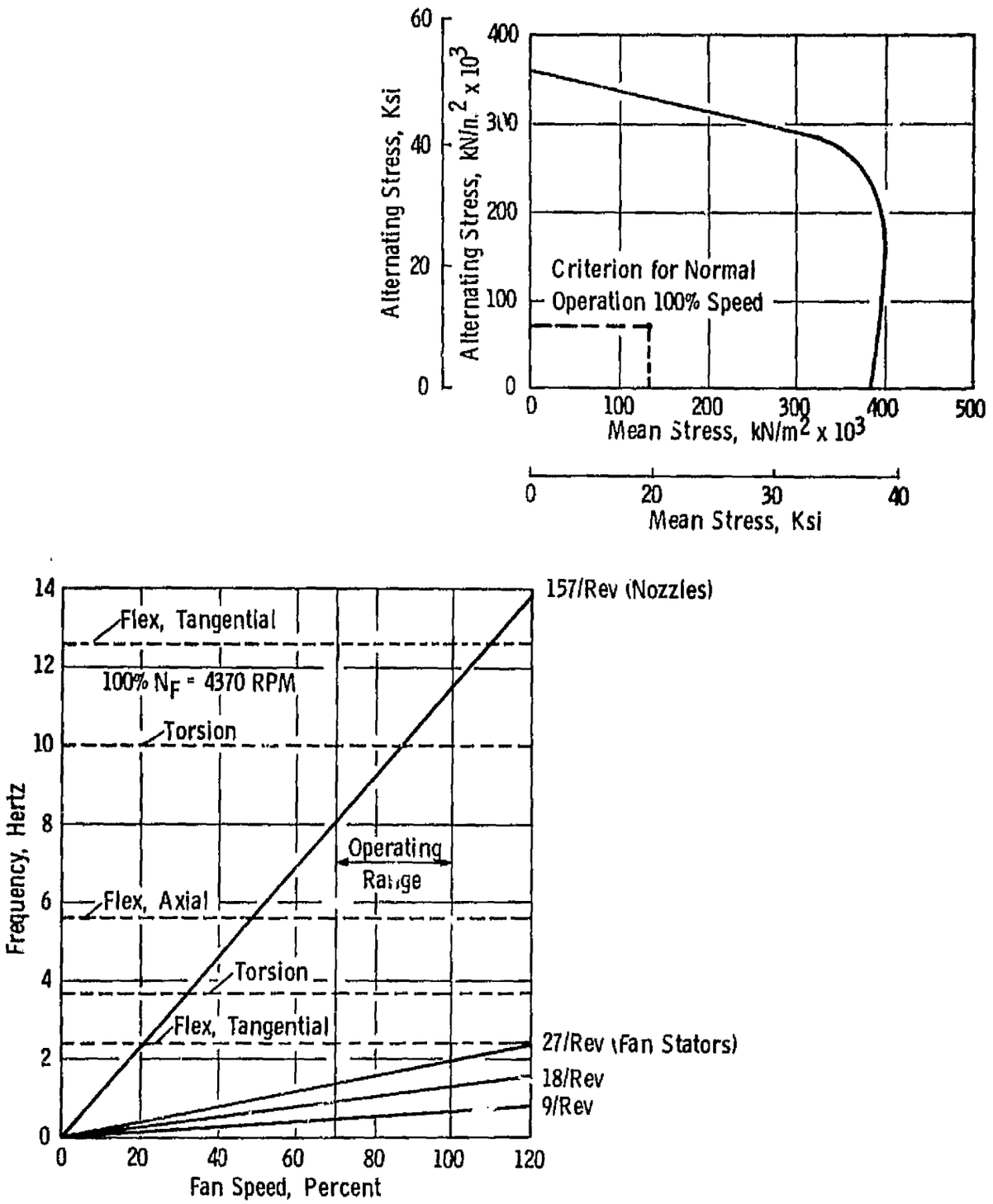

Figure 4.37 Unshrouded Turbine Stress-Range and Frequency-Speed Diagram.

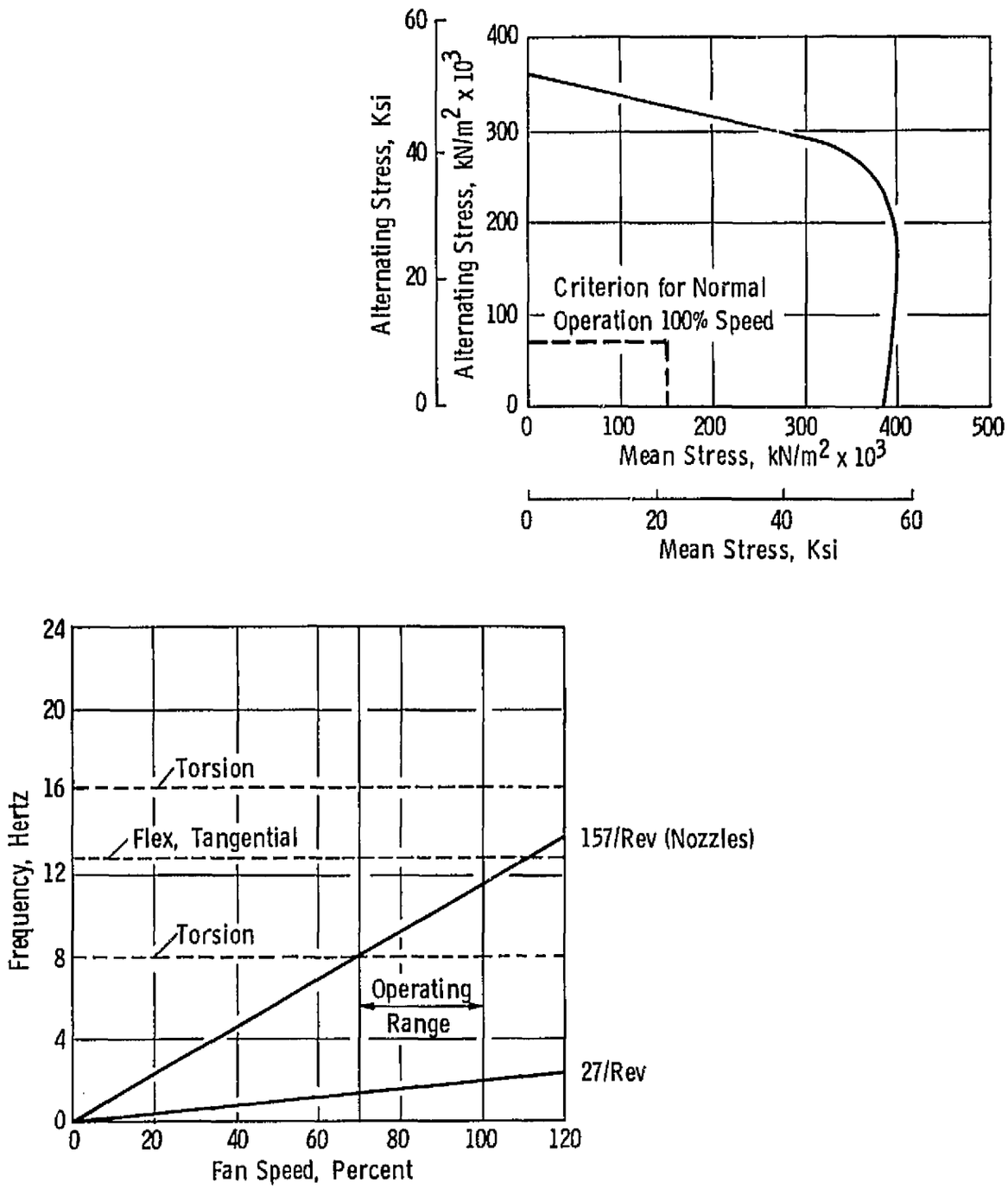

Figure 4.38 Shrouded Turbine Stress-Range and Frequency-Speed Diagram.

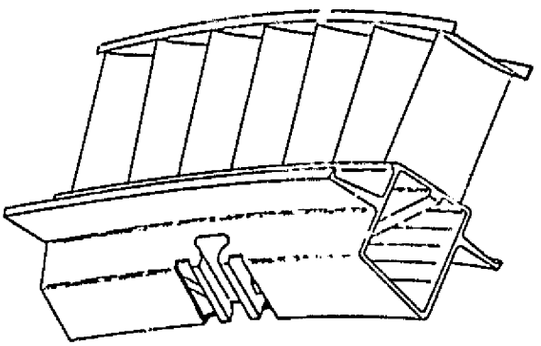

Figure 4.39 Turbine Carrier with Dovetail Slot.

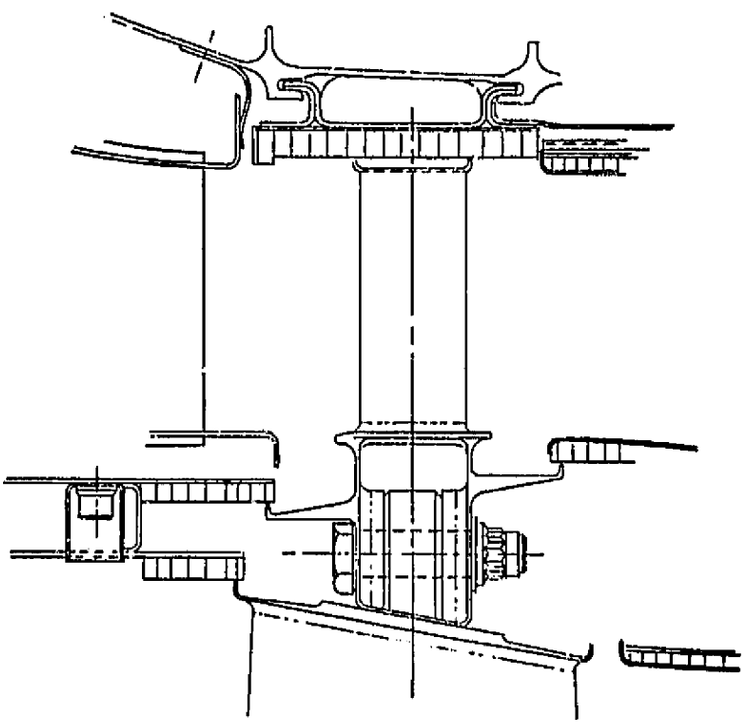

Figure 4.40 Turbine Carrier with Bolted Tang.

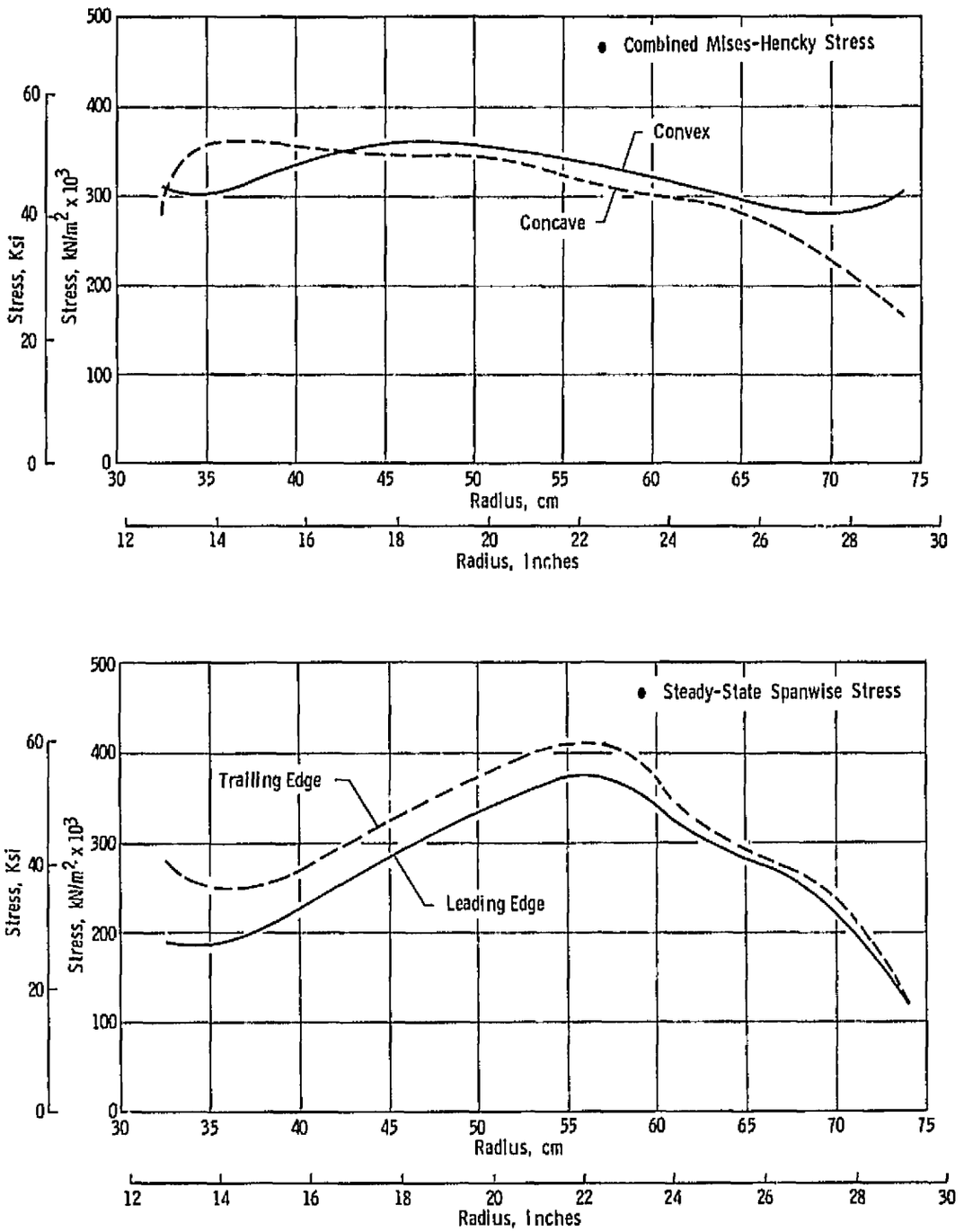

Figure 4.41 Rotor Blade Stress Distributions.

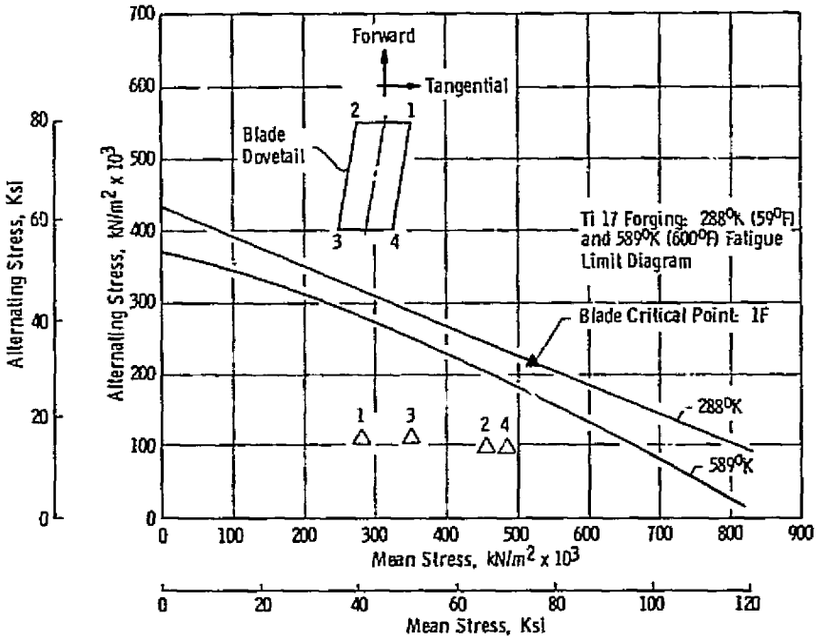

Figure 4.42 Dovetail Stresses.

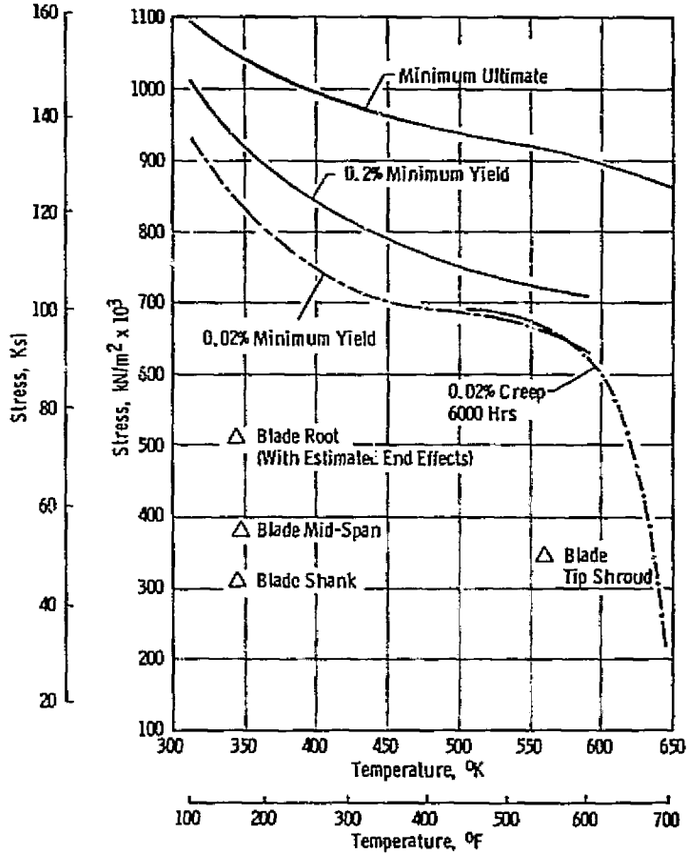

Figure 4.43 Blade Material Properties.

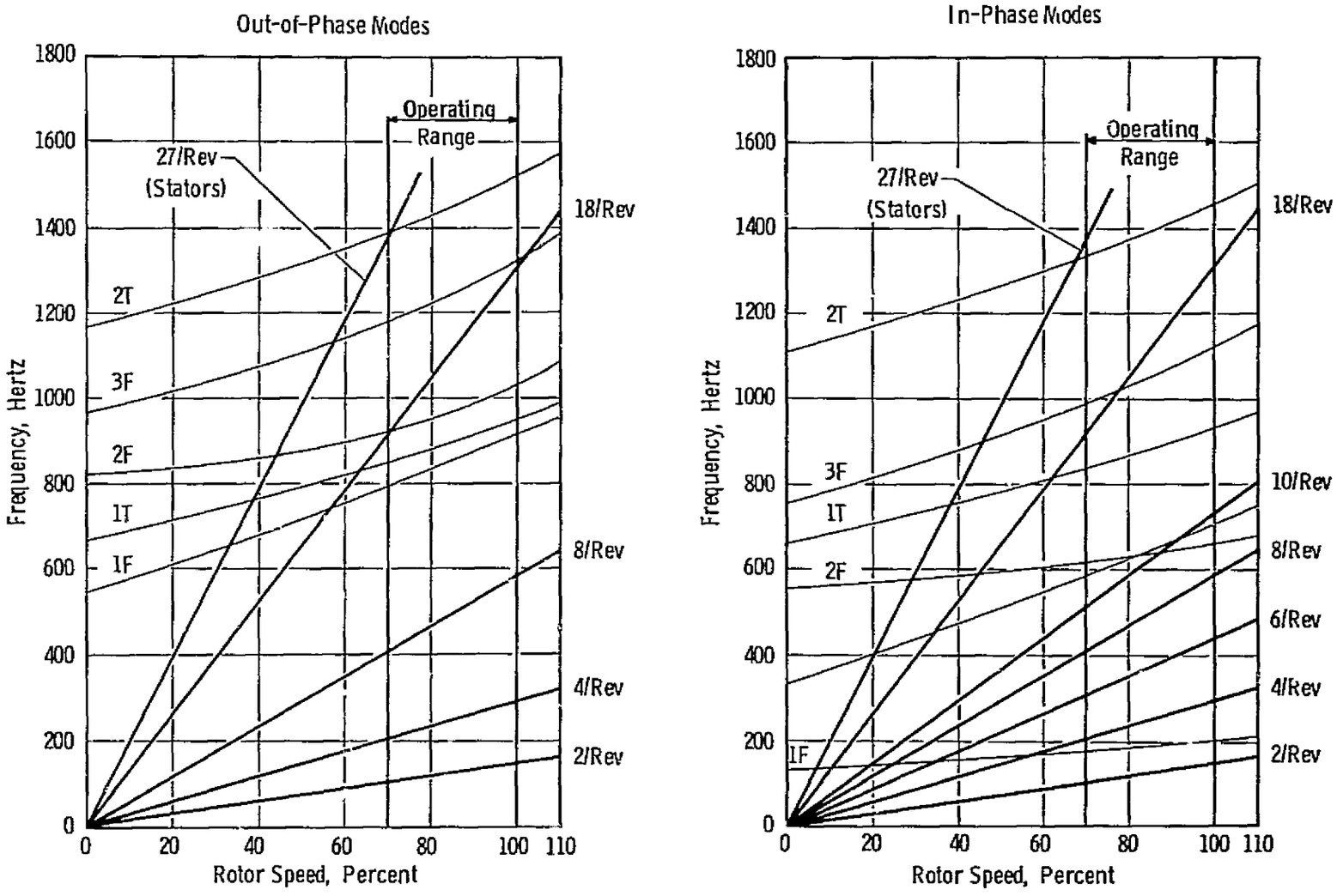

Figure 4.44 Blade Frequency-Speed Diagram.

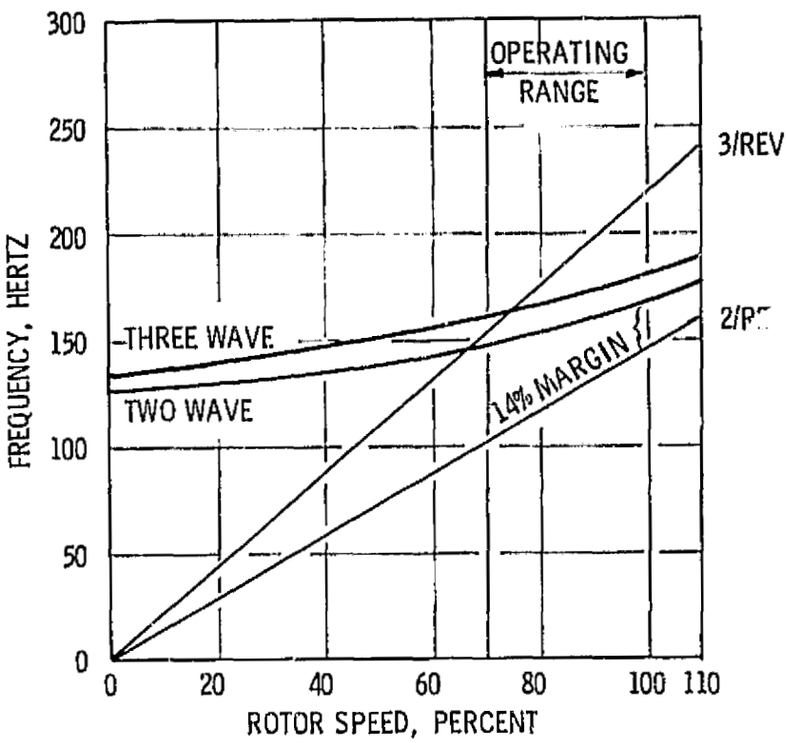

Figure 4.45 Selected Rotor Blade-Disk Mode Frequency Diagrams.

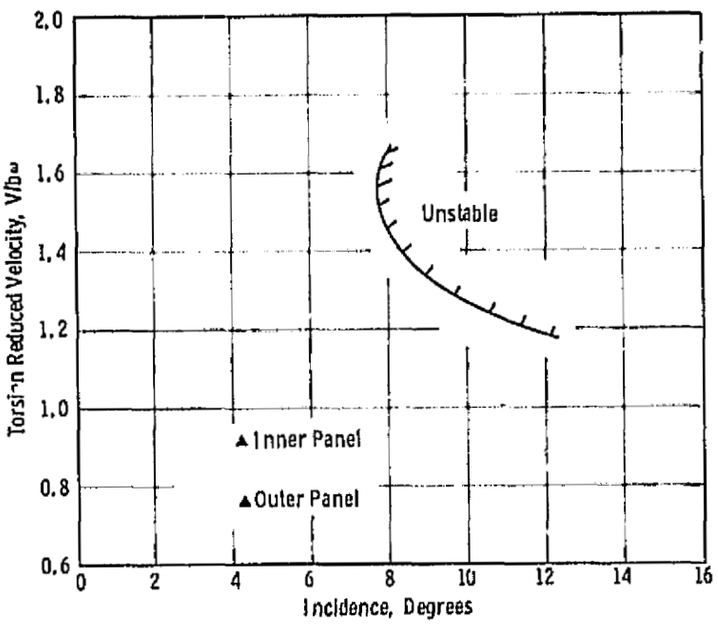

Figure 4.46 Blade Torsional Stability.

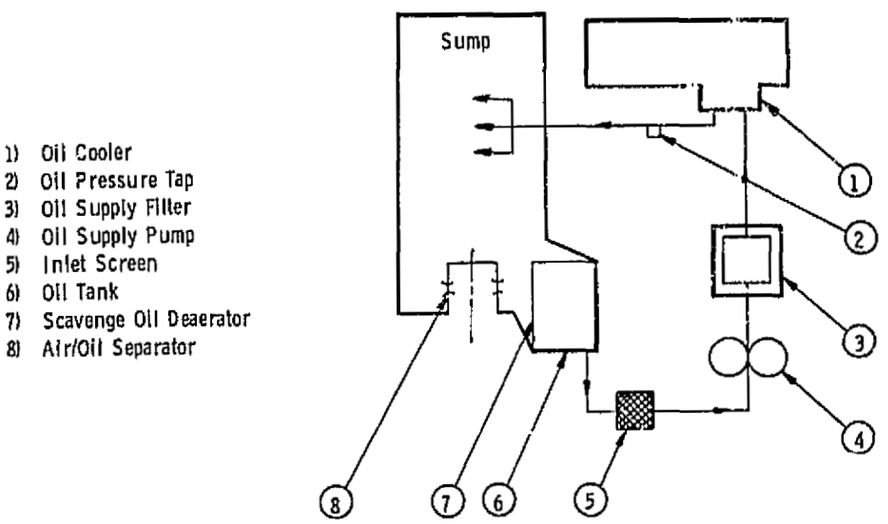

Figure 4.47 Lubrication System Schematic.

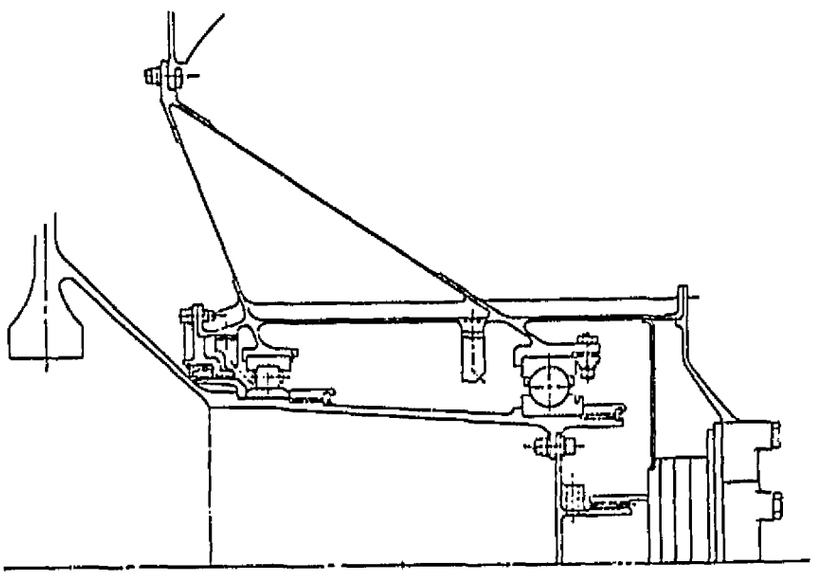

Position	Material	Bore		DN	Capacity		Life
		cm	in.		kN	lb	hr
Roller	M50	19.0	7.48	0.83×10^6	171.3	38,500	6000
Ball	M50	16.8	6.61	0.73×10^6	110.8	24,900	8265

Figure 4.48 Sump Configuration.

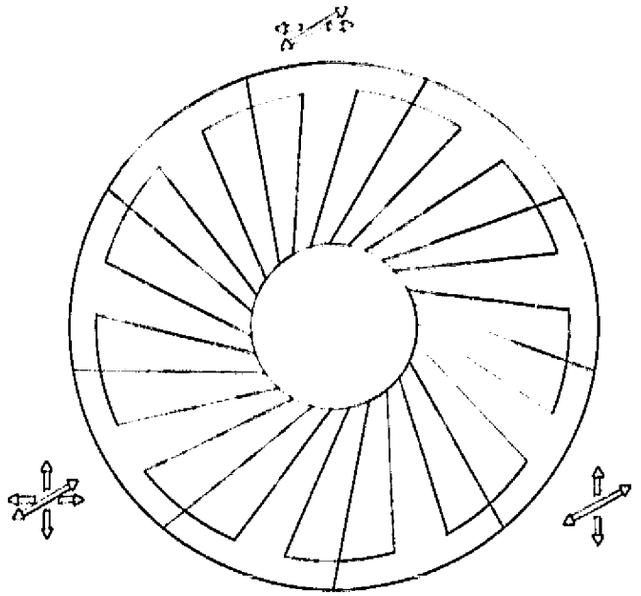

9 Structural Vanes
18 Nonstructural Vanes

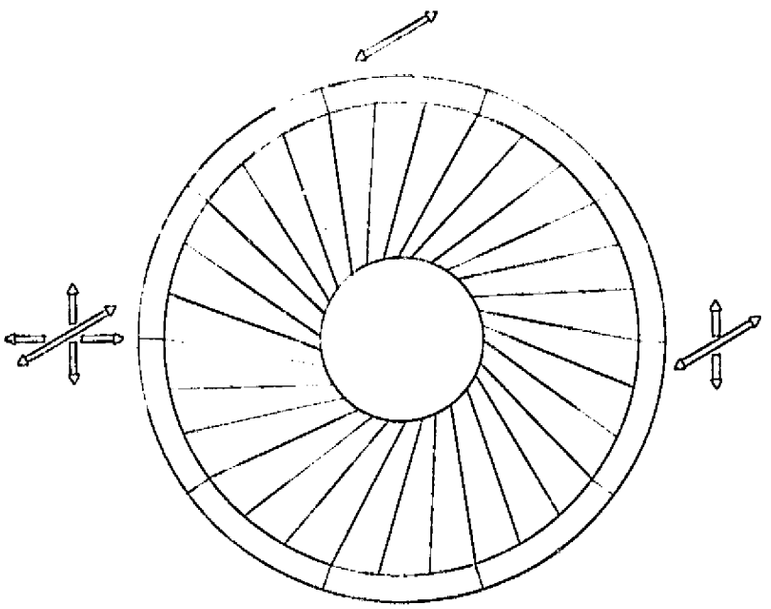

27 Structural Vanes

Figure 4.49 Frame Model.

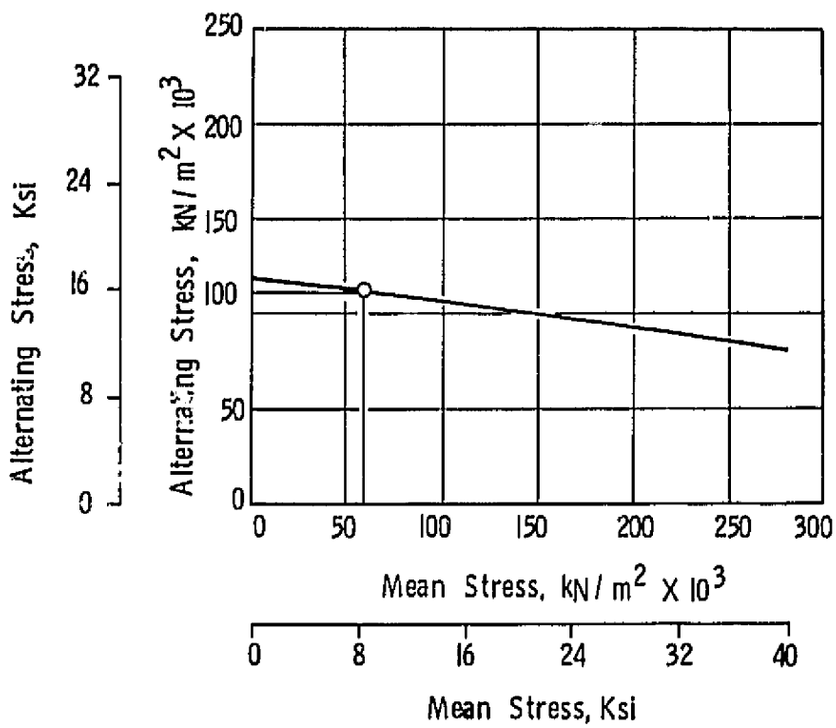

Figure 4.50 Nonstructural Vane Stress-Range Diagram.

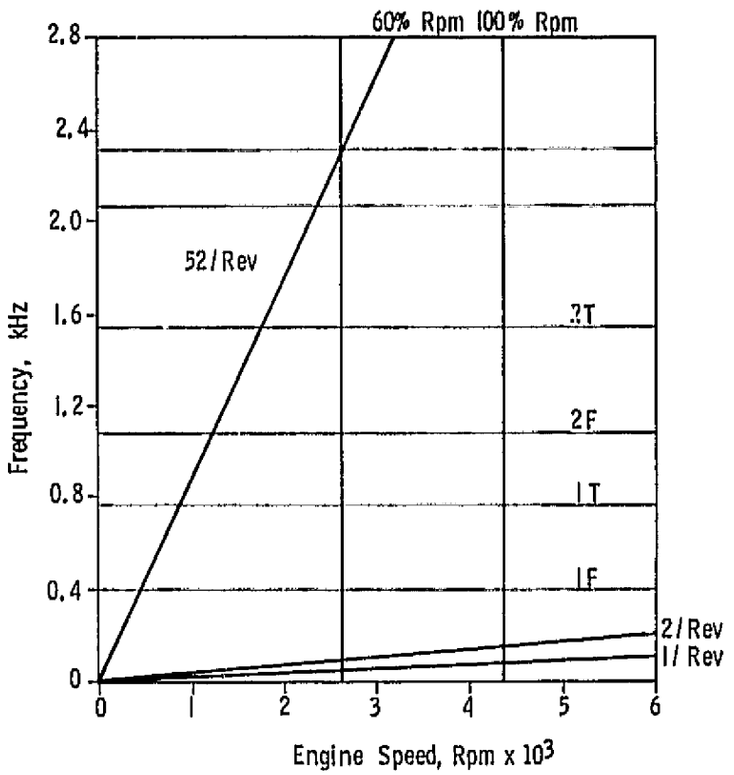

Figure 4.51 Structural Vane Frequency-Speed Diagram.

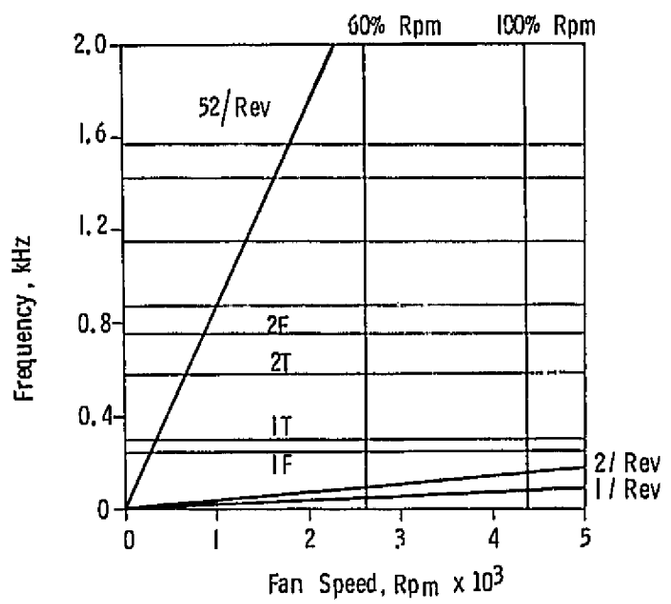

Figure 4.52 Nonstructural Vane Frequency-Speed Diagram.

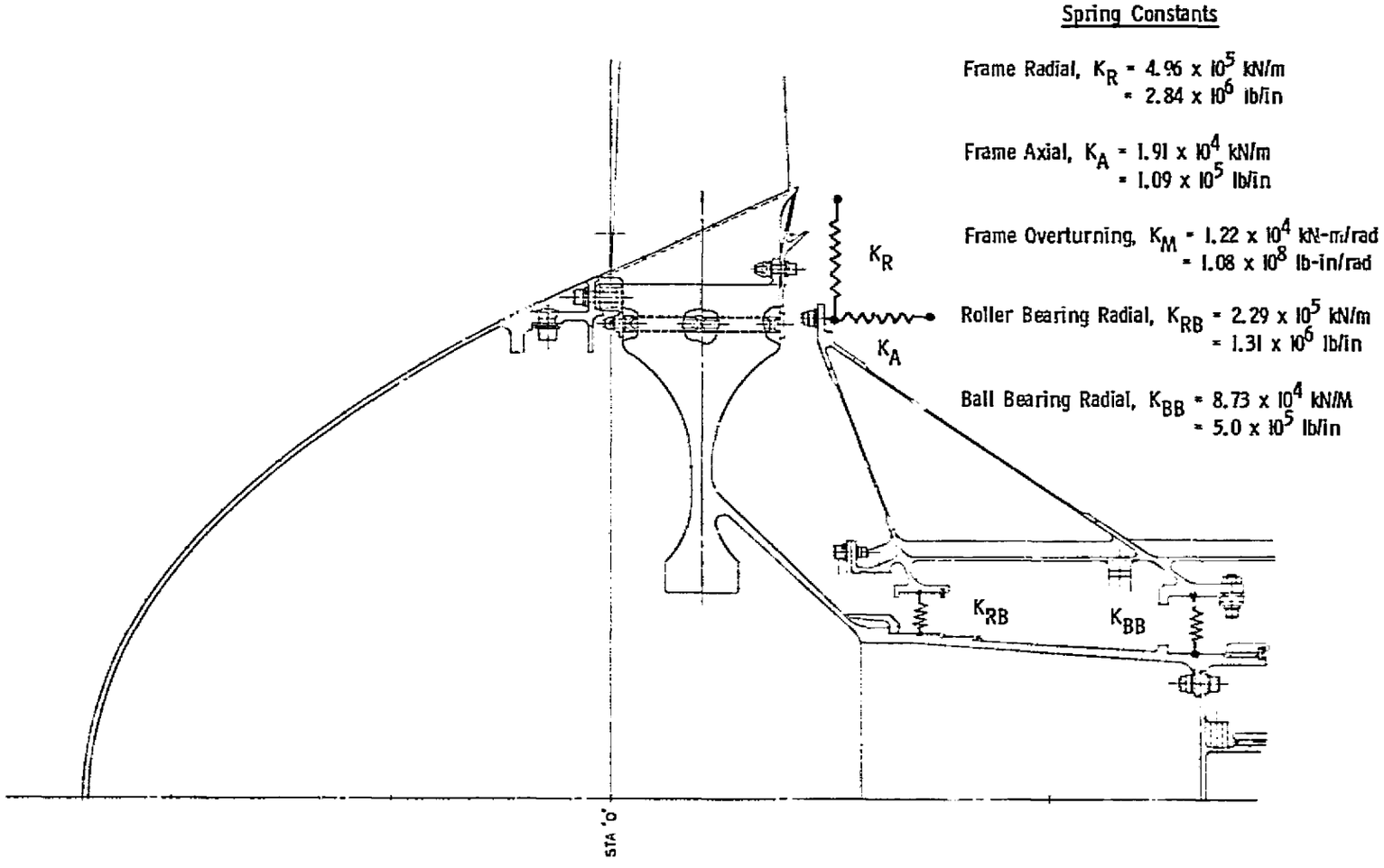

Figure 4.53 Dynamic Model.

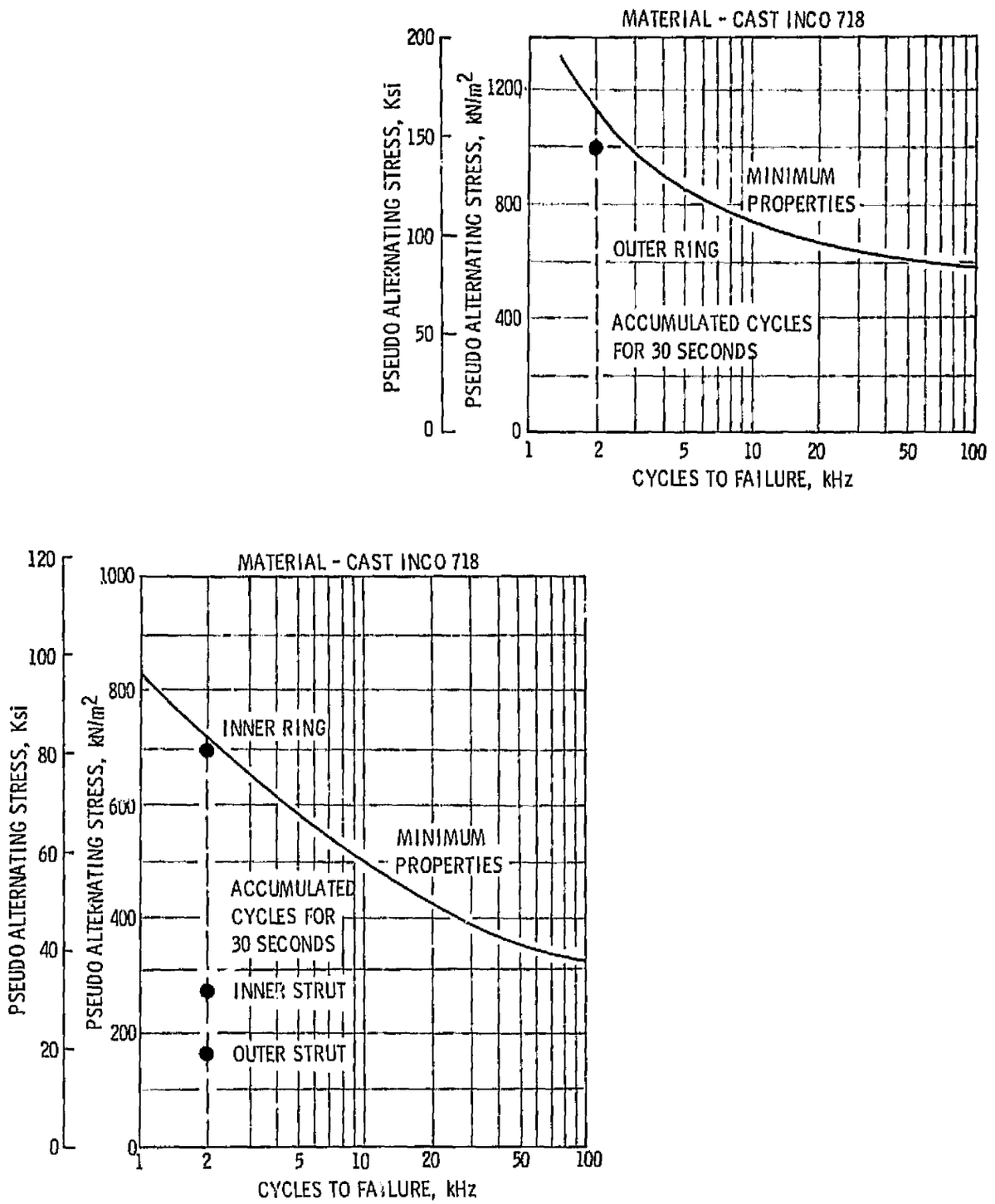

Figure 4.54 Blade-Out Vibratory Stresses.

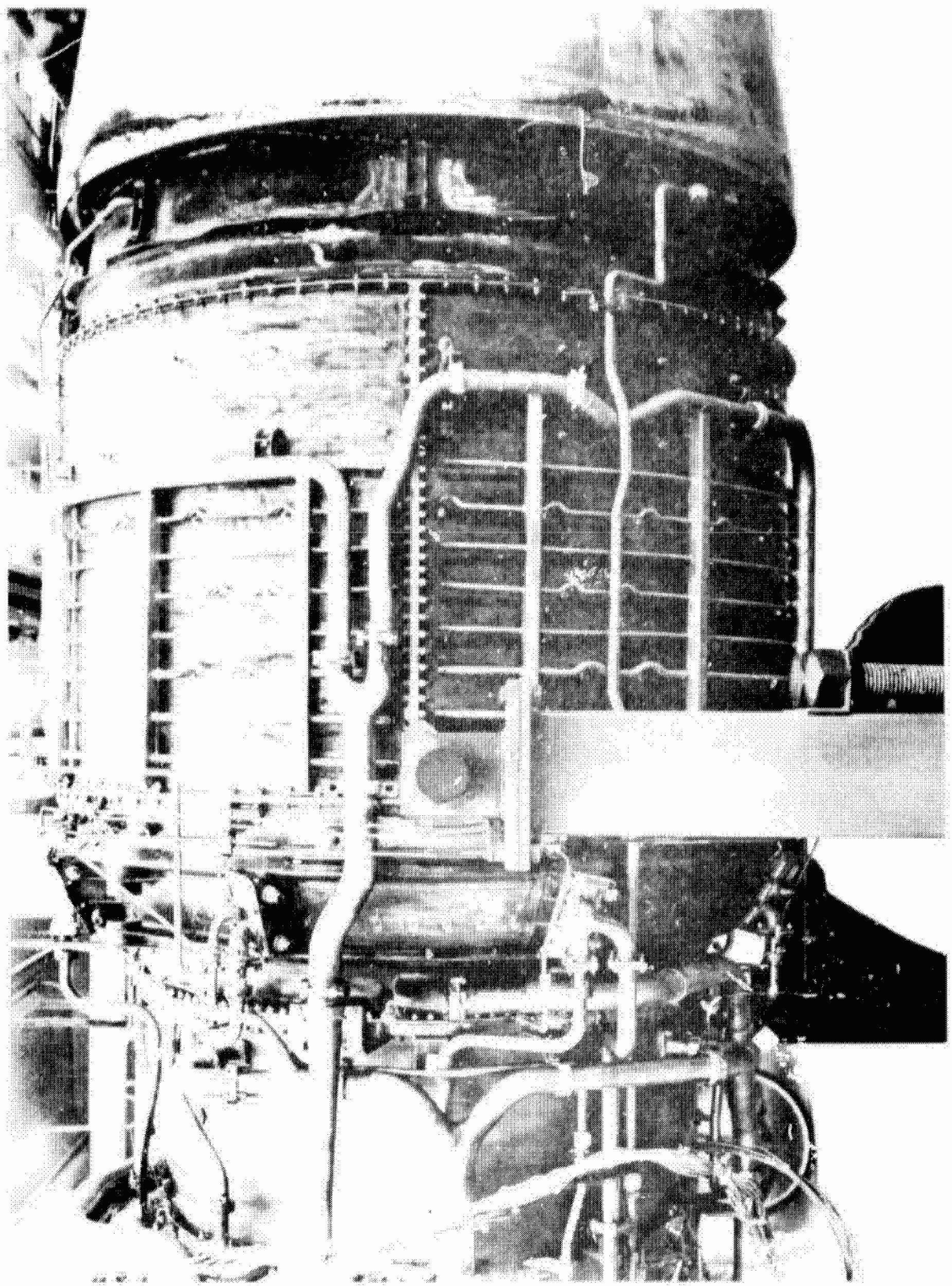

Figure 4.55 TF39 Casing Cooling Manifold.

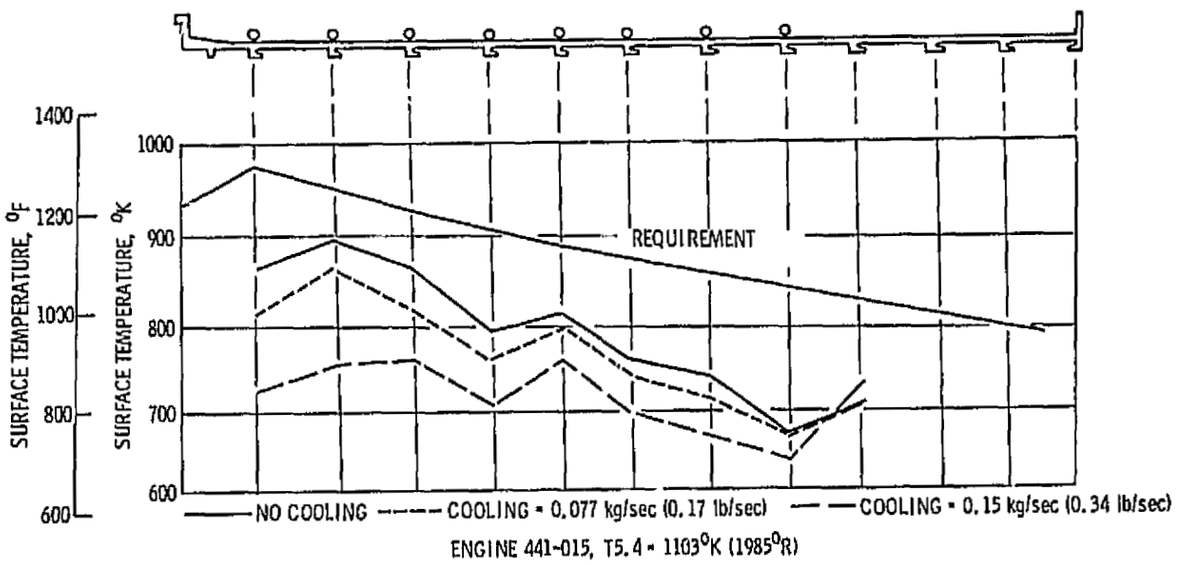

Figure 4.56 TF39 Low Pressure Turbine Case Cooling Tests.

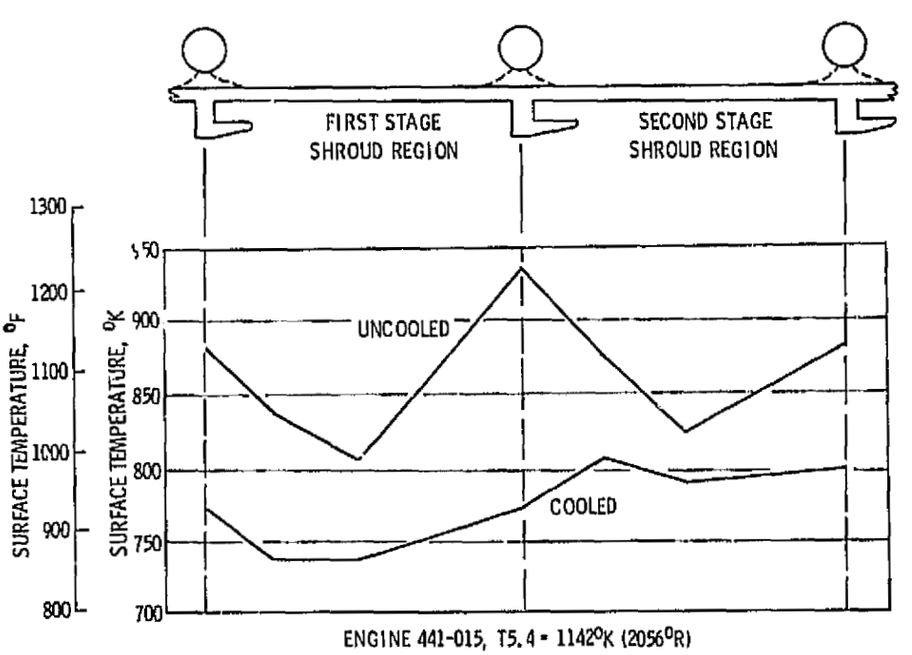

Figure 4.57 TF39 Low Pressure Turbine Case Temperature Profiles.

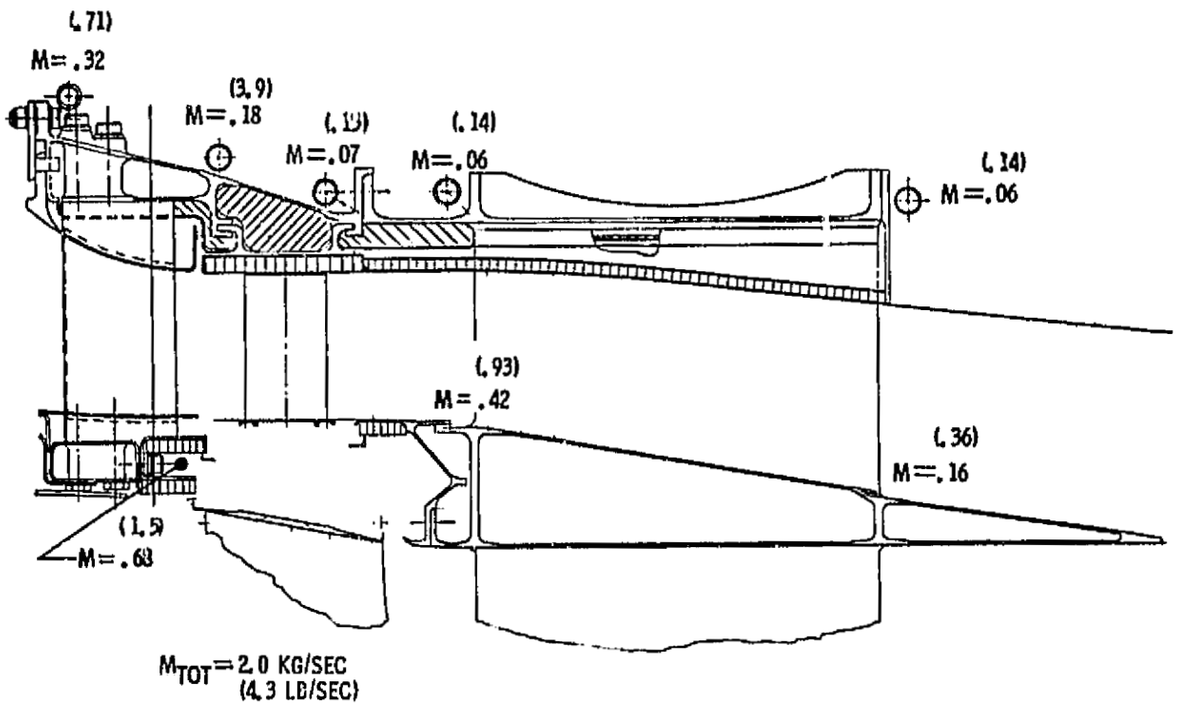

Figure 4.58 Estimated Cooling Flows, Initial Design.

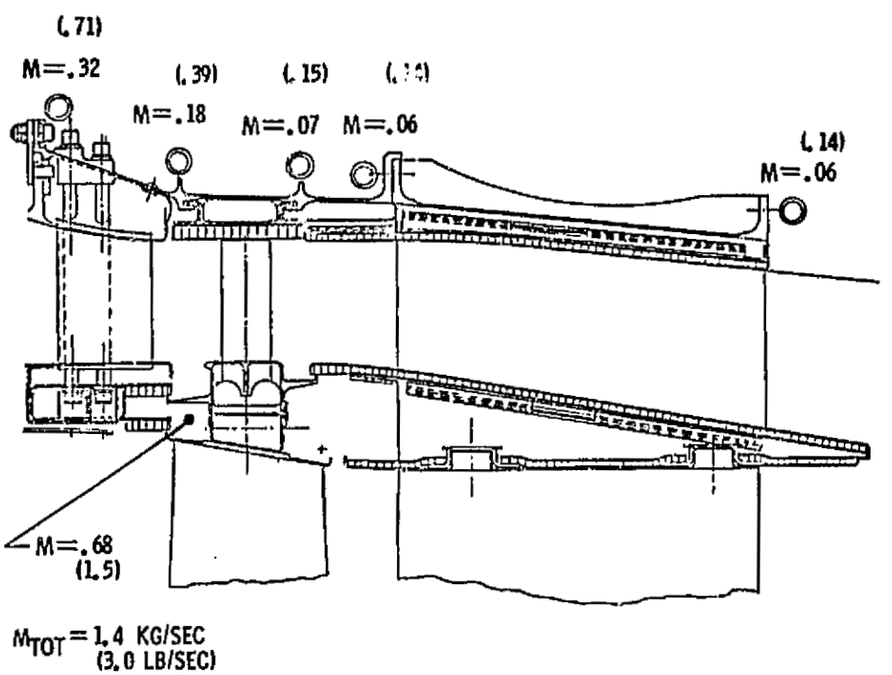

Figure 4.59 Estimated Cooling Flows, Selected Configuration.

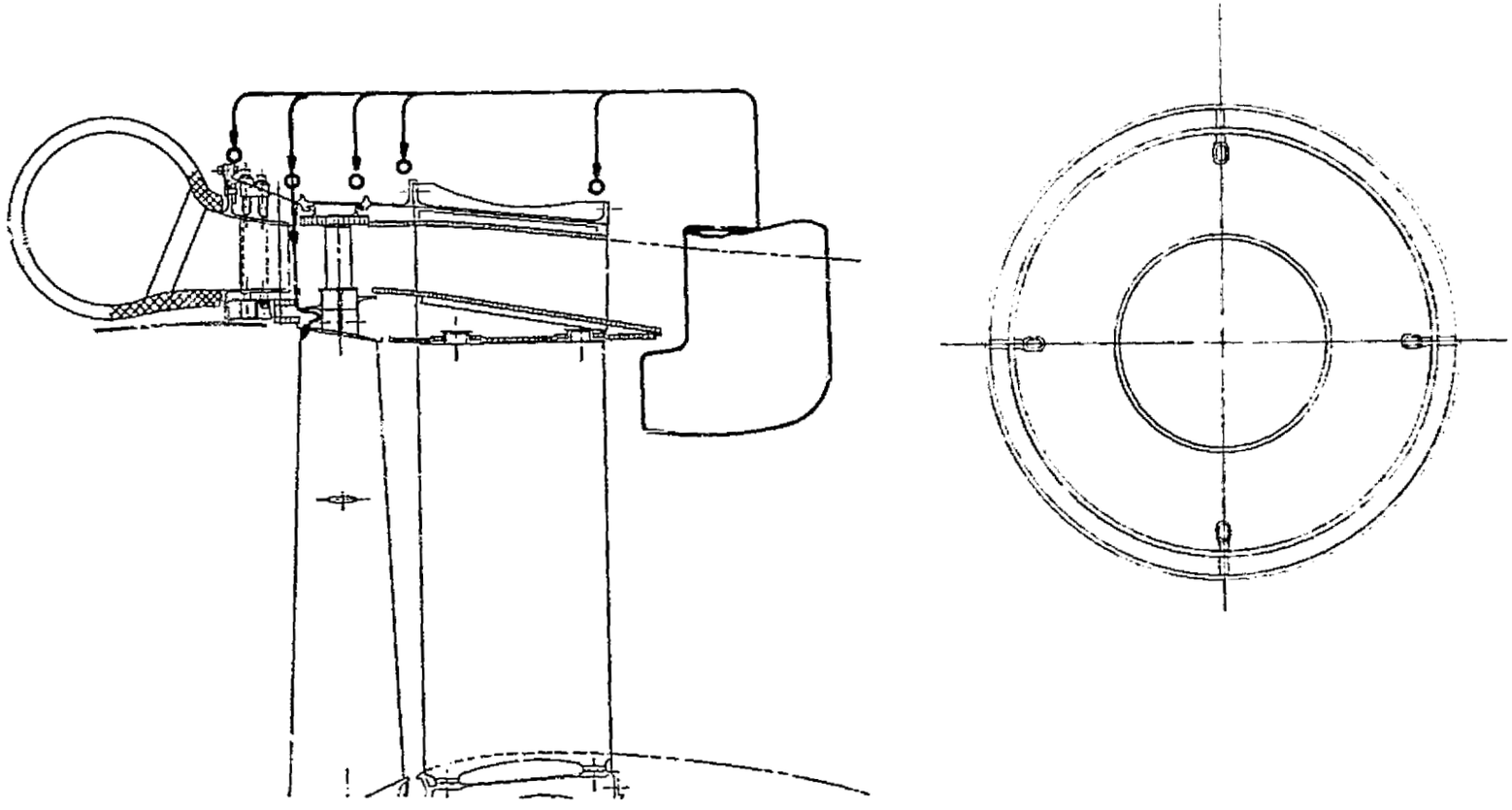

Figure 4.60 Cooling System Schematic.

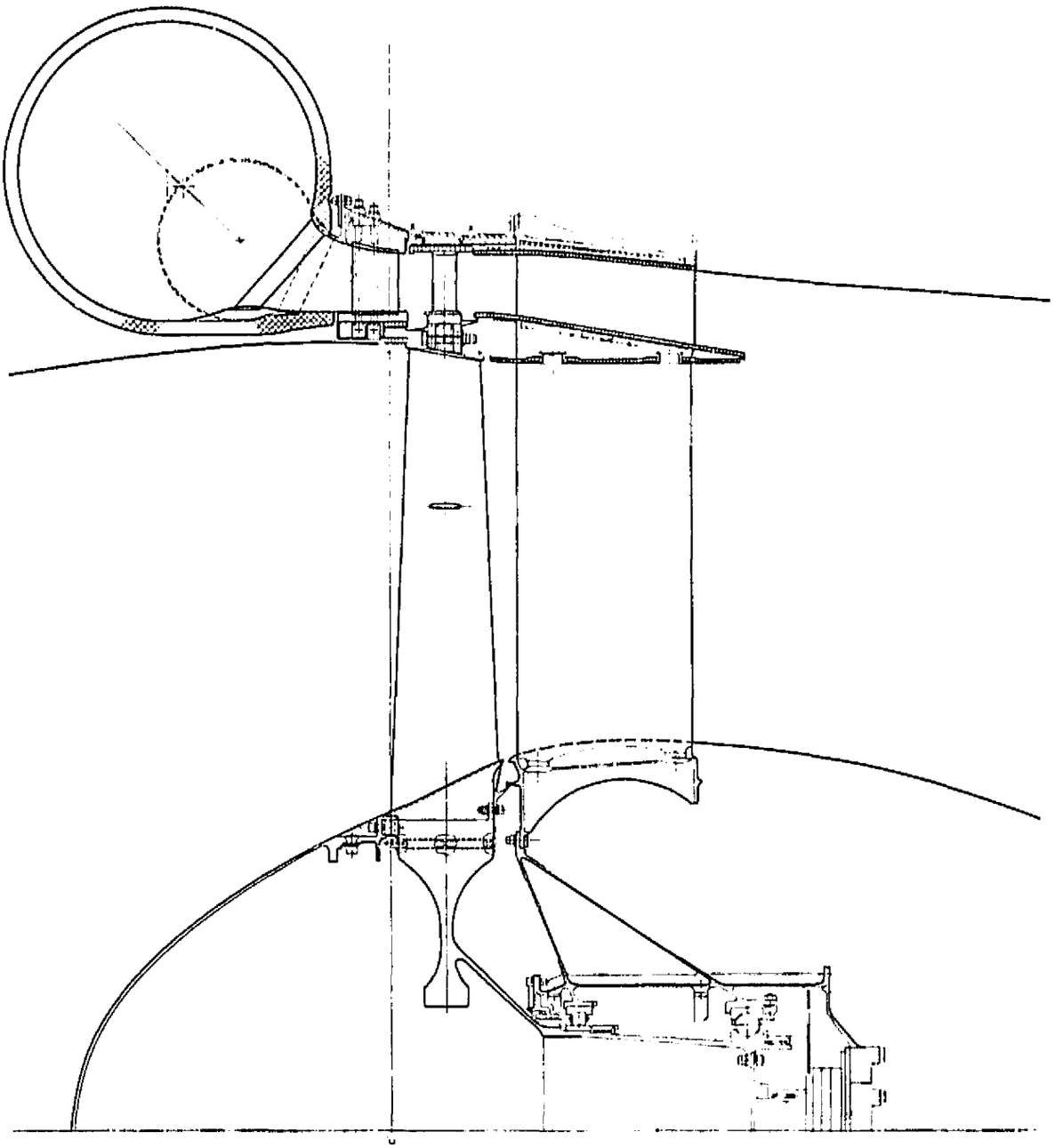

Figure 5.1 LCF459 Cross Section, Circular Scroll.

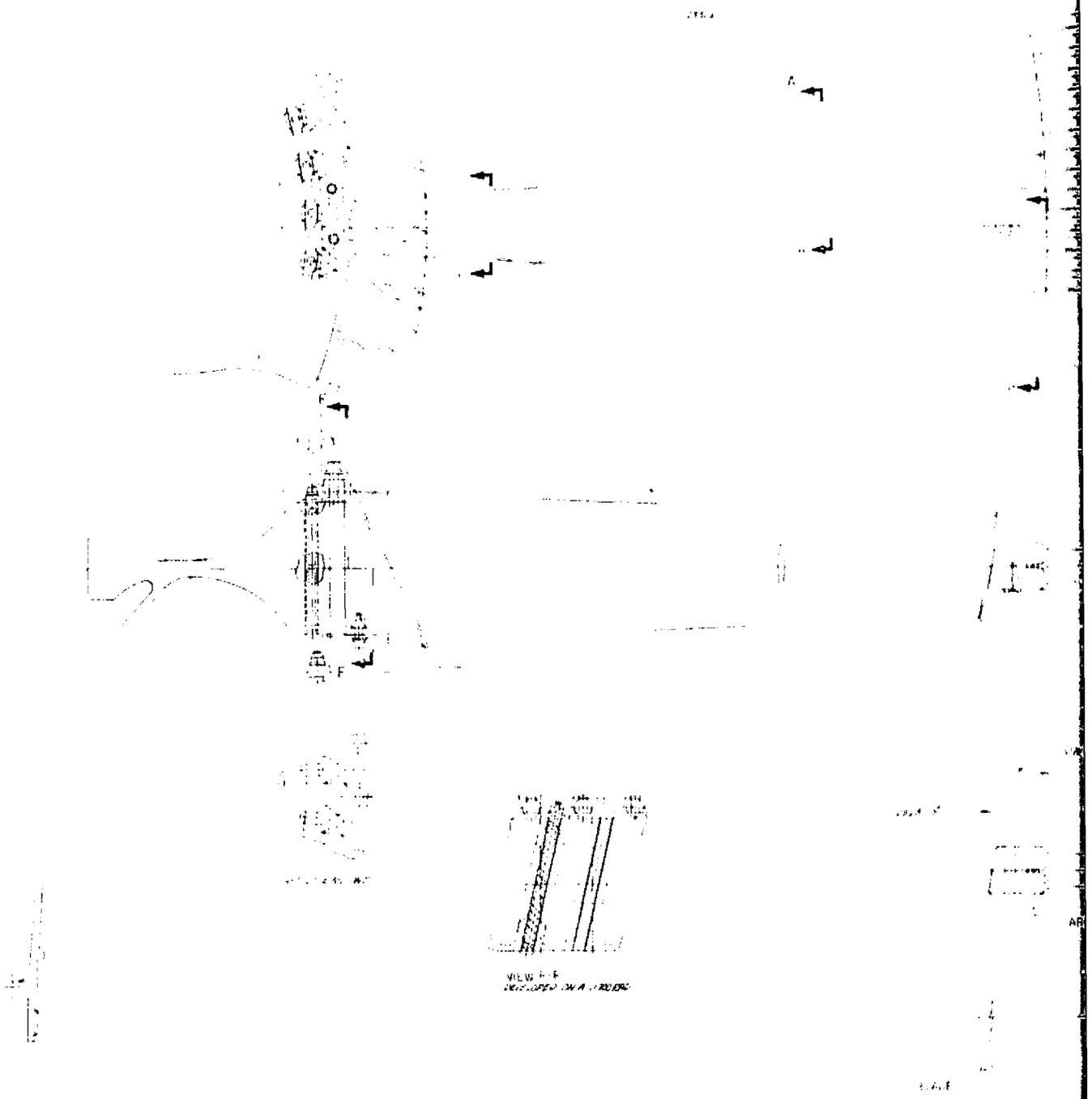

Figure 5.2 Rotor Confi

FOLDOUT FRAME /

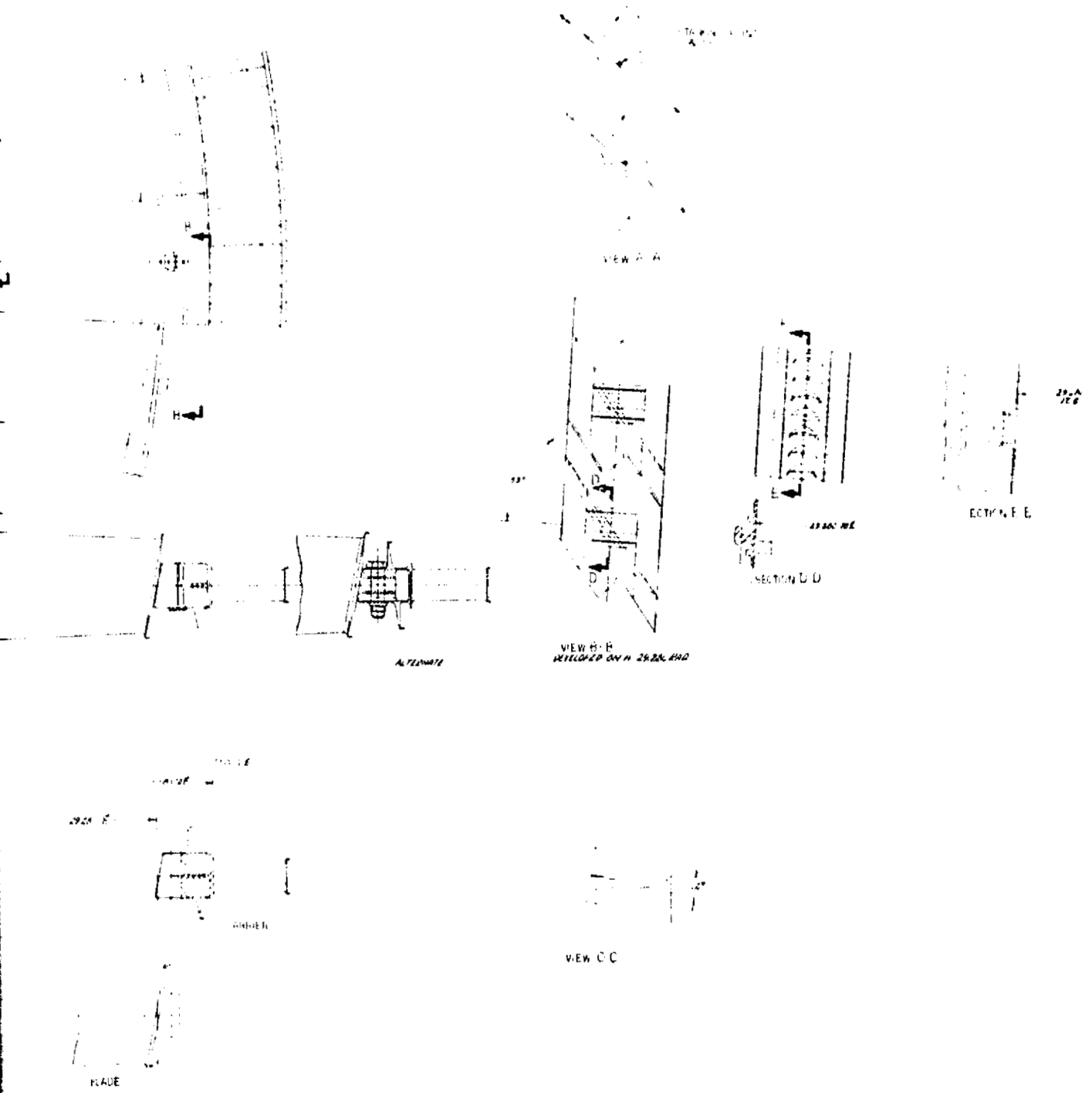

Figure 5.2 Rotor Configuration.

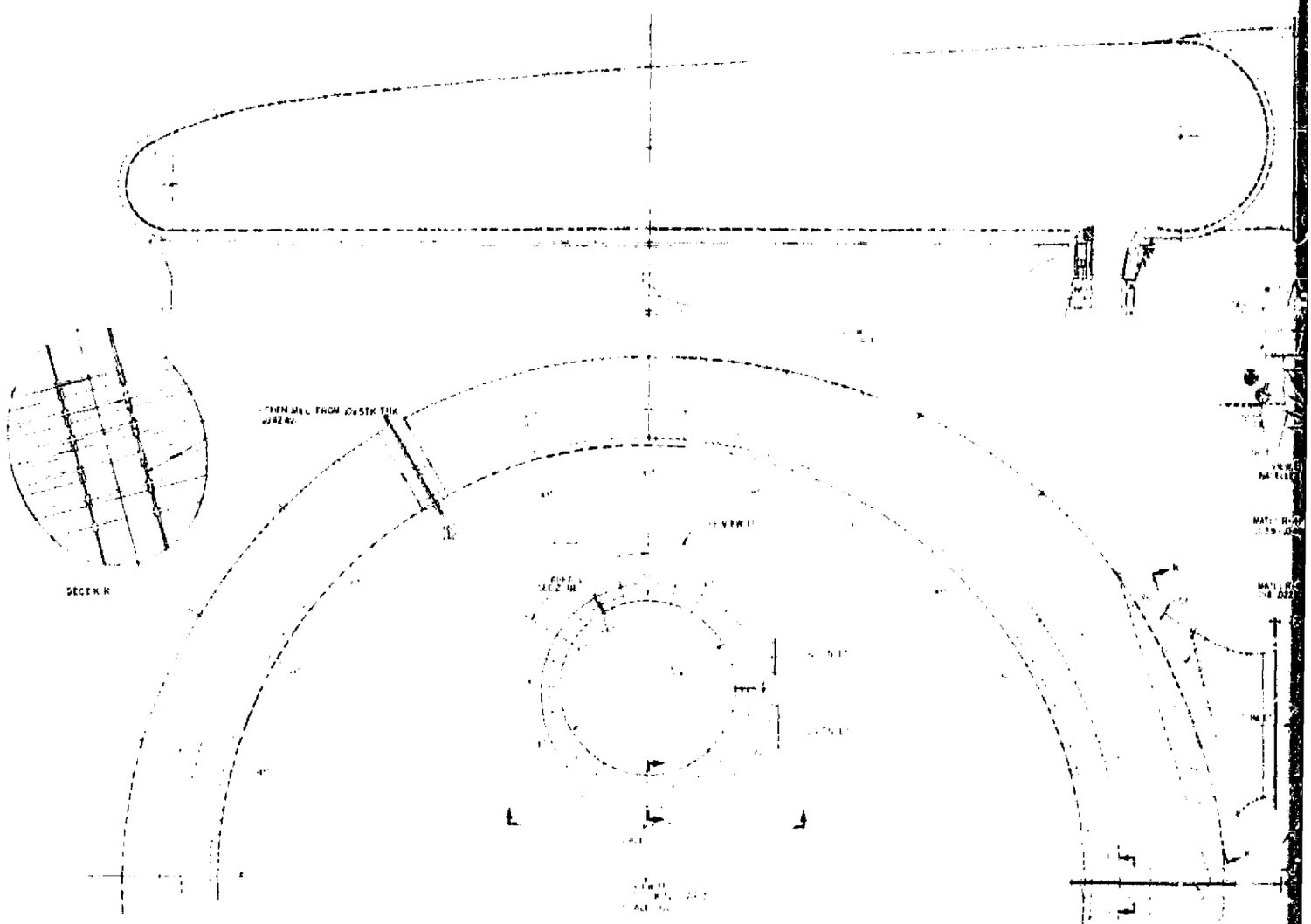

Figure 5.3 Scroll Configuration, Ci

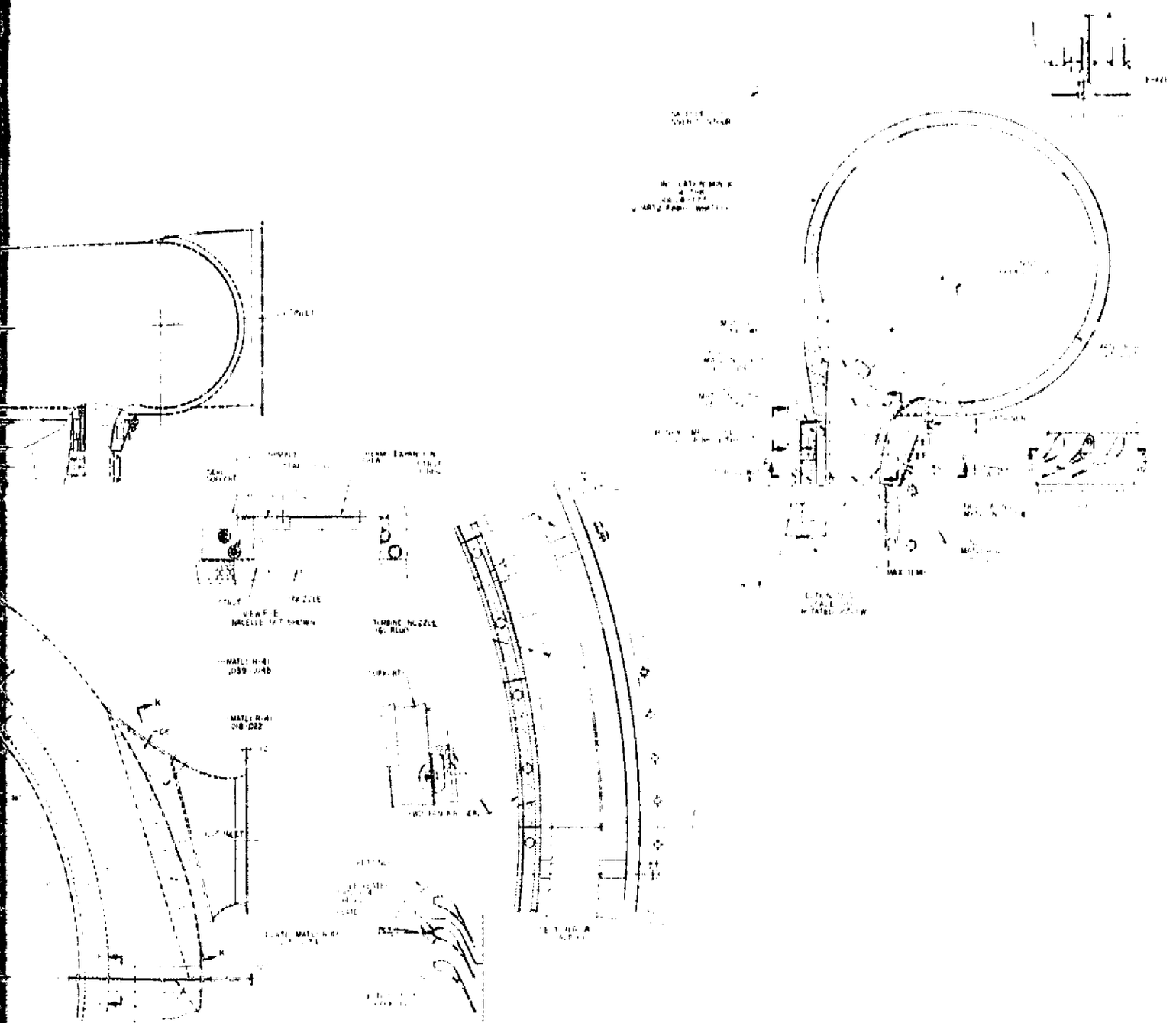

roll Configuration, Circular Bubble.

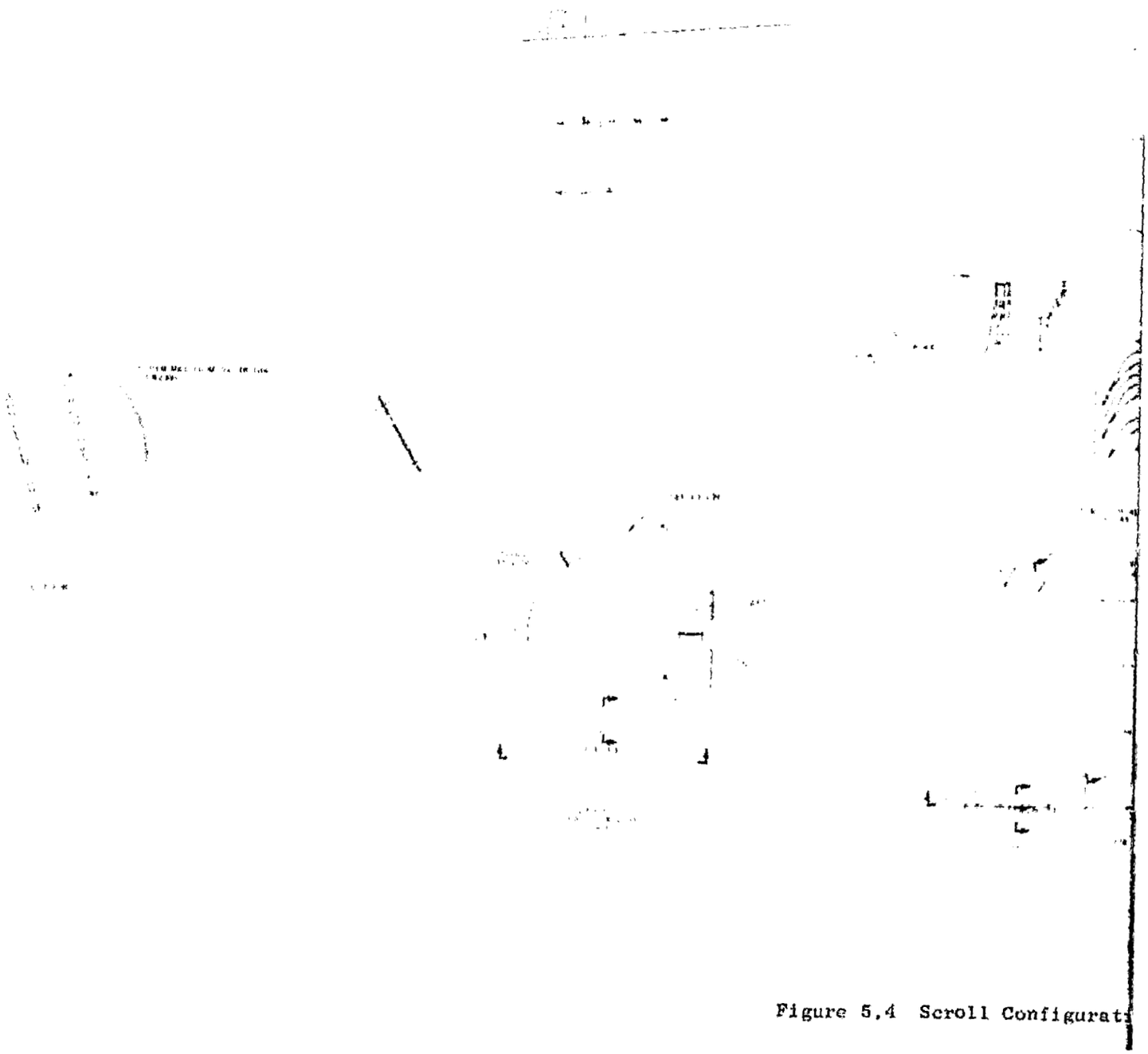

Figure 5.4 Scroll Configurati

4 Scroll Configuration, Multilobe.

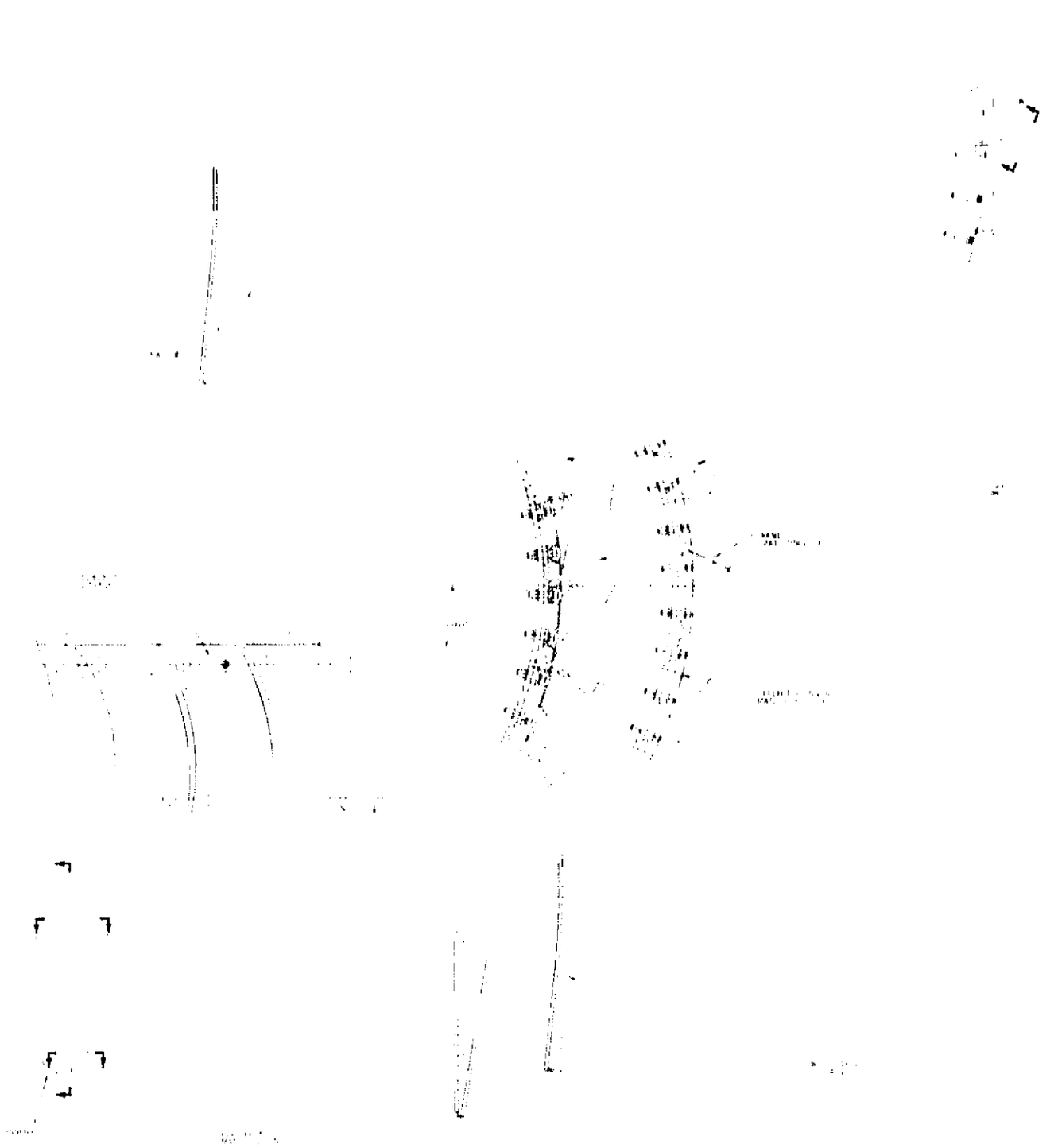

Figure 5.5 Frame Confi

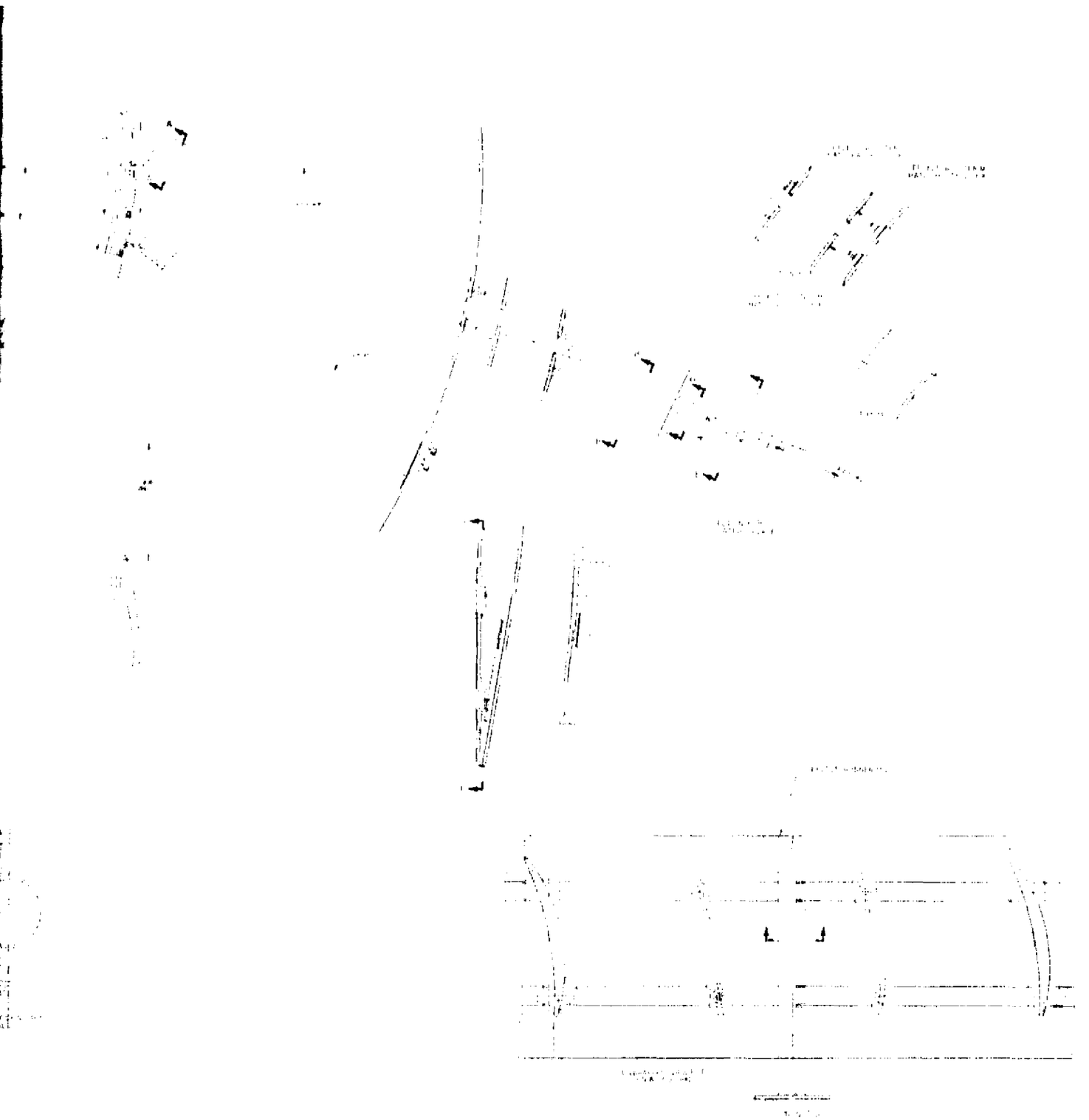

igure 5.5 Frame Configuration.

FOLDOUT FRAME

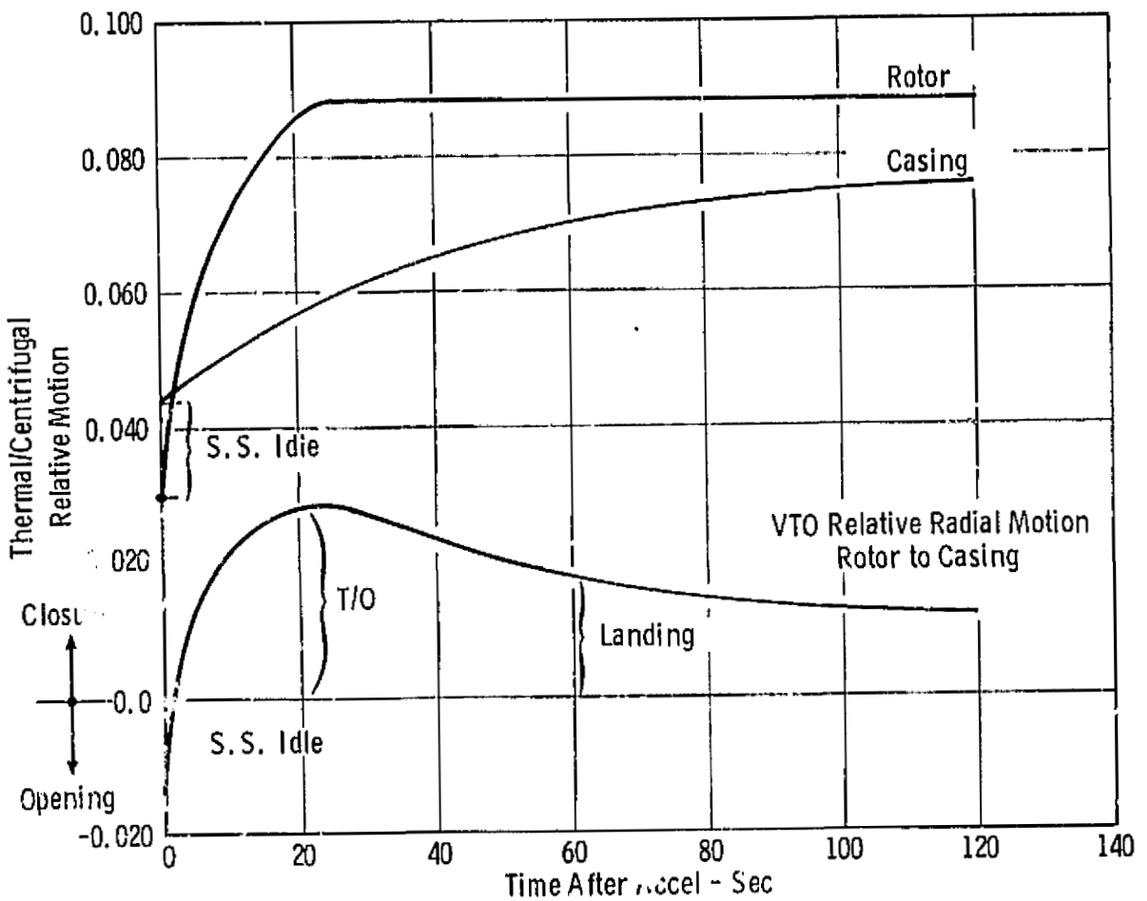

Figure 5.6 Estimated Case Temperature Transients.

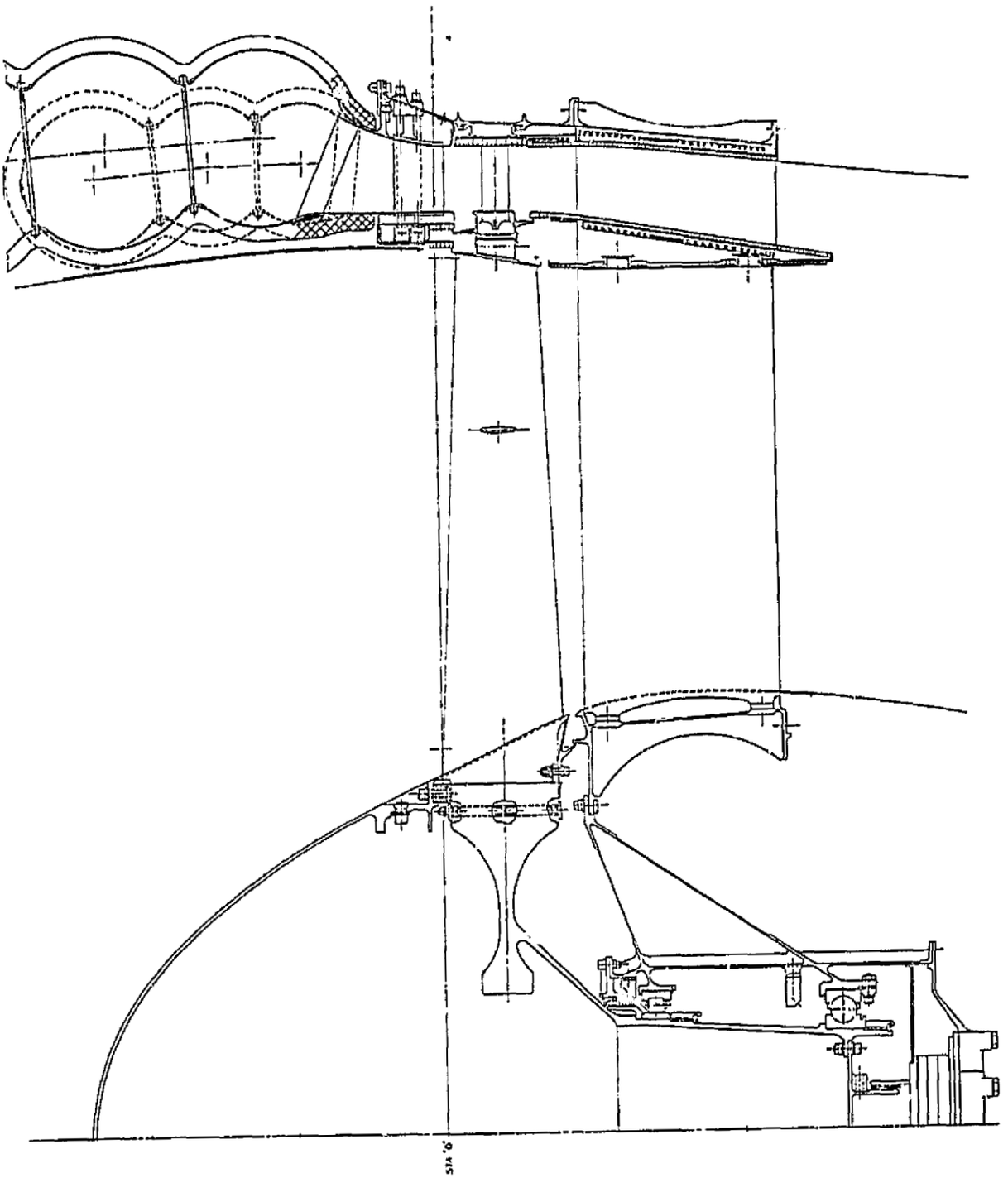

Figure 5.7 LCF459 Cross Section, Multilobe Scroll.

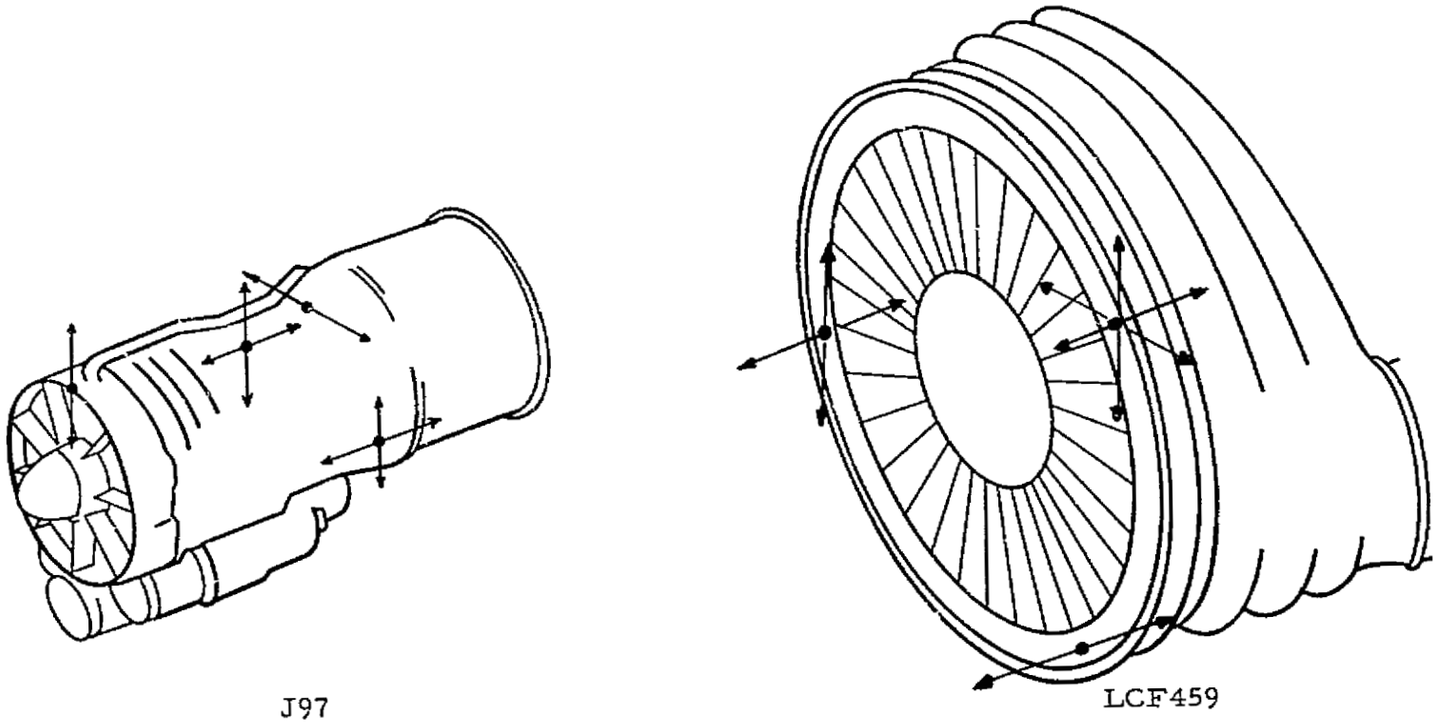

Figure 5.8 Mounting System.

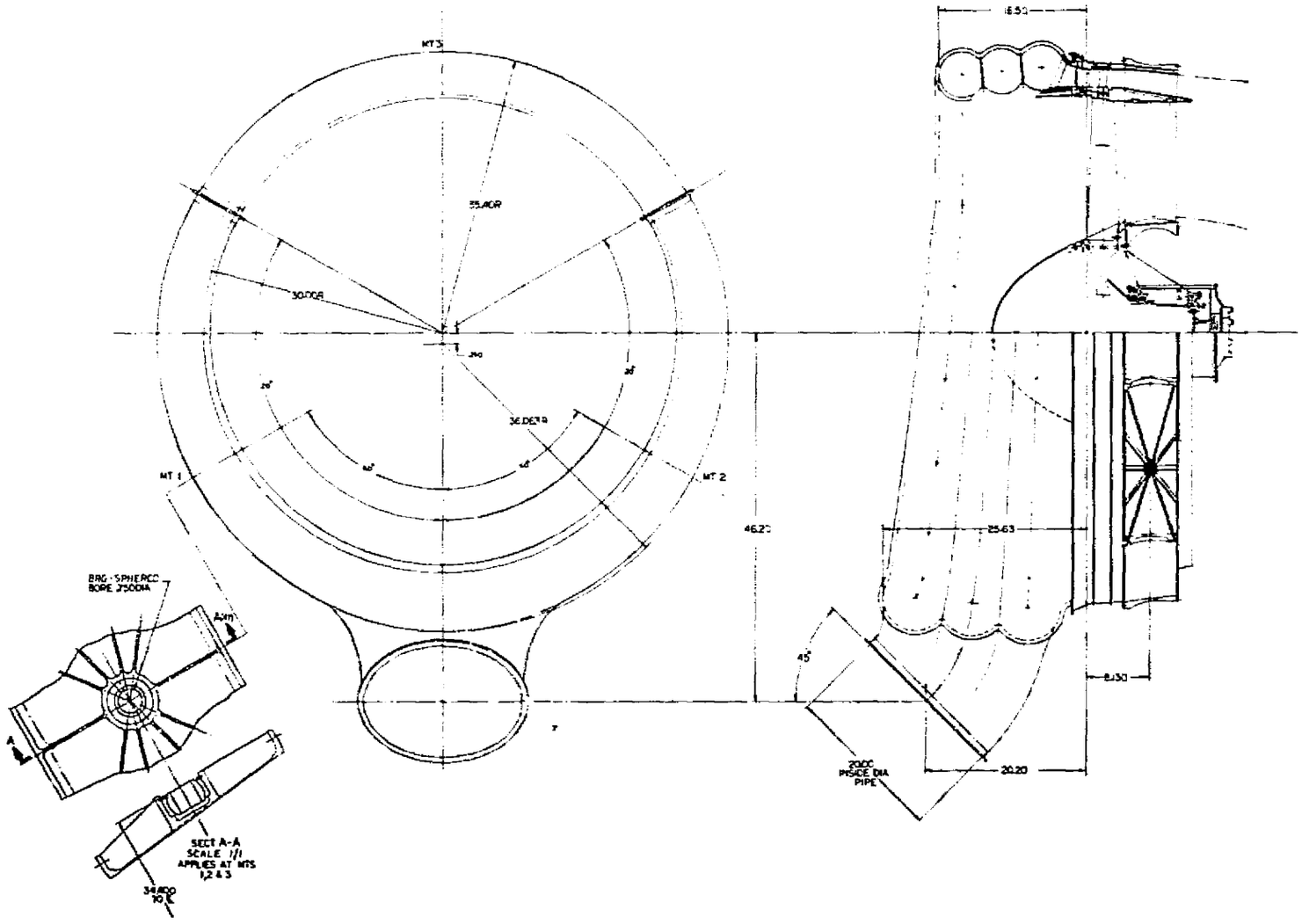

Figure 5.9 LCF459 Installation, Single Inlet Multilobe Scroll.

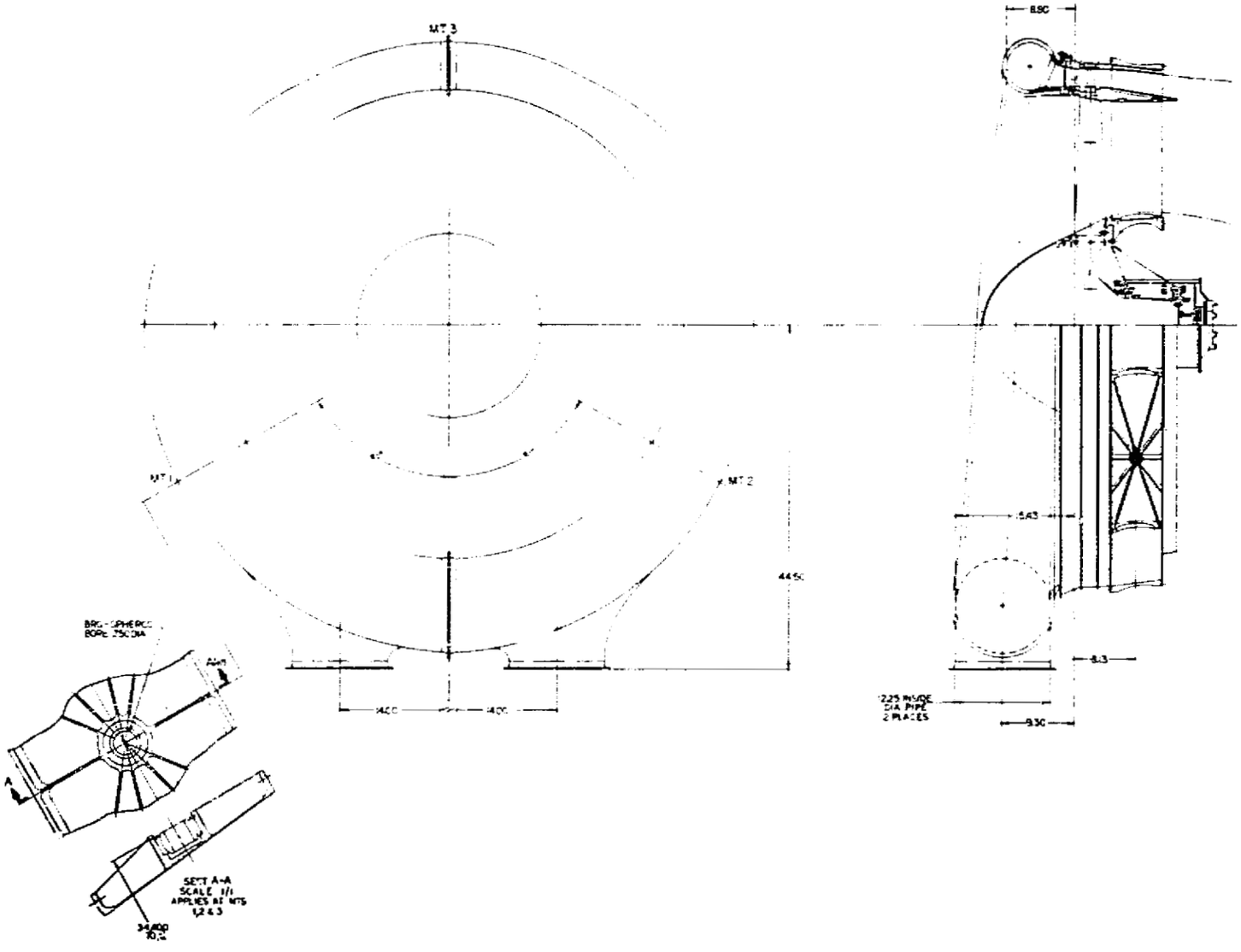

Figure 5.10 LCF459 Installation, Double Inlet Circular Scroll.

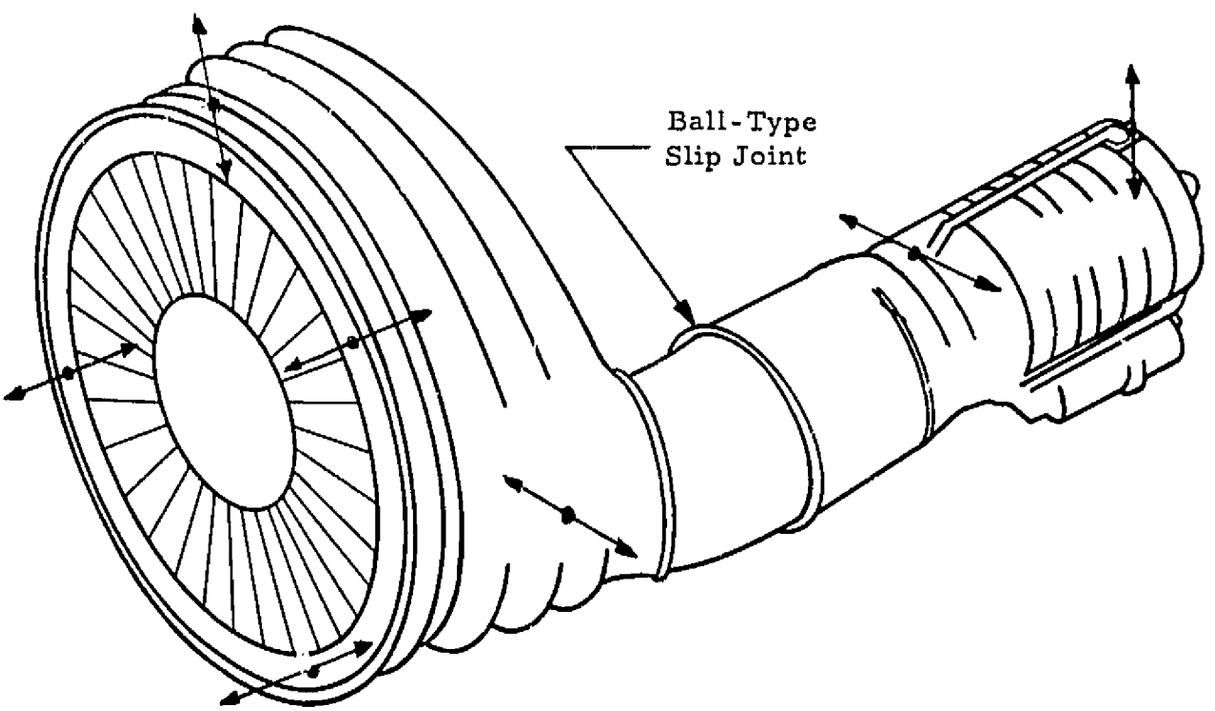

Figure 5.11 Integrated Fan/Engine Mounting System.

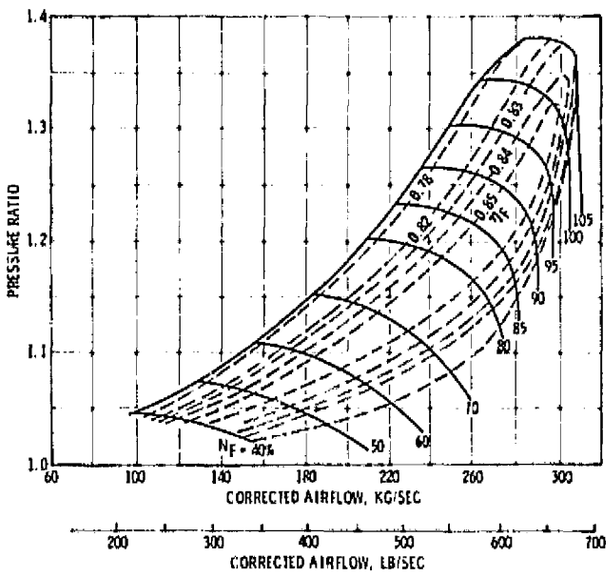

Figure 5.12 Estimated Fan Map.

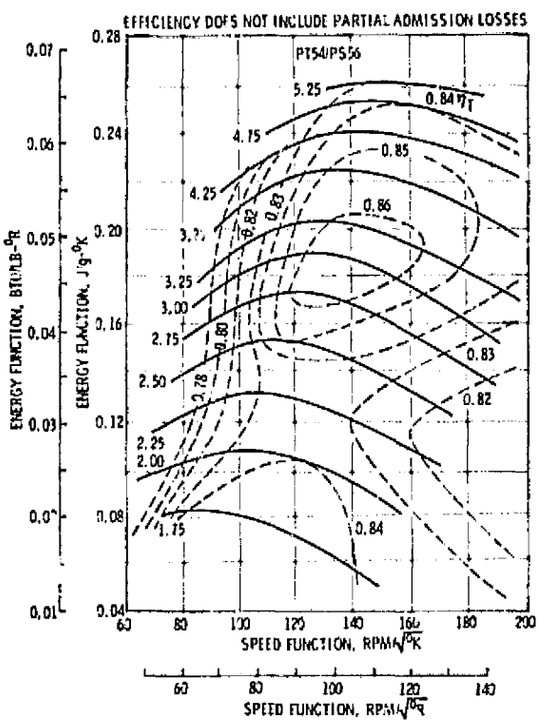

Figure 5.13 Est'mated Turbine Map.

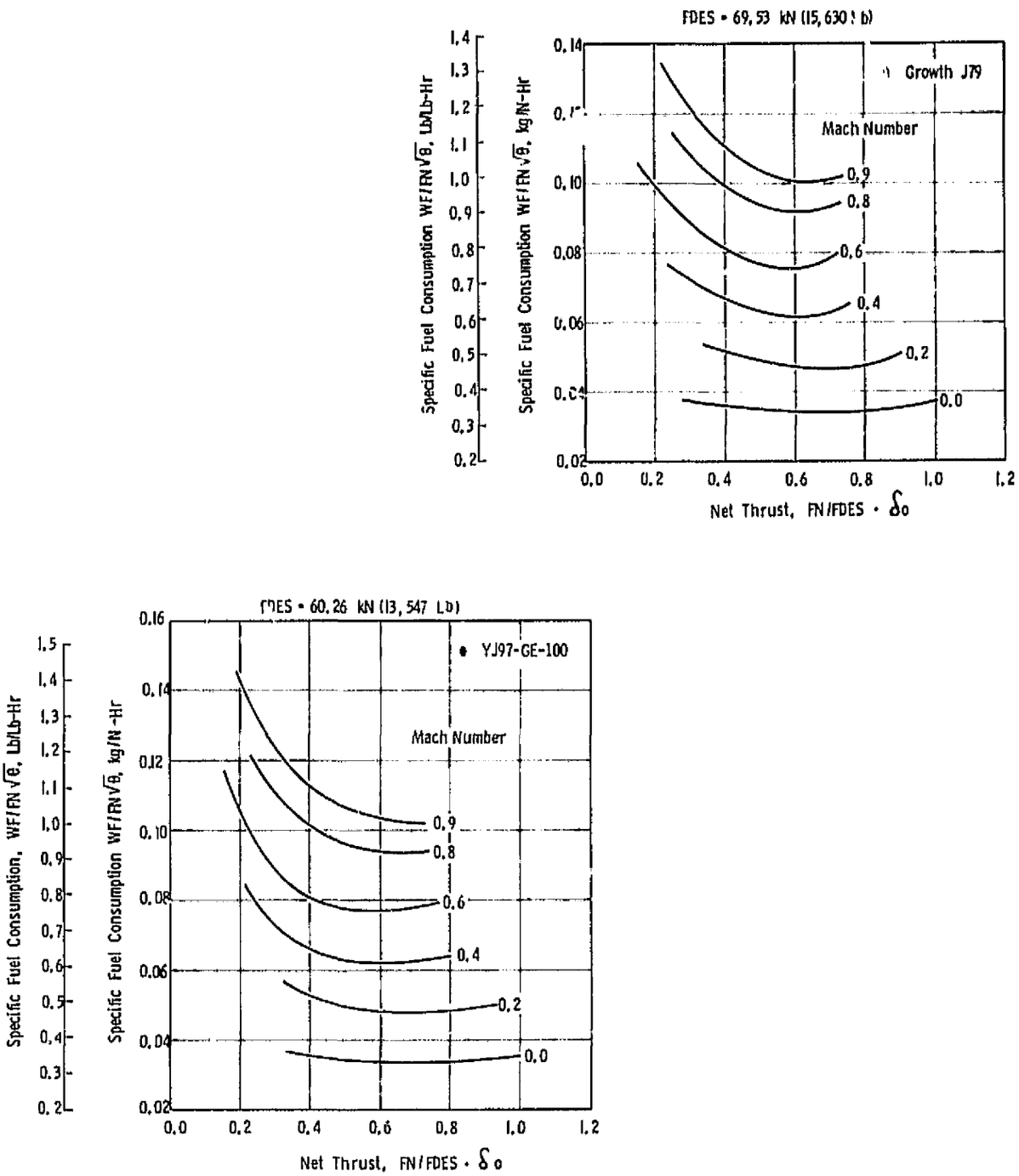

Figure 5.14 Corrected Thrust/SFC Charateristics.

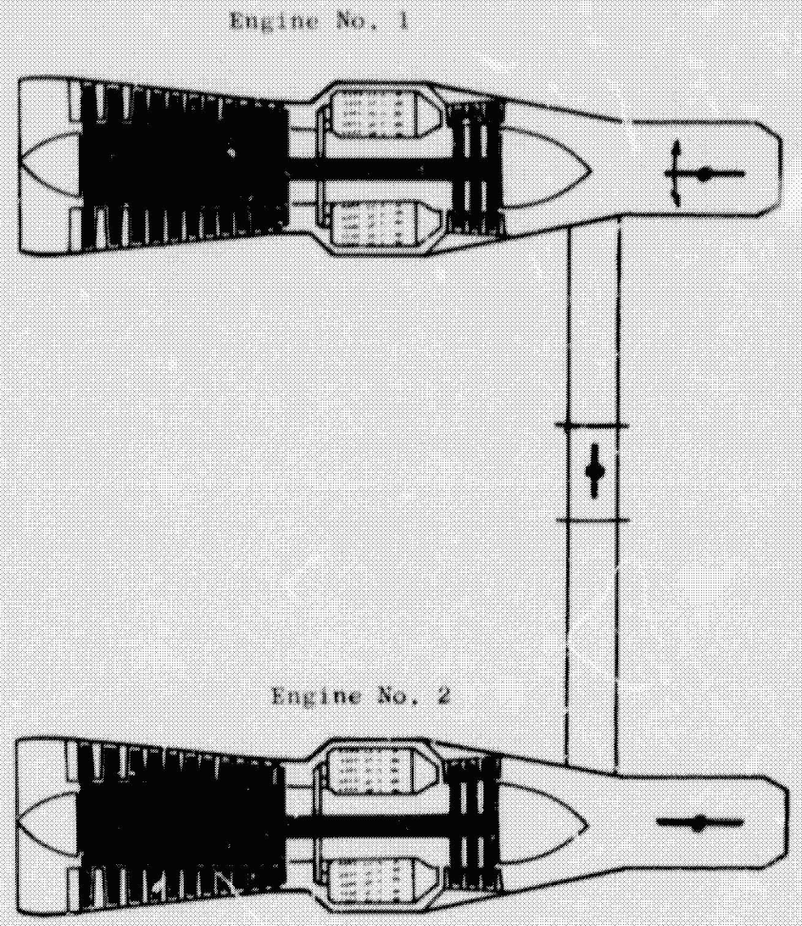

Figure 5.15 Engine Interconnect Schematic.

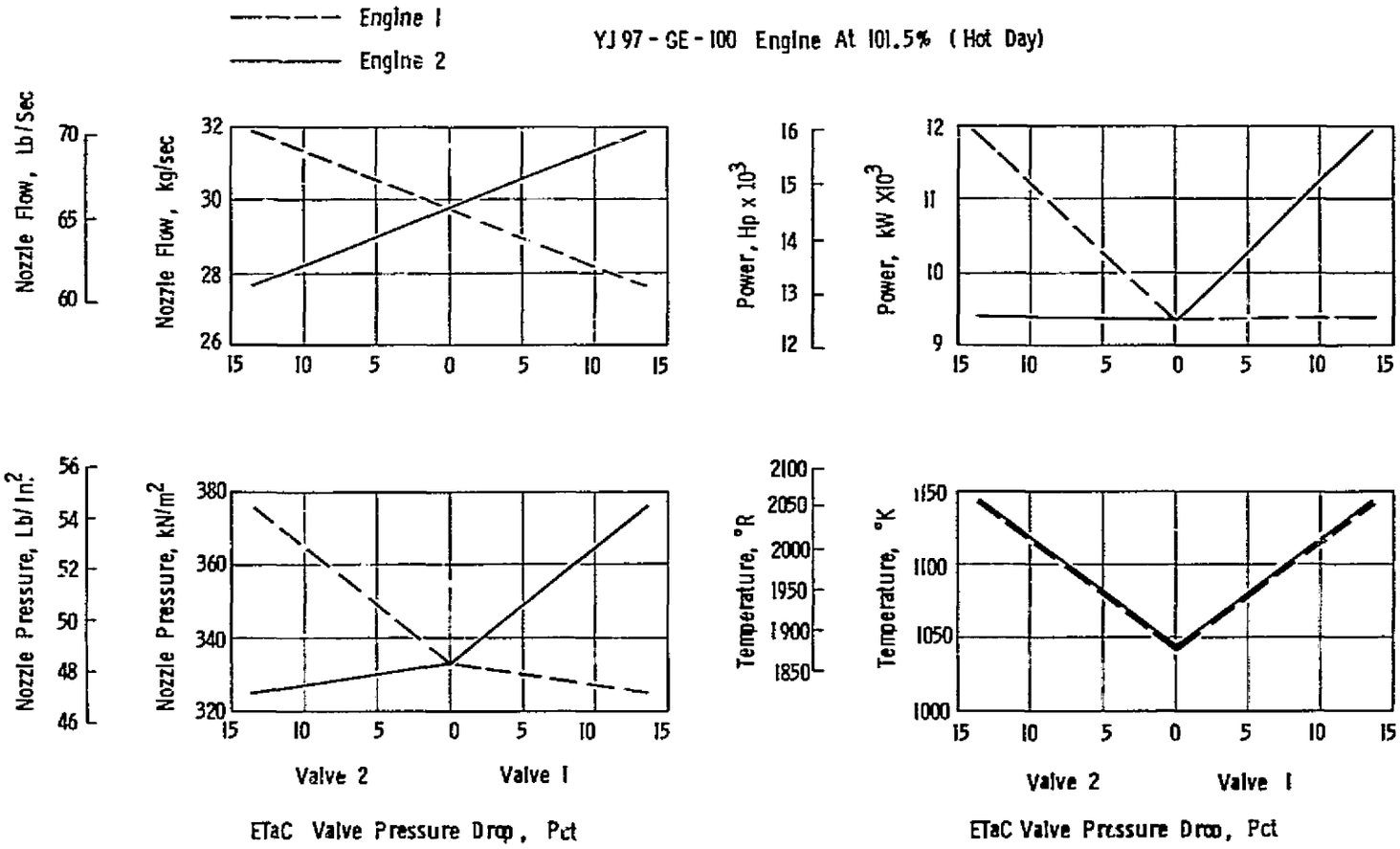

Figure 5.16 Engine Conditions During Control Inputs.

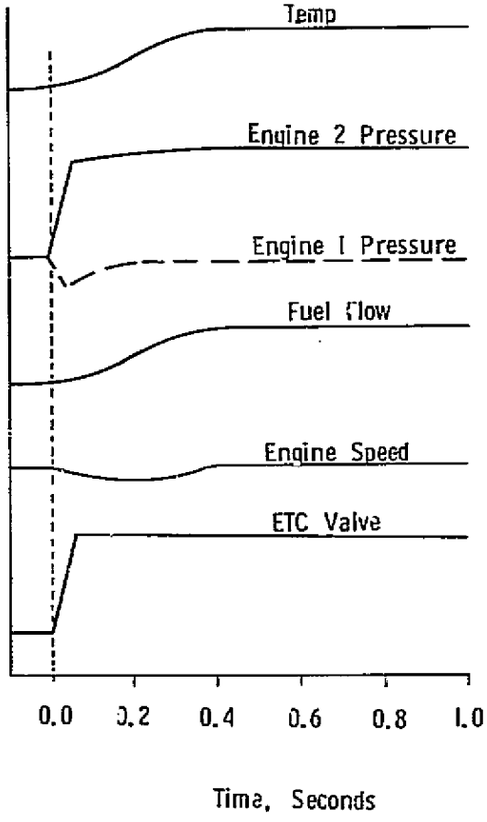

Figure 5.17 Engine Transients During Control.

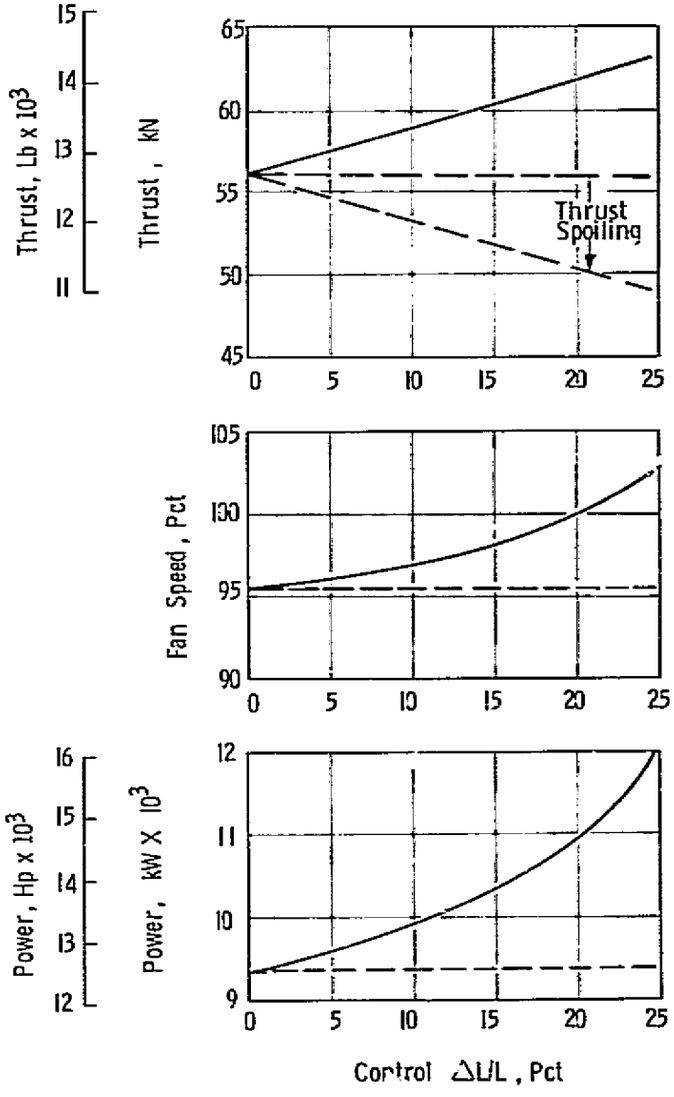

Figure 5.18 Fan Conditions During Control Inputs.

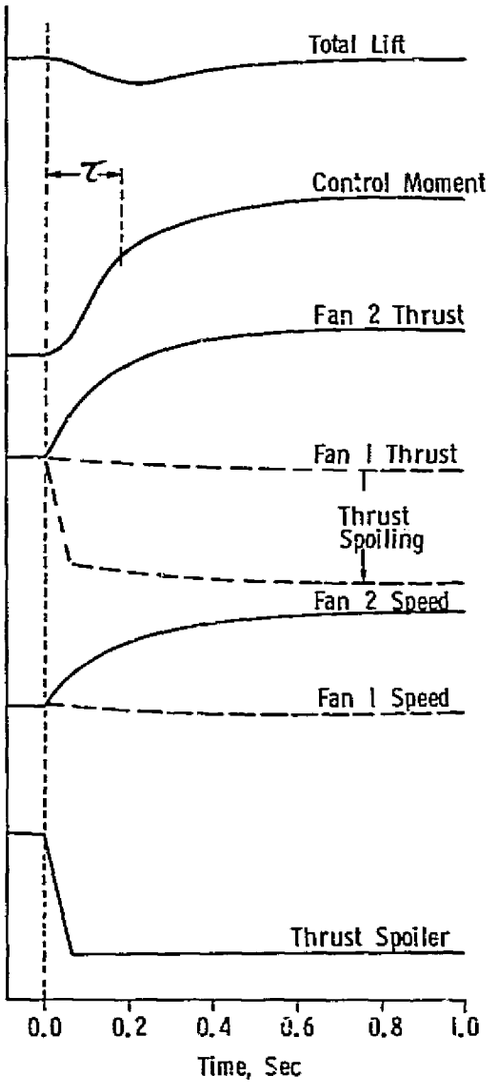

Figure 5.19 Fan Transients During Control.

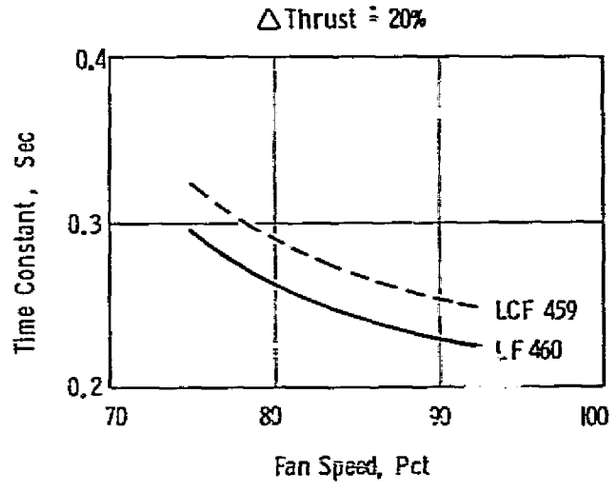

Figure 5.20 Estimated LCF459 Transient Response